LICENTIATE THESIS

Sampling from large flotation cells

An investigation of spatial distributions

Lisa Malm

Mineral Processing

LULEÅ
UNIVERSITY
OF TECHNOLOGY

LULEÅ
UNIVERSITY
OF TECHNOLOGY

Sampling from large flotation cells - An investigation of spatial distributions

Lisa Malm

Luleå University of Technology
Department of Civil, Environmental and Natural Resources Engineering
Division of Minerals and Metallurgical Engineering

Printed by Luleå University of Technology, Graphic Production 2019

ISSN 1402-1757
ISBN 978-91-7790-314-7 (print)
ISBN 978-91-7790-315-4 (pdf)

Luleå 2019

www.ltu.se

Till pappa

Abstract

The general trend in flotation technology today is towards larger flotation cells, which enables higher throughput. However, adverse effects such as segregation and reduced froth transport efficiency have also been observed in larger cells. To better understand these problems it is of relevance to understand how the minerals of interest are moving and distributed inside flotation cells.

A sampling investigation of industrial scale tank cells has been carried out. The samples have been analyzed by their physical properties, such as grade, solids concentration, particle size distribution and mineral composition. A novel method of measuring the wettability has been validated against traditional techniques for characterizing the surface properties of mineral samples. Different techniques and devices for sampling have also been evaluated.

The results show segregation inside the cells, with the quiescent zone having lower particle size (P_{80}) and lower weight % solid. The grade profile in the vertical direction was relatively constant even though the P_{80} and weight % solid decreased in the quiescent zone.

The smaller particles in the quiescent zone contained a higher fraction of soft clay particles, which also correlated with a higher degree of hydrophilicity.

Papers included in the thesis

I- Malm, L., Sand, A., Rosenkranz. J., Bolin, N-J., (2016). *Spatial variations of pulp properties in flotation. Implications for optimizing cell design and performance.* Proceedings of the 28th International Mineral Processing Congress, September 11- 15, Quebec, Canada, paper 354.

II- Malm, L., Kindstedt Danielsson, A-S., Sand, A., Rosenkranz, J., Ymén, I., (2018). *Application of Dynamic Vapor Sorption for evaluation of hydrophobicity in industrial-scale froth flotation.* Minerals Engineering, 127, pp. 305-311.

III- Malm, L., Kindstedt Danielsson, A-S., Sand, A., Rosenkranz, J., Ymén, I., (2018). *Dynamic vapor sorption- A novel method for measuring the hydrophobicity in industrial- scale froth flotation.* Proceedings of the 29th International Mineral Processing Congress, September 17-21, Moscow, Russia, paper 431.

IV- Malm, L., Sand, A., Bolin, N-J., Rosenkranz, J., Ymén, I., *Dynamic Vapor Sorption measurements and identification of mineral species in industrial-scale flotation cell samples*, submitted to Powder Technology.

Author's contribution to the papers:

Paper I:

All experimental planning, all data processing and most of the writing.

Paper II:

Planning of the test work and sampling, most of the writing.

Paper III:

Planning of the test work. Half of the experimental work and most of the writing

Paper IV:

Planning of the test work. Most of the writing.

Supporting papers and manuscripts

I- Malm, L., Sand, A., Rosenkranz, J., Bolin, N-J., (2016). *Internal material distribution in flotation cells at Aitik- Sampling and characterization.* Proceedings Conference in Mineral Processing, Luleå University of Technology, pp. 53-67.

II- Rosenkranz, J., Sand, A., Malm, L., Bolin, N-J., (2017). *Untersuchung des Einflusses der Zellengeometrie auf den Flotationsprozess*, Berg- und Huttenmännische Monatshefte (BHM), Vol. 162, (8), pp. 281-288.

III- Malm, Lisa, (2018). Up-scaling in flotation, Manuscript for the training program "PROCHAINE – Design and upscaling in mineral processing"

Acknowledgements

First of all, I would like to thank my academic supervisors, Professor Jan Rosenkranz, for his guidance throughout my work, Dr. Anders Sand and Dr. Tommy Karlkvist who both have given me good advice and helped me with language corrections and writing.

I am sincerely grateful to the company I am working for, Boliden AB, that has supported me in this work, both financially and with resources. In particular, I want to thank my colleagues at the Boliden technical laboratory for all sample preparation, sieving and analyzing. Special thanks to Mikael Widman, who designed the "Widmatic" sampler and was truly a great help during the sampling survey at the Aitik concentrator. The good working environment at the department and all the help and support from all colleagues has of course been appreciated.

I am also thankful for the financial support of the project "HIFLOAT" from the Swedish Governmental Agency for Innovation Systems, VINNOVA.

One of my master thesis students, Sami Lappi, has with his thesis work contributed with interesting results to this work. Dr. Ingvar Ymén at RISE, Södertälje, has with his profound knowledge of the DVS instrument contributed to part of the work. Both contributions are gratefully acknowledged.

My family, Magnus and our three kids, Katja, Olivia and Ludvig, who continuously remind me of what is most important in life.

A special thanks to my parents who always has supported me.

Finally, I would like to thank Dr. Nils-Johan Bolin. Without his initiative to this project, together with all encouragement and support during the work I would probably not be where I am today. Thank you for that.

List of symbols and abbreviations

BET	Brunauer-Emmett-Teller
CFD	Computational Fluid Dynamics
DVS	Dynamic Vapor Sorption
GVS	Gravimetric Vapor Sorption
H&S	Heath & Sherwood
RH	Relative humidity
XRF	X-ray fluorescence
XRPD	X-ray powder diffraction

A_s	Impeller aspect ratio [-]
d_b	Mean bubble size [mm]
d_{32}	Sauter mean bubble size [mm]
d_{bi}	Bubble diameter [mm]
G	Gravity constant [m/s^2]
h	Height of a flotation cell [m]
J_g	Superficial gas velocity [cm/s]
k	Flotation rate constant [-]
K_f	Rate constant of fast floating [1/s]
K_s	Rate constant of slow floating [1/s]
K_n	Rate constant of non floating [1/s]
N_s	Impeller tip speed [m/s]
S_b	Bubble surface area flux [s^{-1}]
P	Floatability component [-]
P_{80}	Particle size where 80 % of the material is finer [m]
p	Pressure [Pa]
p_0	Atmospheric pressure [Pa]
R_∞	Maximal theoretical recovery [-]
$R\ or\ R_f$	Flotation recovery [-]
t	Flotation time/ residence time [s]

$\gamma_{s/a}$	Surface tension between solid and air [N/m]
$\gamma_{w/a}$	Surface tension between water and air [N/m]
$\gamma_{s/w}$	Surface tension between solid and water [N/m]
θ	Contact angle [degree]
$\emptyset$	Fraction [-]
$\emptyset_f$	Fraction of fast floating [-]
$\emptyset_s$	Fraction of slow floating [-]
$\emptyset_n$	Fraction of non floating [-]

Chemical formula

Cu	Copper
Pb	Lead
CuPb	Copper/ lead product
SiO_2	Silica
PAX	Potassium amyl xanthate

Boliden sites

Aitik	Low grad copper deposit, located in the north of Sweden
Garpenberg	Lead/ Zinc deposit, located in the middle of Sweden

Contents

1 INTRODUCTION 4

1.1 Research background 4

1.2 Objectives and Scope of the work 6

2 FLOTATION THEORY AND ANALYSIS 8

2.1 Flotation process parameters 8

2.1.1 Flotation kinetics and wettability 8

2.1.2 Air bubbles and particle sizes 12

2.2 Flotation cell and circuits 15

2.3 Sampling methods for large flotation cells 18

2.4 Methods for measuring hydrophobicity 23

3 MATERIALS AND METHODS 26

3.1 Flotation plant 26

3.2 Conceptual design of the Sampling procedure 28

3.3 Material characterization 32

3.3.1 Physical parameters, surface area and particle size .. 32

3.3.2 Wettability 32

3.3.3 Assays 34

3.3.4 Sampling procedures 35

4 RESULTS 37

4.1 Spatial analysis of full scale flotation processes 37

4.1.1 Rougher and scavenger cells 37

4.1.2 Cleaner cells 43

4.2 Practical implications from the sampling procedure 49

4.3 Hydrophobicity measurements..... 51
4.3.1 Evaluation of DVS method 51
4.3.2 DVS measurements for rougher cell samples 54
4.3.3 Concept development for using DVS in production 57
5 SUMMARY OF MAIN FINDINGS 59
6 CONCLUDING REMARKS..... 60
7 SUGGESTED FUTURE WORK..... 63
8 REFERENCES..... 66

1 INTRODUCTION

1.1 RESEARCH BACKGROUND

Froth flotation is one of the most cost-efficient unit operations in mineral processing when it comes to selective separation of certain mineral species. As many of the easily accessible, high quality deposits around the world have been mined out, the typical ore grades are getting lower. While ore grades are decreasing, the enhanced utilization and optimization of flotation becomes even more important, thereby presenting new challenges to flotation plant operators.

Lower ore grades can cause inefficiencies in the flotation process, which result in reduced recovery and grades of the target minerals. If for instance the Boliden concentrator of the Aitik mine, north of Sweden, which has a typical feed grade of 0.3% Cu, has to process a feed with a grade decreased down to 0.2% Cu, the plant needs to process at least 50% more feed to yield the same amount of concentrate tons.

To deal with the lower feed grades, mine operators therefore often try to compensate with a higher throughput in order to maintain the metal value production. A higher throughput decreases the residence time in the flotation process, leading to the trend towards larger flotation cells, which allows keeping the investment and operating costs down even though the water consumption and the necessary tailings treatment costs increase.

When a flotation bank is replaced by newer tank cells it becomes even more important to integrate good instrumentation into the flotation circuit as each cell has to produce at top level to maintain an optimum output. This is also a reason why it becomes difficult to compare an old plant with its newer counterparts.

When designing plants with higher tonnage today, the cell size is often chosen to be between 300 to 600 m^3, depending on the desired

throughput. Larger cell diameters tend to require a more turbulent flow inside the cell to keep the slurry in suspension, which also makes it more difficult to simulate the hydrodynamics. A higher tank cell increases the hydrostatic pressure at the bottom of the cell where the bubble-particle attachment shall take place. Today, more attention is paid on kinetic models, lip length loading and froth carrying capacity.

The development and implementation of larger flotation cells has proceeded very fast. In a period of just 30 years of time, the cell size has increased from below 100 m^3 to over 600 m^3. Figure 1 depicts the size of flotation cells over time.

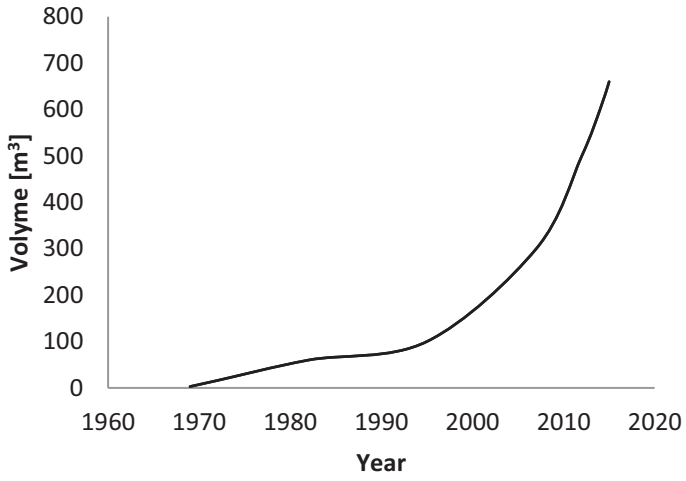

Figure 1. Flotation cell size development throughout the years (Outotec, 2012)

When looking forward, in a Boliden perspective, with regard to constructing new concentrator plants, there is a need to know how to implement the most low cost flotation circuit with retained or improved results. The number of flotation cells needed in order to optimize the flotation recovery and the cell dimensions, like the flotation cell height, are factors that affect the costs and the foot print of the building, as the height of the building has to be twice the flotation cell height (to be able to lift up the agitator during maintenance stops) plus the overhead crane.

Observation at Boliden have indicated segregation effects, particularly inside larger cells and from Boliden's point of view, a topic of discussion has been if it is necessary to have such high cells. From a process view, it is also of relevance to understand how the minerals of interest are moving and distributed inside the cell, depending on its height.

1.2 OBJECTIVES AND SCOPE OF THE WORK

Boliden AB has a long history of building flotation plants, with the first flotation banks being installed in 1934 with the largest cell size of 1 m^3. Many flotation bank and cell designs later, Boliden has, during the last decade, built two new flotation plants, one at the Aitik and one at the Garpenberg mine. The new concentrator in Aitik is a particularly good example of cost-efficient production planning, where a low grade ore deposit could be successfully put into production, the cut-off grade could be reduced and the mineral reserve and life length of the mine could be significantly prolonged as a result of the increased plant throughput.

As a consequence of increased production and larger cell sizes, however, adverse effects, such as segregation in the cells, have also been observed. Under which conditions this segregation occurred and whether it has potential negative or positive effects on the process, is not well known. Even though segregation may be caused by sub-optimal cell design, little scientific work has been devoted to understanding the optimal size, aspect ratio and design of industrial-scale flotation cells.

This work aims at increasing the understanding of the material distribution in large-scale flotation cells and provide input for flotation circuit design. The tasks of the thesis therefore involved investigating the spatial distribution of materials in large flotation cells, both in terms of the distribution of various phases as well as individual minerals. The spatial distribution has also been described in terms of the surface

properties of the mineral particles (i.e. their degree of hydrophobicity), which has not been done before at the same level of detail as in this work.

Research tasks

The work involved a plant-scale sampling campaign in Aitik, where samples were taken from different positions in existing large flotation cells and evaluated with the intention to describe the material distribution inside the cell:

One research task addressed was to investigate different sampling techniques which would enable accurate and representative characterization of the different phases in terms of grade, slurry density and the hydrophobicity. This all together should be of use for describing the spatial distribution inside the cells.

A second research task was to investigate mineral grades in the froth in rougher, scavenger and cleaner cells, which may also give input for enhanced understanding of froth transport mechanisms.

Due to the low reproducibility and inherent problems with standard surface characterization methods used in industry, a third task was to identify whether there are any new or alternative methods for a more accurate description of such properties, particularly hydrophobicity. A measurement of the surface wettability on particles at different phases in a flotation cell will contribute to the knowledge of the distribution of hydrophobic material in flotation cells.

2 FLOTATION THEORY AND ANALYSIS

2.1 FLOTATION PROCESS PARAMETERS

2.1.1 Flotation kinetics and wettability

Froth flotation is one of the most important unit operations in mineral processing. It is based on different surface properties of materials, i.e. differences in their hydrophobicity, which can be utilized for physico-chemical selective separation most often with air as the carrying gas. Hydrophobicity on mineral surfaces is often controlled by using chemical surfactants which are monitored to attach on wanted minerals.

In mechanical flotation cells, the air addition is done through the shaft of the agitator and via the force of the impeller speed, smaller air bubbles are formed after collision against the stators. The smaller air bubbles attach to the hydrophobic particles on their way up through the cell to the surface where a froth will carry them to the launder as a concentrate. A schematic picture of such a flotation cell can be seen in Figure 2.

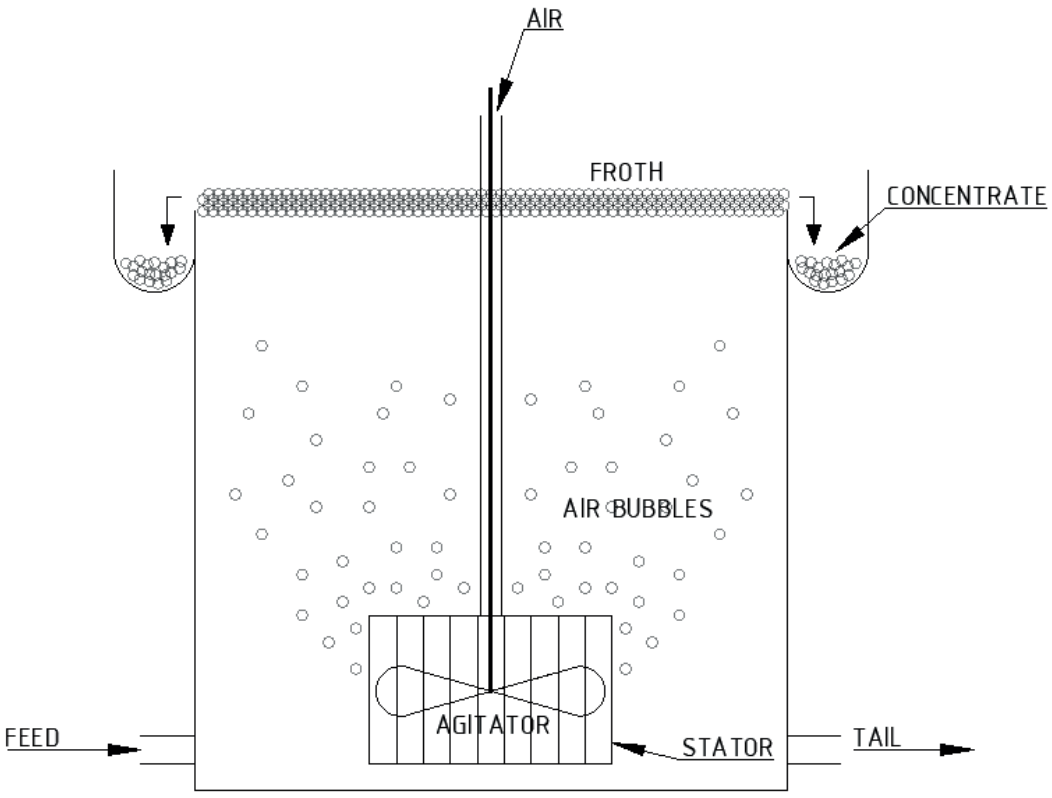

Figure 2. Schematic picture of a flotation cell

The flotation process is conducted in a three-phase system where mechanical, physical and chemical aspects can affect the flotation result such as grade and recovery. The sub processes and parameters affecting the flotation performance are many. Figure 3 lists the most common parameters (Hay, 2018).

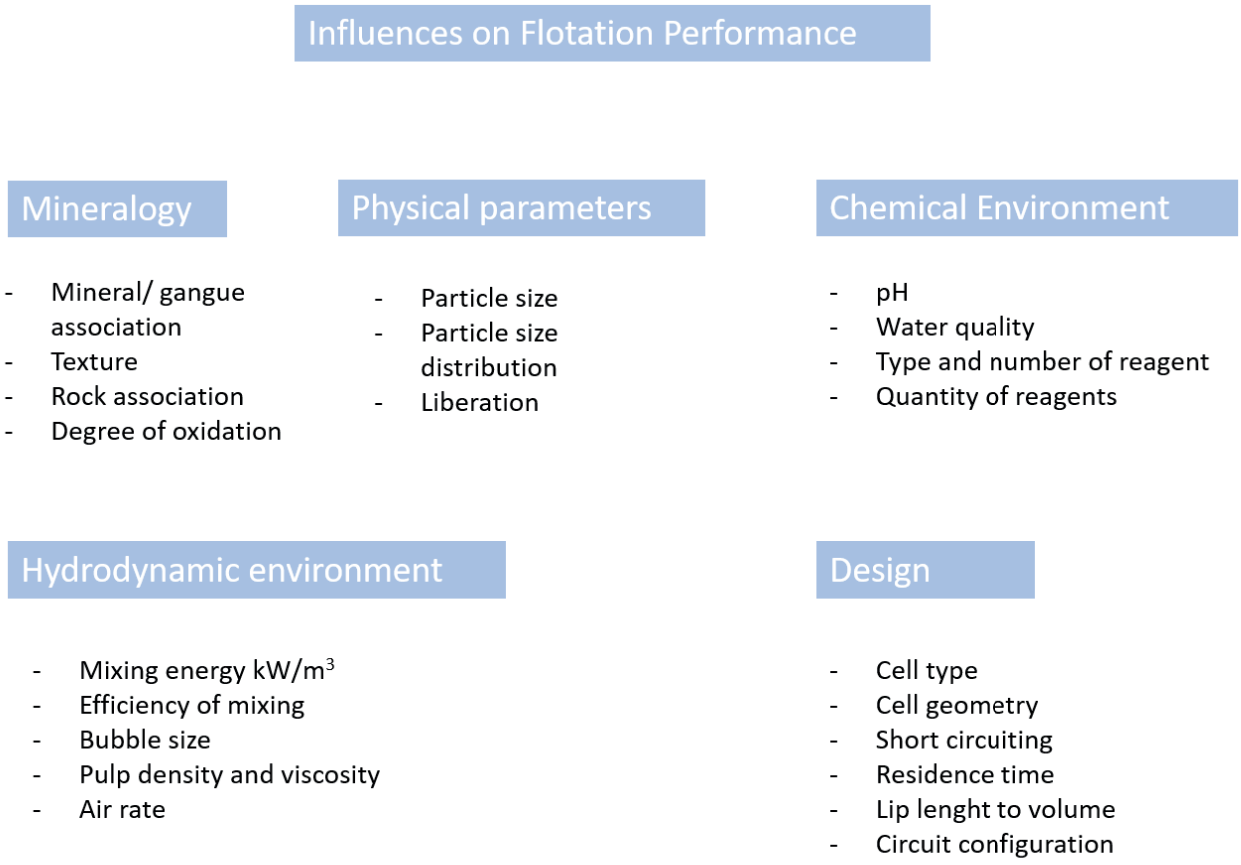

Figure 3: Influences on flotation performance

In order to study the various mechanisms occurring in these sub processes, several directions of flotation research have evolved. A way forward has been to establish ratios between several parameters, like for instance the bubble surface area flux which includes the bubble size, gas hold-up and superficial gas velocity. Describing the flotation system by the process kinetics is another way of combining the parameters. The flotation kinetics are describing how fast mineral particles will float and when the different mineral species are floating. This depends on the cell

configuration, aeration, mineralogy, particle size, liberation, chemical environment and hydrodynamics like the slurry movements inside the cell.

There are several approaches to describing the kinetics by a formula that can be found in the literature (Mavros, 1991; Xiangning et al., 2017).

The first order model, which has also been used for scale up of flotation systems, is given in equation 1 (Amini et al., 2016).

$$R = R_{\infty}(1 - e^{-Kt}) \quad (1)$$

where K is the average flotation rate constant and R is the recovery and R_{∞} is the maximal theoretical recovery. Using two or three material fractions, which incorporates two or three rate terms, usually gives a better model fitting. The corresponding model equations are given by equation 2 and 3 where separate kinetic constants are used for slow floating (s), fast floating (f) and non-floating (n) particles together with their mass fractions.

$$R = (1 - \emptyset)\left(1 - e^{-K_f t}\right) + \emptyset(1 - e^{-K_s t}) \quad (2)$$

$$R = \emptyset_f\left(1 - e^{-K_f t}\right) + \emptyset_s(1 - e^{-K_s t}) + \emptyset_n(1 - e^{-K_n t}) \quad (3)$$

where R is the recovery at time t, ø: Fraction (%) of material (fast floating f, slow floating s, non-floating n). K_s is the kinetic constant of the slow floating material, K_f is the kinetic constant of the fast floating and K_n is the kinetic constant of the non-floating material

The physical meaning of kinetics for plant design can for instance be, that if there is a slow floating gangue mineral in the feed, the residence time should be kept short. Depending on how easily the gangue mineral is separated from the valuable minerals in the cleaning step, the number of scavenger cells should be determined (Hay, 2005).

From the chemistry viewpoint, interest has been devoted for instance towards the selection or tailoring of collectors, frothers and other reagents

that influence the surface properties of particles, froth stability, etc. (Kawatra, 2011; Nagaraj and Farinato, 2016).

The collectors are typically amphiphilic molecules with polar and non-polar end groups. Under the right conditions, the polar ends of the collector molecules can selectively adsorb to the surface of certain minerals, thus leaving them with a surface more or less covered with non-polar molecular tails. This renders these mineral particles more hydrophobic compared to mineral particles where no collector molecules have attached. These differences in hydrophobicity between the different minerals forms the basis of the flotation process. The choice of collector reagent, together with the chemical conditions in the pulp, affects the degree of floatability of selected minerals (Wills, 1997).

To be able to predict the floatability of a certain mineral, it is of interest to measure its degree of hydrophobicity or wettability. To be able to measure the forces of the mineral surfaces several methods have been developed. One way of characterizing the wettability of surfaces is to measure the contact angle, θ, which is defined as the intersection of the liquid-solid and liquid-gas interface for a liquid drop on top of a flat surface of a material or as an air bubble added on a flat surface in a liquid solution, see Figure 4. At equilibrium the surface energies between solid and air ($\gamma_{s/a}$), water and air ($\gamma_{w/a}$) and solid and water ($\gamma_{s/w}$) can be described by the Young equation (4).

$$\gamma_{s/a} = \gamma_{s/w} + \gamma_{w/a} cos\theta \quad (4)$$

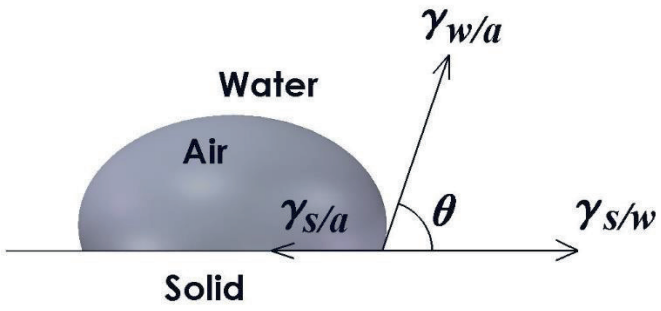

Figure 4. Profile of an air bubble on a flat solid surface in water. The contact angle, θ, formed between the solid surface and an air bubble

The contact angle can be measured either by applying a droplet on a flat surface of a mineral (sessile drop method) or as a capillary method. These are further described in section 2.4.

2.1.2 Air bubbles and particle sizes

The agitator has to disperse the air addition against the stator in order to create smaller air bubbles with a certain velocity to allow for bubble-particle collisions. There has to be a balance between the micro-turbulence and macro-scale laminar flow velocities to increase the recovery by sizes. The bubble-particle aggregates rise by buoyancy towards the froth zone (Wills, 1997).

The air bubble attachment to the mineral particles is an essential process needed to float the particles in conventional flotation cells. It requires the right tip speed of the impeller and the right air addition to create an environment where the mineral particles get the chance to attach to the air bubble. A batch laboratory flotation cell can be regarded as a perfect mixer where particles get many chances to attach to the air bubble. In a full-scale, continuous cell, there is a bottom inlet and bottom outlet where the material can by-pass the cell (short circuiting). This means that for some particles there is only a low probability to get attached per cell in a series, which is the reason why at least five cells in a row are

recommended to mitigate the risk of short circuiting. Another way of by-passing is if the bubbles formed are too small, usually less than 0.8 mm. Then the bubbles can follow the fluid flow and even go with the tailings. Conventional flotation tank cells usually produce air bubbles between 0.5 and 2 mm (Gorain et al., 1997; Miettinen et al., 2010). Smaller bubbles may float smaller particles but they also have a longer rising time in the tank, which increases the flotation time and the overall bubble residence time. Smaller bubbles also have a tendency to float more entrainments, probably due to the larger amount of water in the froth phase and the entrainments are following the water recovery (Schwarz and Grano, 2005; Trahar and Warren, 1976). The movement of gas dispersion in the flotation cells is usually described by the bubble surface area flux, S_b, (Finch and Dobby, 1990; Gorain et al., 1997). The bubble surface area flux is the rate at which the bubble surface area moves through the flotation cell per unit of cell area. The value can be calculated using equation 5, by measuring the superficial gas velocity (J_g) and the mean bubble size (d_b)

$$S_b = \frac{6J_g}{d_b} \tag{5}$$

The superficial gas velocity represents the velocity at which gas moves upwards in a flotation cell. The factor has been identified to have a direct effect on the flotation kinetics of both wanted minerals but also entrainments of gangue minerals (Ahmed and Jameson, 1989).

The effect of gas dispersion is often described in relation to the first order rate constant and can be defined as equation 6 (Gorain et al., 1999).

$$K = P \cdot R_f \cdot S_b \tag{6}$$

where K stands for the first order rate constant, R_f is the froth recovery and S_b stands for the bubble surface area flux. P stands for the floatability component, a dimensionless parameter that represents the ability of a certain mineral to float and is determined by fitting the equation to the test results (Ata, 2012).

The bubble surface area flux can also be expressed by comparing several data sets from different base metal flotation plants with the formula presented in equation 7 (Gorain et al., 1999).

$$S_b = 123 J_g^{0.75} N_s^{0.44} A_s^{-0.10} P_{80}^{-0.42} \quad (7)$$

where J_g is the superficial gas velocity (m/s), N_s is the impeller tip speed (m/s), A_s is the impeller aspect ratio (dimensionless) and P_{80} is the particle size where 80 % of material is finer.

How the physical parameters, e.g. the particle size distribution for different minerals and grade of liberation, affect the flotation recovery has been investigated during many decades. Today, it is well known that the optimal flotation recovery is achieved for particles between around 20-100 μm, depending on the mineral system and the flotation circuit (Gaudin et al., 1942; Lynch et al., 1981; King, 2012; Klimpel and Hansen, 1988). Smaller particles have lower flotation velocity/ kinetics due to lower collision efficiency with conventional flotation bubbles with a given size and velocity (Trahar and Warren, 1976; Miettinen et al., 2010). Losses in the coarser size range are typically attributed to non-liberated particles but also because of turbulences, buoyancy constraints combined with lower stabilities in the froth phase which may cause drop back (Van Deventer et al., 2002; Kohmuench et al., 2018). Coarser particles tend to float further down in the flotation banks and may need more reagents (Bazin and Proulx, 2001).

In an operational plant, there is the need for keeping control of the recovery by size to determine the losses in each size classes and analyze the reason. This can be presented as a so called “elephant curve” (Kohmuench et al., 2018). An example is given in Figure 5 showing production data from Boliden Aitik.

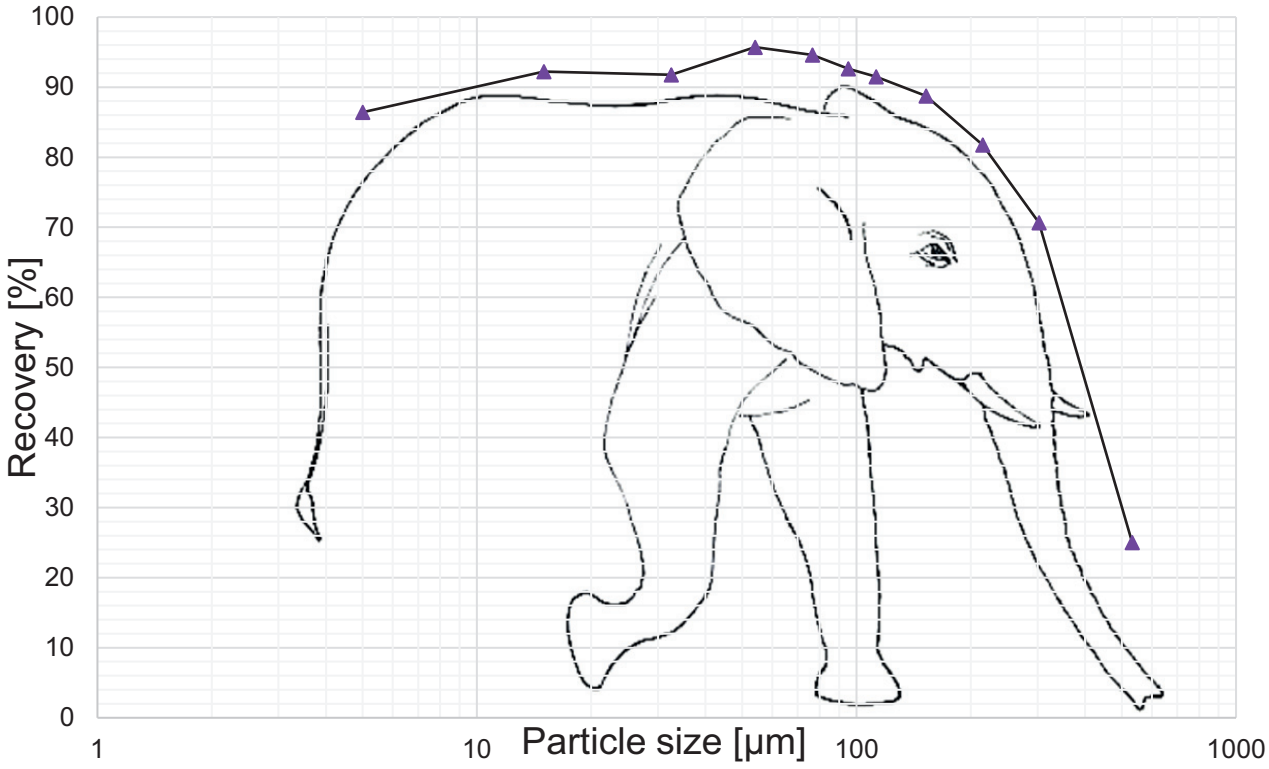

Figure 5. Particle size vs. recovery at Aitik concentrator (Adam Isaksson, Aitik mine)

The particle size is determined by the grinding circuit, i.e. recovery losses in the flotation circuit should be investigated by first looking at the grinding circuit. A monthly fractional analysis of the flotation feed is a good way to understand the flotation process and optimize the recovery. There is always an economical balance between grade and recovery which is plant specific and may even vary depending on metal prices.

2.2 FLOTATION CELL AND CIRCUITS

How to design a flotation circuit depends on the purpose. As an example, the process description for a traditional base metal flotation circuit, with rougher, scavenger and cleaning steps, is given in the following.

The flotation reagents are added before the first flotation step which is the *rougher flotation*. The most fast floating minerals enters the froth phase in the rougher flotation cells and the froth concentrate has its highest grade

in the first cell. Thereafter, it is decreasing further on in the flotation bank (Hay, 2005). Flotation reagents are in general added stage-wise along the flotation bank.

The tailings from the rougher bank are continuously floated in the *scavenger flotation* bank where a relatively low grade concentrate is captured. This product can either be sent back to the feed to the roughers or to a first *cleaning step*.

The purpose of the cleaning cells is to depress entrainments and increase the grade of the final concentrate. If the cleaning stage consists of more than one bank, the froth from the first cleaner bank is pumped to the next cleaner and so forth. The tailing from each cleaner cell is typically sent back one step. The rougher flotation concentrate is quite often sent further on in the cleaning step due to its higher grade, compared to the scavenger concentrate. An example and simplified flotation flow sheet is presented in Figure 6.

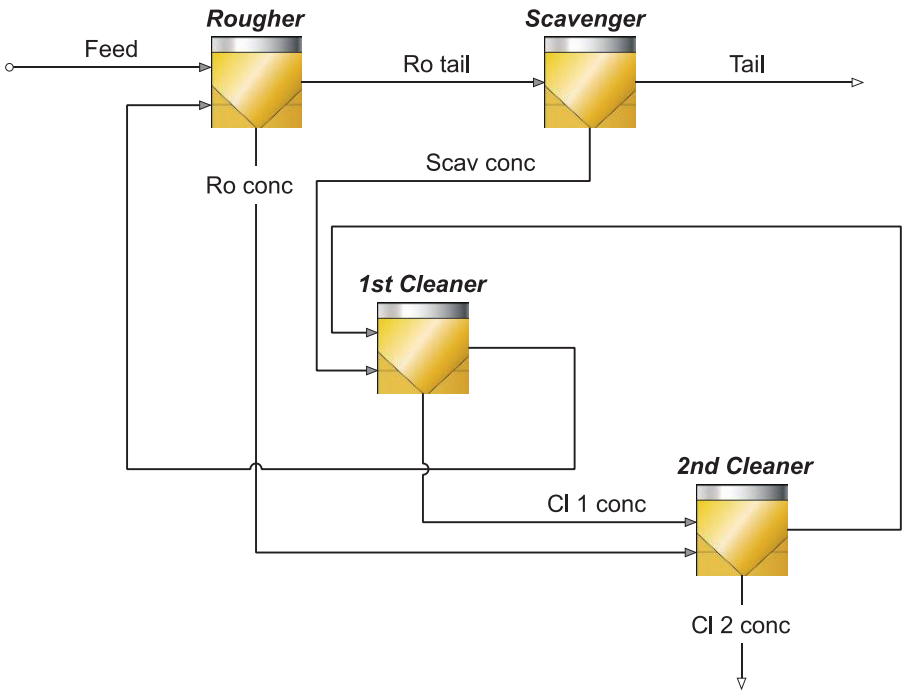

Figure 6. Example of a simplified flowsheet with direct flotation

In some cases a regrinding mill is used before the cleaning circuit to increase the degree of liberation or refresh the mineral surfaces which also can increase the separation process efficiency (Wills, 1997).

The capacity in a flotation plant is most often defined by the grinding capacity, which is the most cost intensive part of the plant and should act as the bottleneck in the system. In order to not let the flotation circuit be a limitation, flexibility in the flotation circuit should be installed to handle variation in grade and tonnage or mechanical failure of single cells.

The increase in cell size has changed the hydrodynamic effects in the cells, such as dispersion and mixing efficiency and bubble-particle collision rates. This has led to more research on systematically investigating the material distribution in different regions within the pulp and in the froth layer (Tabosa et al., 2016; Van der Westhuizen and Deglon, 2007; Zhu et al., 2013; Panire et al., 2015). Computational Fluid Dynamics (CFD) and other modeling approaches have been used for simulation in order to optimize the process (Koh and Schwarz, 2006; Shi et al., 2015; Chegeni et al., 2015; Dube et al., 2015; Amini et al., 2016).

Compared to a lab flotation cell, which is assumed to be a perfect mixer, the mechanical flotation tank cell can be subdivided into three process zones; the *mixing zone* at the bottom of the cell, the *quiescent zone* in the middle part where the turbulence is lower and finally, the *froth zone* on top of the cell.

The trend towards larger cell sizes is restricted by the limitation with respect to keeping the slurry in suspension and preventing the cell from silting up. Usually, the up-scaled flotation cells have the same or similar aspect ratio as its smaller counterparts.

This implies that the volume increases with a factor three while the cross sectional area increases with a factor two. The residence time is related to the flotation process by the volume and the froth removal is related to the

surface area. When the flotation cell increases in size, the concentrate flow rate does not increase proportionally to the volume. However, larger cell sizes are usually used to float lower grade ores where it is a benefit of larger volume per surface area. This is due to fewer particles that can form a froth layer which requires less surface area (Farrokhpay, S., 2011; Norori-McCormac et. al., 2017). For the largest cell sizes installed, internal launders are often used to decrease the surface area and also to increase the lip-length and shorten the transportation distance of the froth to the launders.

When scaling up to larger flotation cells the cell height increases and the hydrostatic pressure at the bottom of the cell increases which affects the air bubbles.

The hydrostatic pressure at the impeller level of a tank cell can be calculated by equation 8.

$$p = p_0 + \rho_p \cdot g \cdot h \tag{8}$$

where p_0 is the atmospheric pressure and the ratio between the pressure at impeller depth and at the surface depends on the pulp density and the height of the cell.

The increased pressure in the larger cells has resulted in research on enhanced agitator design to keep the slurry in suspension and provide the cell with air through the agitator shaft (Dube et al., 2015).

2.3 SAMPLING METHODS FOR LARGE FLOTATION CELLS

A literature survey has been conducted on how to sample inside the flotation cells to obtain the relevant information while avoiding disturbance of the surroundings.

The flotation cell is a three-phase system that is strongly affected by the mixing energy and rising bubbles. For sampling at different levels in a

tank cell the aim is not to disturb the surroundings with the sampler in order to collect a representative sample. Depending on the purpose of the sample and which parameters are of interest to investigate, there are some techniques available.

If the purpose is to grab a slurry sample from any height in a cell, the simplest way is to use a peristaltic pump connected to a pipe. The flow rate in the pipe has to be high enough to prevent sedimentation causing non-representative samples. At least it is important to be aware of the risk.

The gas-hold up concept is a description of the proportion of air relative to the slurry at a specific volume. It is affected by changes in bubble size, the slurry velocity at the specific location and the turbulence (Prakash et al., 2018). Measuring the gas hold-up can be done in several ways. One way is to utilize the pressure difference between two pressure sensors in the cell (Finch and Dobby, 1990; Tang and Heindel, 2006). Another way is to measure the electrical conductivity between two conductivity cells, one with a known amount of dielectrical material and the other the unknown pulp-gas dispersion (Pérez-Garibay and De Villar, 1998).

If the system allows for comparison of the cell level before and after aeration the difference is the gas-hold up which than can be measured. A capture method is also possible where a slurry sample consisting of both pulp and air is collected.

If the idea is to have a sampler that does not affect the air and pulp flow in order to collect a representative sample, it´s closing mechanism should be quick and the container needs to be sealed tight so that the air or slurry is not leaking out. Since the container volume is known the air content can be calculated.

There are some different samplers available for this purpose. The JK Gas hold-up probe is a 1 liter vertical cylinder with pinch valves on each side

to be opened and closed by air pressure. It is designed to have a straight through flow for the slurry and air. It is lowered down to the desired position in the cells where it will be opened and closed. The sampler is then lifted out of the flotation cell and the content is moved to a bucket, see Figure 7. The difference between the slurry volume and the probe volume is the gas hold-up.

Figure 7. JK Gas hold-up probe

As a complement to the JK gas hold-up probe Boliden has manufactured a similar sampler named the Widmatic sampler. The sampler is using a similar principle as the JK Gas hold-up probe but has a wider cross sectional area and a shorter length. The Widmatic sampler has a capacity to sample one liter of pulp. In opened position the lids are at the side of the tube to have a straight through flow. The sampler can be placed horizontally or vertically and is maneuvered by compressed air. It takes less than 1 second to close the sampler. A schematic picture of the Widmatic sampler is given in Figure 8.

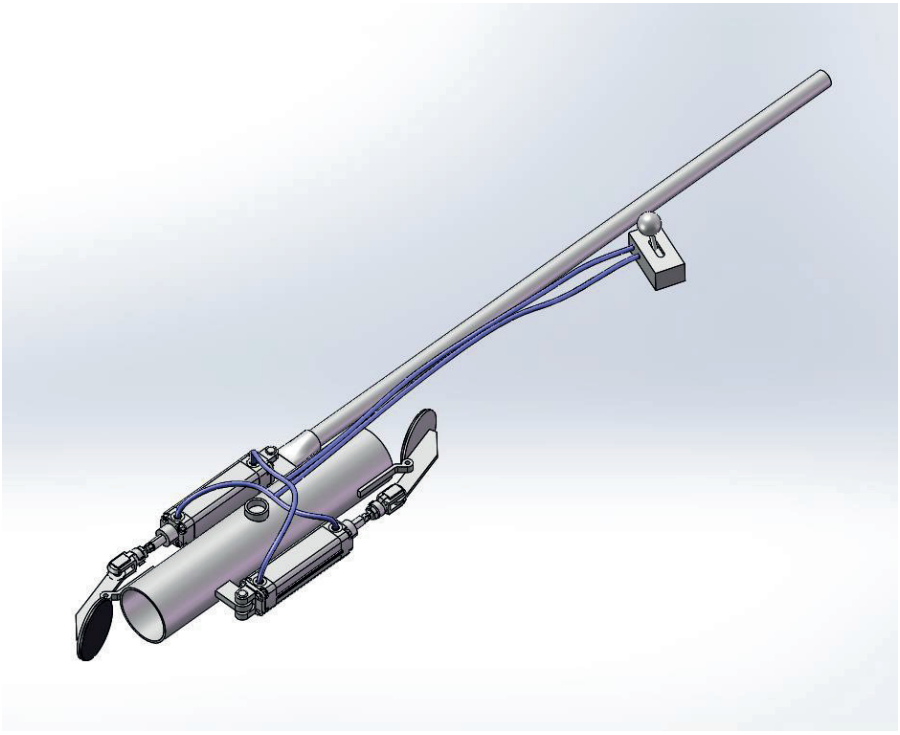

Figure 8. Boliden Widmatic sampler

Another technique for measuring the gas hold-up is using a cylinder attached to a central rod as shown in Figure 9. The upper and lower plunger have O-rings to tighten the seal around the cylinder in closed position. Both, mechanical and pneumatic driven samplers have been used. (Yianatos et al., 2001; Gorain et al., 1995; Vinnett et al., 2016). As for the JK Gas hold-up probe, the cylinder volume is known so that the gas hold-up can be calculated.

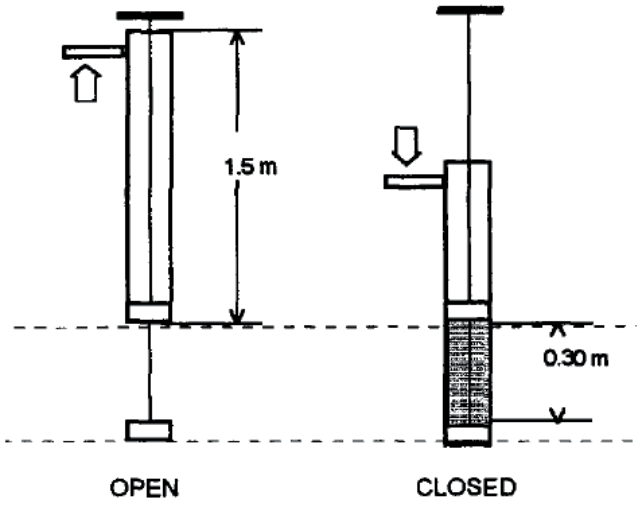

Figure 9. Local gas hold-up measurement (Yianatos et al., 2001)

Heath & Sherwood (H&S) has developed a fully mechanical sampler where the bottom and top have lids attached to a mechanism inside the container, even though this could probably disturb the straight through flow, see Figure 10.

Figure 10. H&S sampler

Sampling the froth on top of the cell has usually been done with a simple cup lowered down until the froth has started to pour into the cup (Yianatos et al., 2016), compare Figure 11.

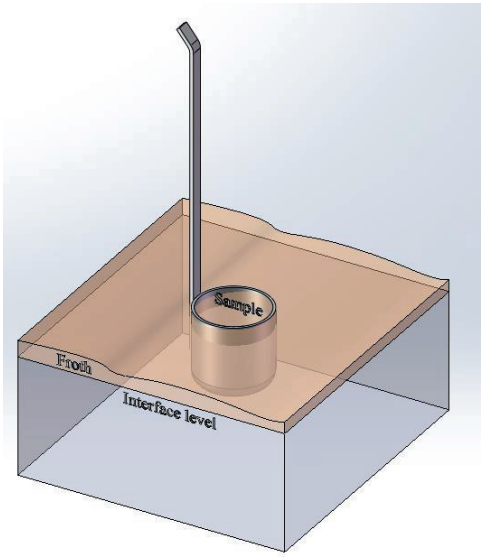

Figure 11. Sampling cup for top of froth sample

Other typical parameters to measure are the bubble size, the air velocity and drop back (Rahman et al., 2013; Falutsu and Dobby, 1989; Besagni and Inzoli, 2016; Prakash et al., 2018).

2.4 METHODS FOR MEASURING HYDROPHOBICITY

The understanding of particle surface properties is essential for the flotation process and evaluation of froth flotation phenomena, particularly in the investigation of various chemicals including collector effects. Even though the wettability is of huge interest for the flotation process, it is not as yet used as a measurement technique on a daily basis at any of Boliden's concentrators.

The traditional way of measuring the wettability is by the contact angle as shown in figure 4. In the most typical setups, it can be measured either by applying a droplet on a flat surface of a mineral (sessile drop method) or as a capillary method.

The sessile drop method requires a flat surface where a droplet of liquid is applied and the contact angle is measured by drawing a tangent to the drop profile using image analysis. The capillary rise test is performed on

a compacted powder and measures liquid absorption by monitoring weight increase or capillary pressure (Nowak et al., 2013; Akdemir, 1997; Qiu et al., 2004; Chau, 2009; Iveson et al., 2004).

The sessile drop method suffers from serious drawbacks, e.g. the direct contact angle measurement must be made on a large, reasonably flat and preferably non-permeable surface. This is not possible on a mineral sample consisting of small particles taken directly from a flotation process. The capillary methods, e.g. Washburn capillary rise, on the other hand are sensitive to particle properties, such as size and shape distributions and heterogeneities in the surface properties. In addition, this method requires the use of packed mineral powders samples where the packing procedure has been shown to affect the reproducibility (Susana et al., 2012; Teipel and Mikonsaari, 2004).

The Washburn measurement utilizes equation 9 to calculate the contact angle.

$$w^2 = kt\frac{\rho^2\gamma_{LG}cos\theta}{\eta} \quad (9)$$

where w is the weight of the liquid that is taken up by the sample, γ_{LG}, ϱ and η are the surface tension, density and viscosity of the liquid, respectively, θ is the contact angle, k is a material constant and t is the time required for the penetration.

The Washburn technique requires two measurements with identical samples and packing procedure. From the first measurement the sample specific constant can be calculated by using an optimally wetting liquid e.g. n-hexane. Under the assumption of complete wetting, the contact angle θ is 0 ($\cos\theta=1$) and the capillary constant can be calculated. The second measurement is made with Milli Q-water and the contact angle can be calculated using equation 4 and the specific constant. The sample amount needed for one measurement is volume specific, as it has to cover

1 cm height of the measuring tube. Depending on the sample density it requires between 1 and 3 g.

In the case of conducting measurements on industrial ore samples, not pure minerals, the mixture of hydrophilic and hydrophobic particles could affect the velocity of the rising liquid inside the capillaries, as well as the pore filling degree. The resulting contact angle will therefore represent some form of average value of the minerals contained in the sample. The selection of liquids has also been shown to have an effect on the results (Teipel and Mikonsaari, 2004; Kirdponpattara et al., 2013).

The Dynamic Vapor Sorption (DVS) technique, or sometimes referred to as the Gravimetric Vapor Sorption (GVS), is an analytical method used for characterization of fine powder materials. The adsorption of water (or solvent) on the particles, is measured as a function of the relative humidity (or the solvent partial pressure) at a constant temperature. In the pharmaceutical industry this technique has been used for a long time, to measure the moisture sensitivity of active pharmaceutical ingredients (Buckton and Darcy, 1995; Heng and Williams, 2011), but no work has been reported regarding applications of the method in mineral processing.

A DVS-instrument is basically a very sensitive balance with a sample cup and an empty reference cup, which are both flushed with an extremely well controlled moisture gas stream. The balance can operate at a constant temperature between 5 and 60 °C, with a sample size between 1– 150 mg with a sensitivity of 0.1 μg and, if water is used, with a relative humidity between 0- 98 % and an accuracy of ±0.5 %. The sample is weighed into a weighing pan and its weight is monitored while the sample is exposed to different relative humidities (%RH).

One measurement is divided into two equal cycles, where the relative humidity is increased stepwise from 0 up to 95% RH and down to 0 again.

The sample is first dried with dry nitrogen gas for 1 hour before the 1st cycle and the same before the 2nd cycle. In both sorption/desorption cycles, at each step, the sample was kept at the set relative humidity until the change in mass was less than 0.002% over a period of 5 minutes.

The DVS does not give the contact angle, which is the common established unit for characterizing wettability in mineral processing. Instead, it is a measure of the sample's ability to adsorb moisture, which hydrophilic materials do, and returns a mass percent difference at 95% relative humidity. The method is affected by particle size since smaller particles have a larger specific surface, which can adsorb more moisture and for a mixture of minerals it will also return an average of moisture uptake.

3 MATERIALS AND METHODS

3.1 FLOTATION PLANT

The sampling campaigns were carried out at the Aitik concentrator, Boliden´s largest copper mine with an annually production of 39 million tons per year. The plant is located in Northern Sweden, 20 km east of Gällivare. A new plant was built and commissioned in 2010. The flotation plant is equipped with a with a parallel rougher flotation circuit in two lines using 160 m^3 cells, each line with four rougher cells, five scavengers and four auxiliary cells for pyrite flotation. The 160 m^3 cells are supplied with Outotec's FloatForce® 1500 agitator and with external launders.

The cleaner circuit consists of four consecutive cleaner banks that handle the froth from the two rougher/ scavenger lines. The first cleaner stage floats the scavenger froth in 50 m^2 Outotec TankCell®. The second, third and fourth cleaner stage are 40 m^2 Outotec TankCell®. The rougher concentrates from both lines are pumped to a pebble mill for re-grinding and classification via hydrocyclones. The cyclone overflow is sent to the

cleaner stage 2. The scavenger concentrate from both lines is pumped to a separate pebble mill for re-grinding and classification via hydrocyclones. The cyclone overflow is sent to the cleaner stage 1. The flowsheet is shown in Figure 12.

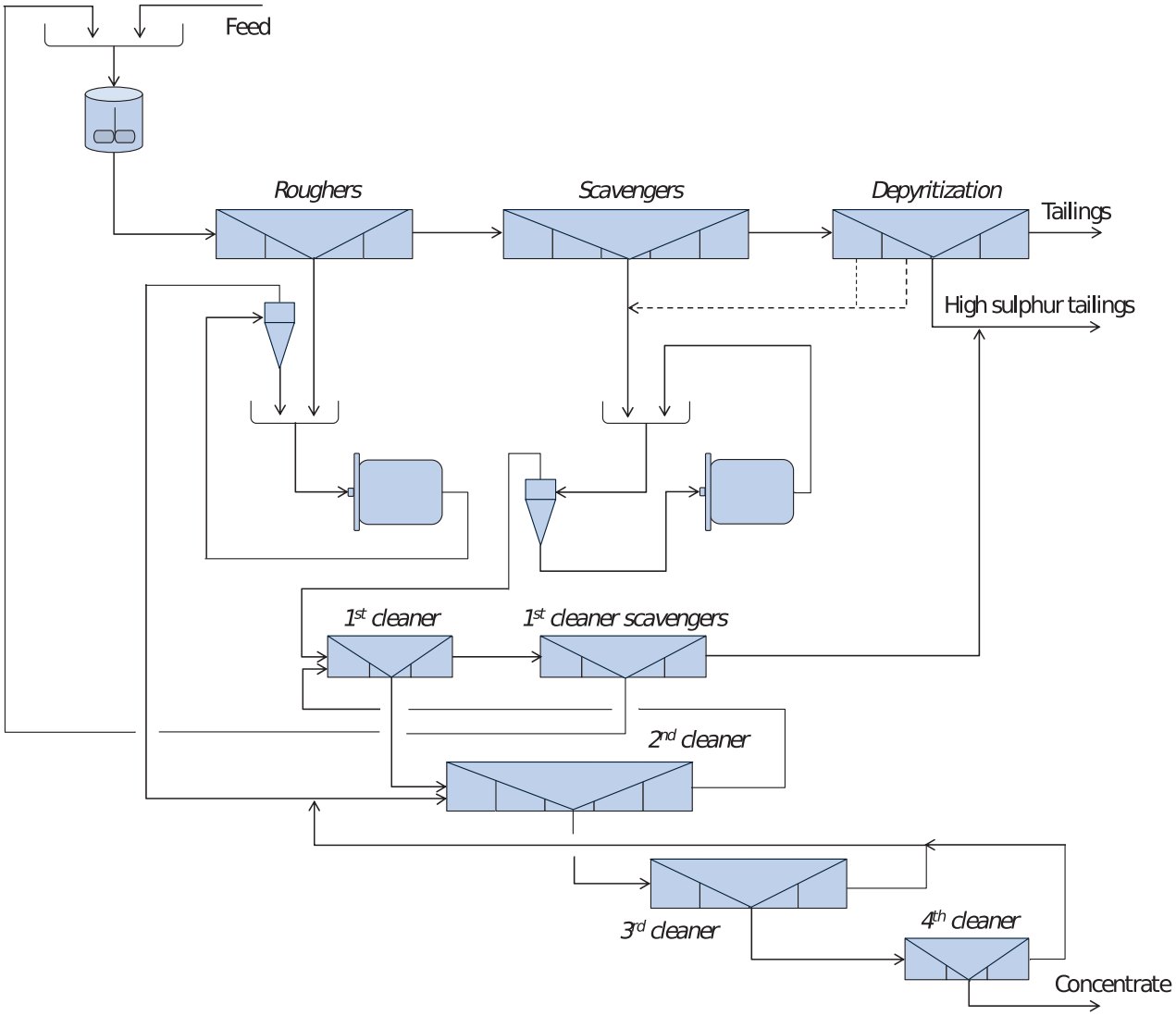

Figure 12. Flowsheet of Aitik flotation circuit

The sampling campaign was conducted in April 2015. At the day of the sampling, the feed grade was 0.14 % Cu, which is lower than the average 0.2 % Cu. The flotation feed contained 44 wt.% of solids. Some relevant process data from the plant are summarized in Table 1. The only collector reagent used in the rougher/ scavenger is PAX (potassium amyl xanthate).

Table 1. Process data from the flotation cells in April 2015

Cell number	Conditioning tank	2	4	5	6	8	9
Air addition [m3/h]		11	10.7	10			15
Froth depth [cm]		21	23	35			30
PAX dosage [g/ton]	2	0.8	0.5	-	1	0.5	

Further sampling was conducted in an additional sampling campaign for the 1st cleaner section in February 2015 and the 2nd, 3rd and 4th cleaners in April 2015 (Lappi, 2015).

3.2 CONCEPTUAL DESIGN OF THE SAMPLING PROCEDURE

To investigate the spatial variation inside the Aitik 160 m^3 cells, samples from different levels inside the cells needed to be taken. The investigated areas was first of all to characterize a vertical profile and also, in some extent, to determine fluctuations in the vertical profile at different positions in the flotation cells. The gas hold-up at different position inside the cell was also a benefit if it could be measured. Finally, the froth transportation on top of the cell was decided to be included in the work.

For analyzing the samples were fractional assays of interest to understand in which fraction the valuable minerals is and where in the flotation cell they are located. The ore density and the degree of hydrophobicity is two other measurement that could give information of the vertical profile. Material needed for the analytical program requires at least 100 g of dried material in each sample. The flotation feed contains around 45 wt.% solids and the minimum of sample volume was 2 dl of slurry. In case there was a lower solid density higher up in the cell the final decision was to collect not less than 5 dl of sample.

There are online analyses available for the feed, rougher tailings and scavenger tail while the sampling campaign covered the first and last rougher and first and last scavenger cells of the plant. I.e. the feed and tailing assays would have reference measurements.

At the time of sampling the very first rougher was by-passed due to failure on the motor, i.e. only three rougher cells were in use. Therefore, the second cell was the first cell used in the rougher series at this time and the one sampled.

The flotation cells in Aitik are almost 5 meters deep and high turbulence was expected below 3.5 meters. Measurements done previously had shown that it was difficult to hold a sampler in strict position at the lower positions. The sampling plan was set from the surface down to, if possible, 3.5 meter. The decision was to take samples inside the cells at multiple levels instead of more replicates except for the first rougher where the samples with two different samplers can be seen as a type of replicate. Therefore, samples were taken from a maximum depth of 3.5 meters and up to 0.5 meter from the interface level, in 0.5 m intervals. Complementary samples from 0.3 m under interface level and just under the froth were also taken as well as from the entire froth.

In the first rougher, three sampling positions were prepared for sampling, to compare the radial variations. All the sample positions chosen for this work are presented in Figure 13 where the vertical positions are shown together with the radial positions (A, B and C) and the top of froth sampling positions.

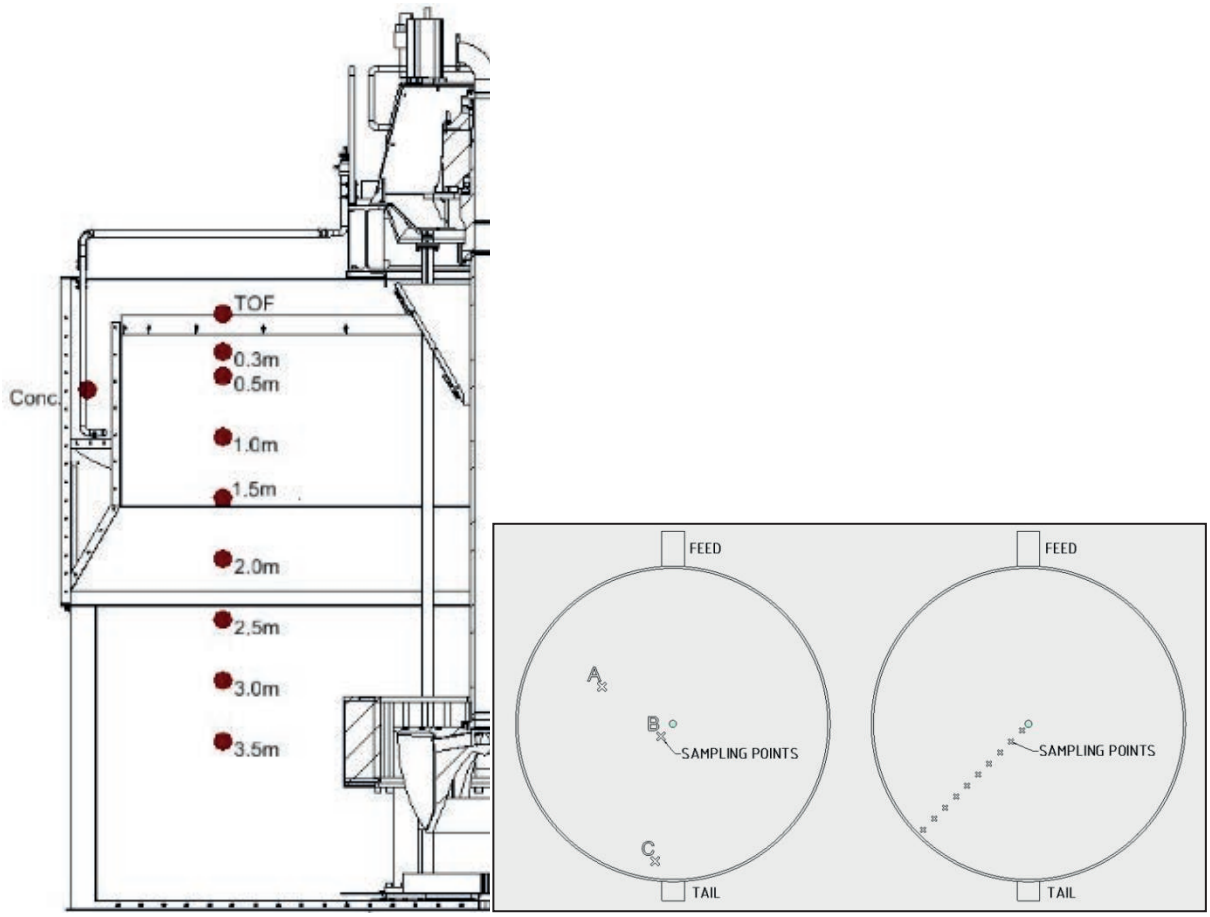

Figure 13. Sampling position in Aitik TC 160 m³ cell (left) and a top view of radial sampling position (middle) and top of froth sampling (right)

The Widmatic sampler was chosen instead of the JK Gas hold-up probe due to the larger cross sectional area and its shorter length. For sampling in 50 centimeter intervals it is a benefit to have a shorter sampler.

Two additional samplers were bought from Heath & Sherwood. One was a 3 dl container (model 5033) for sampling higher up in the cell where the sampling intensity is higher and a smaller sampler container is needed. The other sampler was a 1 liter sampler (model 5105) with a 5 m long rod to be used for the deeper positions and was used to compare the sampling results and sampling procedure with the Widmatic sampler.

For the deeper positions (3.5 - 2.5 m) in the first rougher the Boliden Widmatic sampler was used together with the one liter sampler from Heath and Sherwood (model 5105). For the other cells only the Widmatic sampler was used for these positions. For the positions between 0.5 and

2 m down in the cell the 3 dl sampler from Heath and Sherwood (model 5033) was used. At the highest position (0.3 m) in the cell, the sample were collected in a bottle with a lid that, triggered by a rod, could be opened and closed at a specific depth.

Since the plunged samplers had to pass through the froth phase the outside of the container was rinsed with process water before emptying into a bucket.

It is known that there is transportation of valuable minerals in the froth from the center of the cell out towards the edge of the cell (Zheng et al., 2004). It was, therefore, decided to sample a full radial froth profile, with samples taken in 20 cm increments starting from the center and moving outwards to the edge of the cell.

The froth layer was sampled by a simple cup with an extended handle, lowered down just far enough for the top of froth to pour into the cup. The samples were taken in 20 cm increments starting from the center and moving outwards to the edge of the cell. At the same radial position the middle of the froth was also sampled. A container with a lid was used that was opened and closed at the desired positions.

There are no easily accessible sampling points for feed and tail for the individual cells in the Aitik flotation plant. Those streams were sampled with a peristaltic pump connected to a 6 m long pipe with 12 mm diameter placed as close as possible to the inlet or outlet, respectively. During pumping a high volumetric flow of 10 l/ min was used to prevent sedimentations in the pipe.

The cells were sampled in sequence and all the samples were collected from one cell before the next cell was sampled.

3.3 MATERIAL CHARACTERIZATION

3.3.1 Physical parameters, surface area and particle size

All samples were weighed and analyzed for wt.% of solids before dividing into smaller sample sizes for further analysis.

The density measurements were conducted with a pycnometer, Micrometrics AccuPyc II 1340, with helium as the analysis gas.

Particle size distributions were measured with a Malvern Mastersizer 2000 using a dispersant (Miglyol, RI of 1.449 and an absorption value of 0.05) and with and without ultra-sonication prior to the measurement.

Specific surface area measurements were done according to the BET (Brunauer-Emmett-Teller) method. The BET surface analysis uses nitrogen gas to adsorb on the mineral surfaces at the temperature of liquid nitrogen and the amount of adsorbed gas (i.e. a mono-molecular layer) correlates with the specific surface area of the particles (Brunauer et al. 1938).

3.3.2 Wettability

The wettability measurement by using DVS (Dynamic Vapor Sorption) was conducted at the RISE laboratory of Bioscience and Materials/ Surface, Process and Formulation in Södertälje, Sweden. The instrument used here was a Surface Measurement Systems DVS Advantage instrument to measure the water uptake as a function of the relative humidity at 25.0 C. Two cycles were used with one hour drying with nitrogen before each cycle. The relative humidity was increased stepwise up to 95 %RH (10, 30, 50, 70 and 95 %RH) and then down to 0 %RH again. The sample was now once again dried for 1 hour at 0 %RH, before another identical cycle, the 2nd sorption/desorption cycle, was run. In both sorption/desorption cycles, at each step, the sample was kept at the set relative humidity until the change in mass was less than 0.002% over a

period of 5 minutes. In Figure 14 a schematic picture of the DVD instrument is presented.

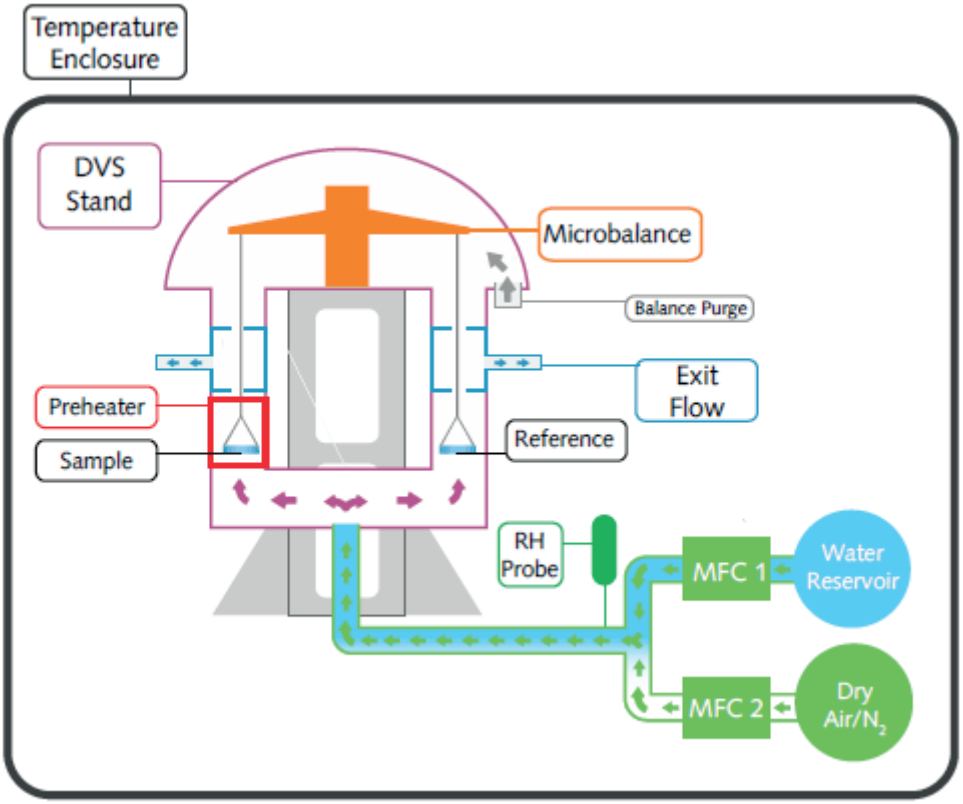

Figure 14. System schematic of DVS instrument (DVS Adventure)

For the evaluation of the DVS technique a comparative study was conducted where DVS and Washburn measurement were carried out on a copper/ lead ore from Garpenberg. The instrument used for Washburn calculations was a Krüss tensiometer K100 (Krüss, 2018).

At least 1 cm height of packed samples has to be used and due to the high bulk density of the lead ore, 3 g of material was used for each test. The material was weighed on a calibrated scale to reach 3 ± 0.01g. The material was packed manually using a piston with a 2 kg weight from the top, also supplied by Krüss. The packing procedure involved manually lowering the piston through the top of the glass tube and slowly letting the piston compress the material, so that the whole weight of the piston was finally placed on top of the sample before it was slowly removed. This procedure was carried out carefully since the packing procedure, as well as the

roughness or pores in the particles, have shown to have an impact on the result (Galet et al., 2010; Kirdponpattara et al., 2013).

Five measurements with n-hexane were carried out on each sample, in a random order, to calculate an average capillary constant for each sample. The mean value from the five capillary constant calculations was used in the equation for contact angle when five measurements with Milli-Q water was conducted. In Figure 15 the Washburn measurement technic is schematic presented.

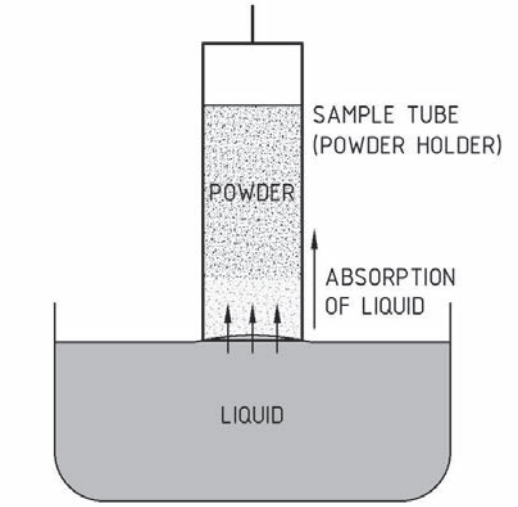

Figure 15. Schematic picture of the Washburn measurement

3.3.3 Assays

All samples were divided into five fractions by sieving and all fractions were analyzed by a table-top ED-XRF (energy dispersive X-ray fluorescence spectrometer). The samples were measured as a powder in a cup using a pre-calibrated fundamental parameter model. Without extra sample preparation, such as fine grinding, pelletizing of glass borate smelting, the inaccuracy (expressed as one standard deviation) of XRF (X-ray fluorescence) performed on different size fractions can be expected to be up to 20- 30 % relative error. This inaccuracy is the probable deviation from the true value for ore powders independent of ore type and size fraction. Within a group of samples with the same ore type and size

fraction the relative uncertainty inside the group will typically be smaller than 5- 10 % relative (one standard deviation).

The samples from the first rougher were also analyzed by XRPD (X-ray powder diffraction). The analyses were performed at 22ºC on a PANalytical X'Pert PRO instrument, equipped with a Cu, long fine focus X-ray tube and a PIXcel detector.

3.3.4 Sampling procedures

For the sampling campaign in Aitik, compare paper I and IV, the sample procedures for analysis are presented in Figure 16 where the dotted line only covers the first rougher.

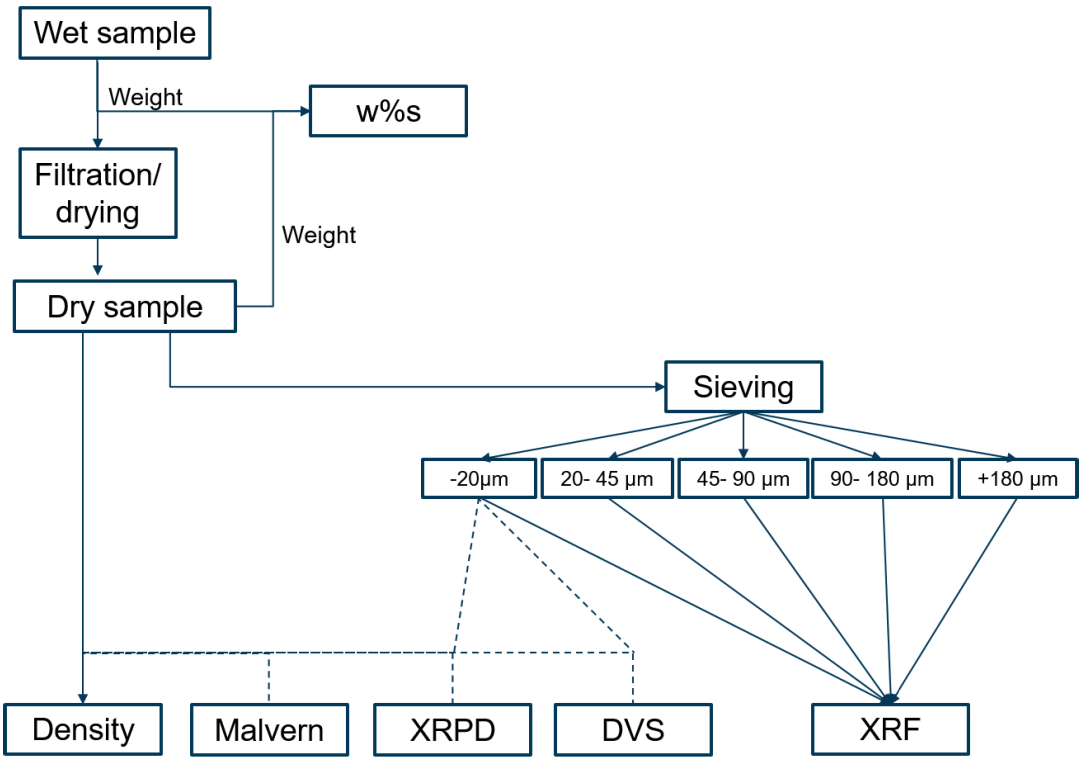

Figure 16. Sample preparation and analysis procedure for the sampling campaign in Aitik, Paper I and IV

Paper II covers the first test work with DVS as an analytical method of wettability in ore powders. The sample procedure for those tests is presented in Figure 17.

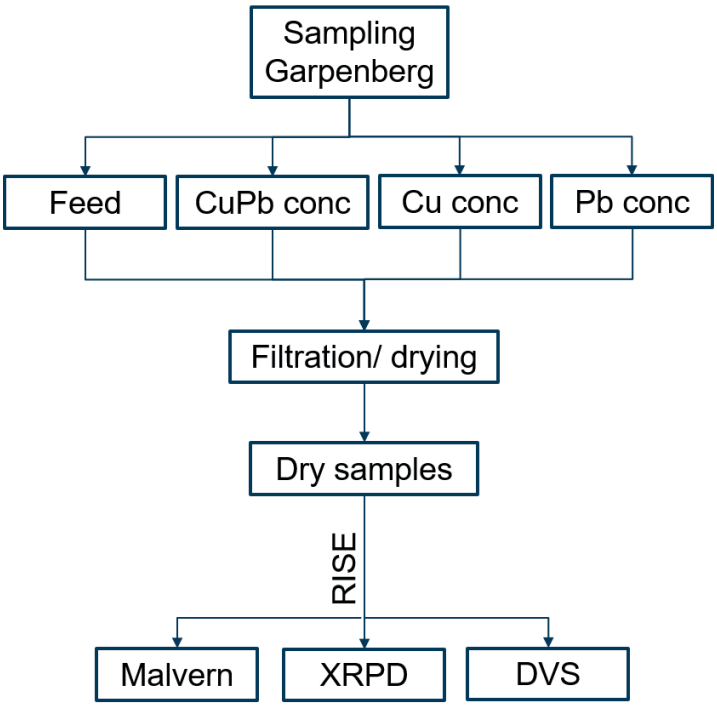

Figure 17. Sample preparation and analysis procedure corresponding to paper II

Sample procedures for evaluation of DVS as a technique of measuring the wettability was done according to the schematic picture in Figure 18 and presented in the corresponding paper III.

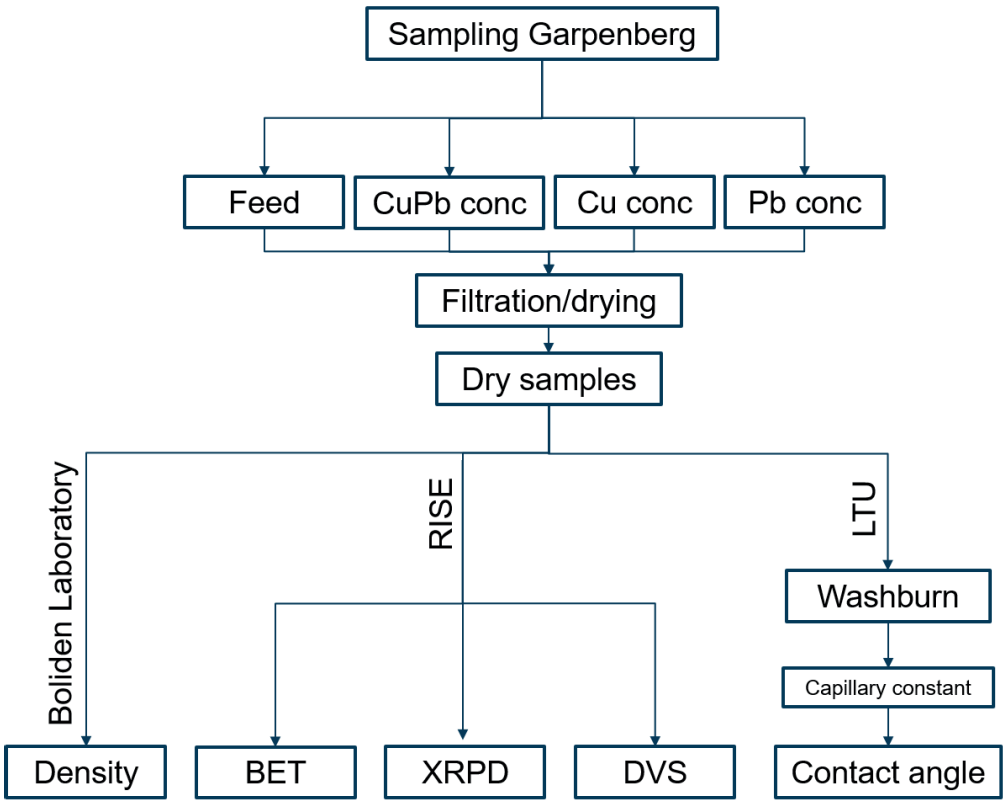

Figure 18. Sample procedure for DVS evaluation, paper III

4 RESULTS

4.1 SPATIAL ANALYSIS OF FULL SCALE FLOTATION PROCESSES

4.1.1 Rougher and scavenger cells

The three positions A, B and C in the first rougher cell (lateral direction) did not show significant differences, in terms of density, grade and weight % solids. That is why the following results from the first rougher are only presented from one position (A), compare Figure 13.

In the vertical direction, the solids concentration inside the flotation cells in Aitik decreased higher up. In the last rougher and the last scavenger it was clear that a segregation occurred. The solids concentration for the rougher and scavenger cells are shown in Figure 19.

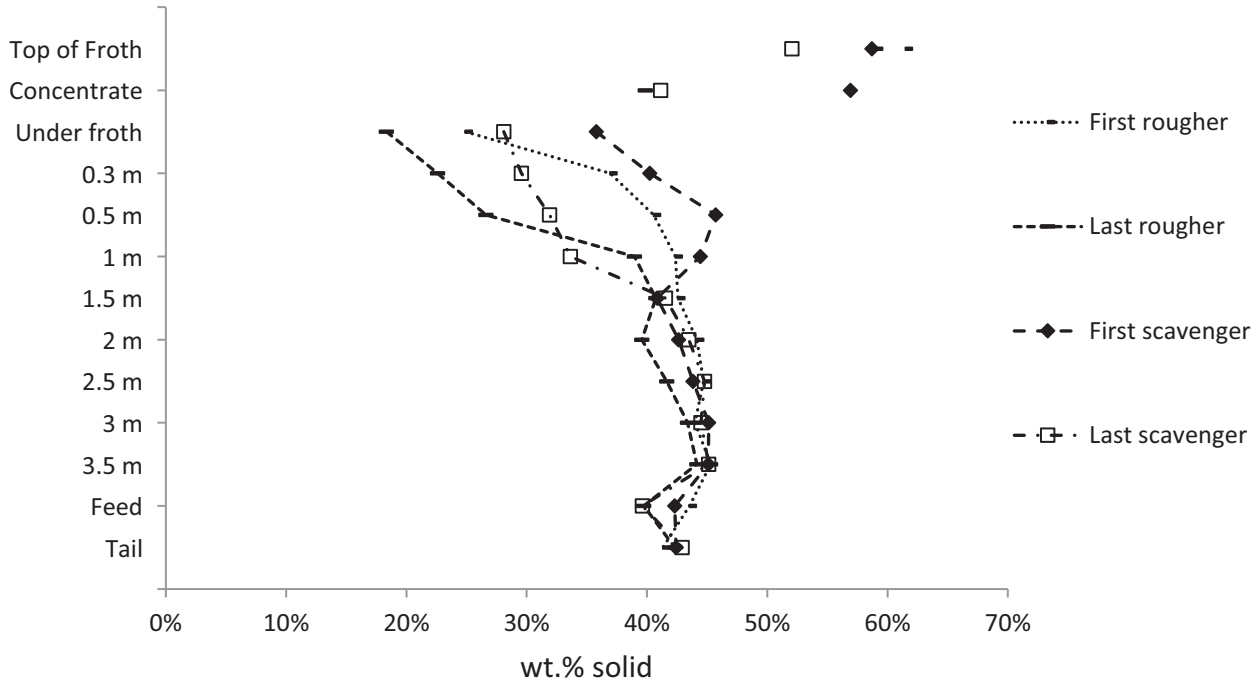

Figure 19: Distribution of solid concentration at different depth under pulp/froth interface level

The P80 increased with distance from the pulp/froth interface up to 1.5 - 2 m depth, before stablishing, as shown in Figure 20.

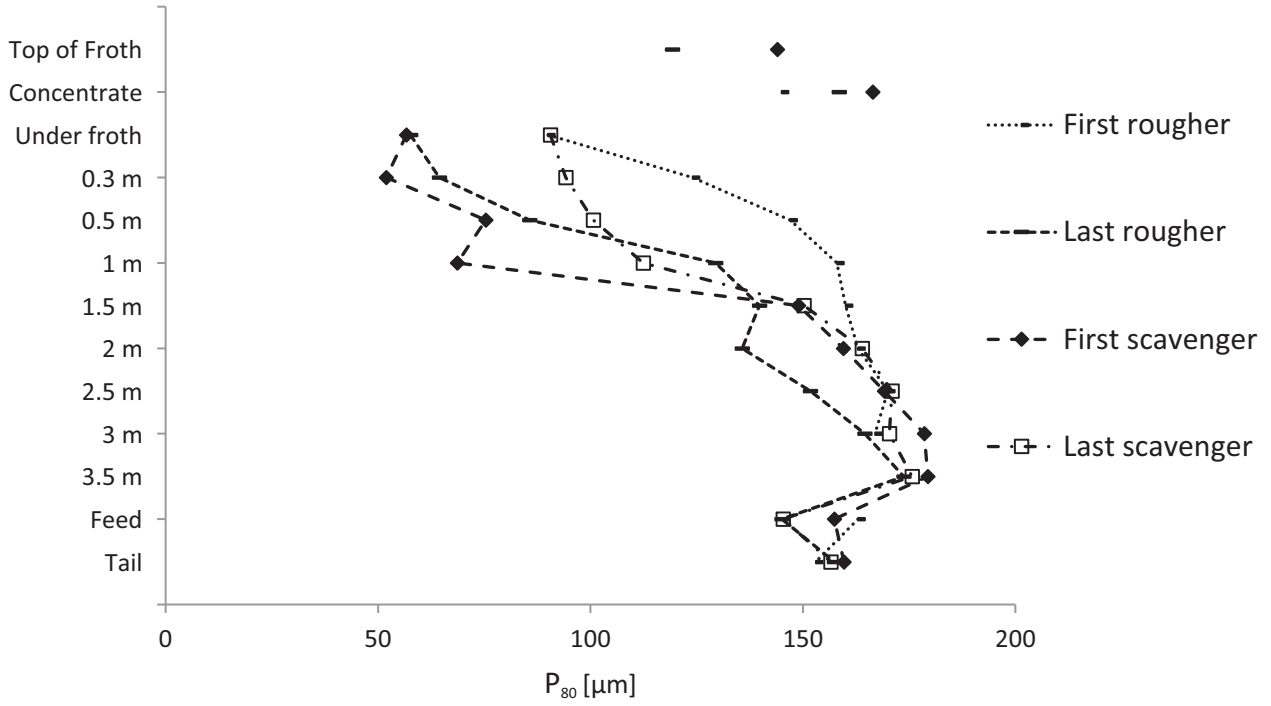

Figure 20. P_{80} in the solids at different depth under pulp/froth interface level

Based on these results, the mixing zone can be defined from the bottom of the cell up to 1.5-2 m from the pulp/ froth interface level. The quiescent zone is from there up to the froth zone. The decrease in particle size in the quiescent zone may explained by the inertia of coarser/ heavier particles preventing them from staying suspended/ attached to bubbles in the quiescent zone and settling back to the mixing zone.

The mineral grades inside the flotation cells showed a similar trend in all cells, with only small variation in grade from the bottom of the cell to the froth zone. Figure 21 shows the grades per size fraction from the four investigated cells and the axis scale for low grade material has been enlarged, therefore the concentrate has been omitted to make the charts presentable. It is notable that the composition of copper grade had only

small variation in vertical direction even though the wt.% solid was lower at the higher position, in the quiescent zone as presented in Figure 19.

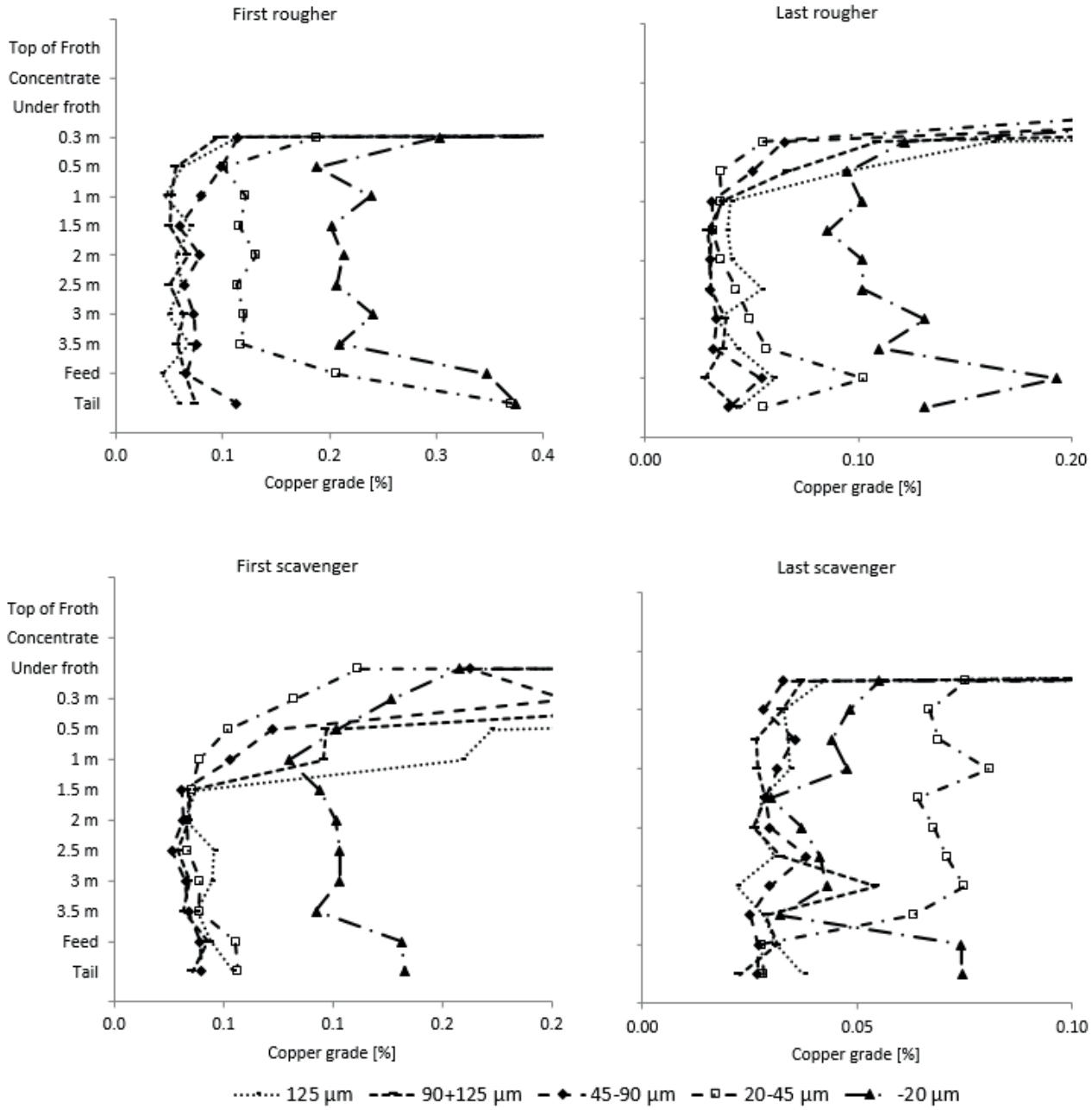

Figure 21. Copper grade for each fraction inside the cells at different depth under the pulp/ froth interface level

Further, it has to be emphasized that the grade of chalcopyrite in the first scavenger concentrate was higher than in the last rougher in all fractions, which indicates better flotation, compare Figure 21 and Figure 22. The air rate was the same in both cells but it is possible that the differences in grade can be accounted to the conditioning time needed for the collector

reagent (PAX). The reagent is added at the inlet of the last rougher, which might not allow sufficient conditioning time for it to be efficient in that cell. Reagent not reporting to the concentrate of the last rougher will continue to the first scavenger.

The copper grade at the vertical profile shows a higher value in the first rougher cell which sticks out from the other three investigated cells, where the first rougher cell has a grade twice as high. The grade is still more or less constant at the vertical profile in the first rougher as well.

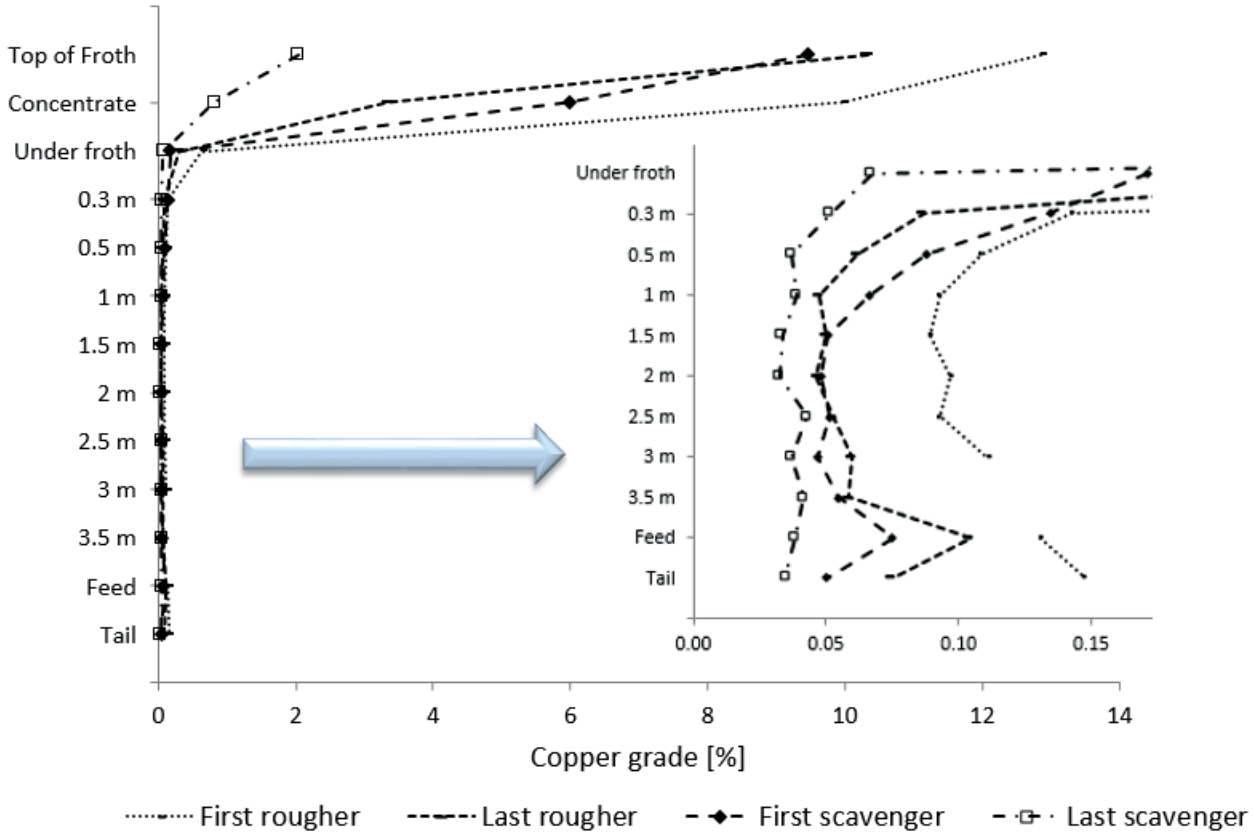

Figure 22. The grade of chalcopyrite at different depth under the pulp/ froth interface level. The inserted diagram shows an enlargement of the lower grades.

Samples taken from the top of the froth showed an increase in grade of chalcopyrite, from the center and outwards, in all the cells investigated. The highest value of chalcopyrite was obtained ca 20 cm from the edge. In all the cells the grade went down close to the edge of the froth lip, see Figure 23. The grade was highest in the first cell, with an increase from

30% chalcopyrite at the center point to 40% chalcopyrite just before the edge where it again went down to 35% chalcopyrite.

The last rougher and the first scavenger showed a similar trend, with an increase from 15- 20 to 30% chalcopyrite and a small drop just at the edge. The last cell showed grades between 5 and 7% chalcopyrite, and also exhibited the typical grade drop at the edge of the cell.

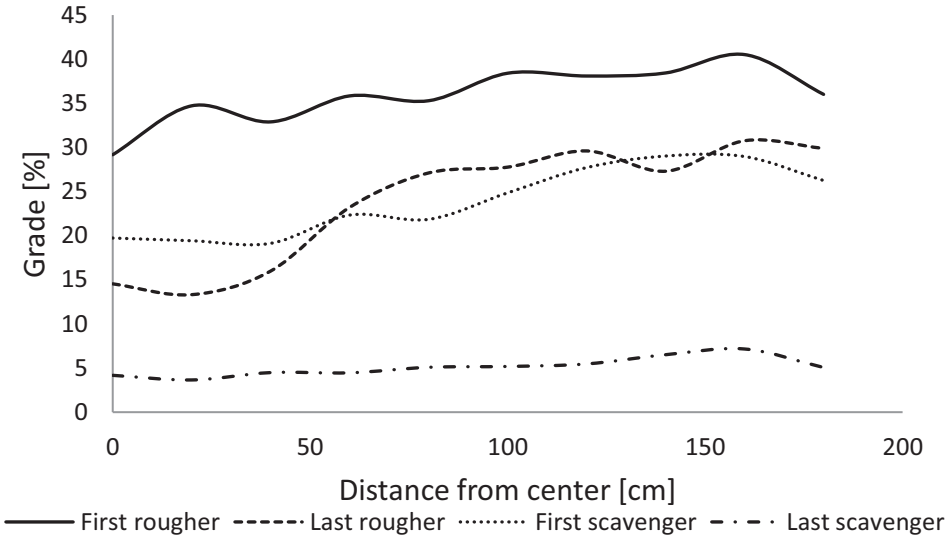

Figure 23. Top of froth measurements of chalcopyrite

The drop may arise from floated material along the edge of the cell which will not have any time in the froth zone to decrease gangue entrainment. The launders are also installed inside the cell, compare Figure 13, which may generate turbulence along the edge of the cells and can be a reason for the slightly lower grades.

Along with the increased content of chalcopyrite at the top of the froth, quartz showed the opposite trend with the highest grade being found at the center of the cells, compare Figure 24.

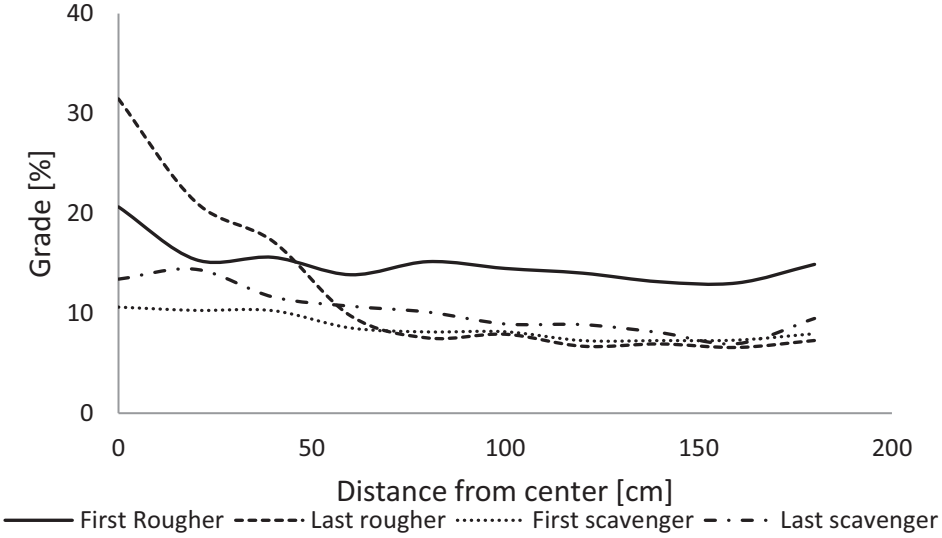

Figure 24. Top of froth measurements of quartz

Figure 23 and Figure 24 indicate of upgrading at the froth surface along the froth transportation to the edge of the cell, where the quartz grade is decreasing and the copper grade is increasing. This could arise from the difference in wettability, where quartz is depressed through the froth phase, due to the more hydrophilic copper bearing particles being floated up and competing for the top of froth location. Another explanation could be a higher turbulence in the froth phase along the shaft of the agitator where gangue minerals are thrown up in the froth.

Most of the copper-bearing particles in the scavenger tailings were found in the coarsest (+125 μm) and in the smallest (-20 μm) fraction, around 30 and 40 % respectively. Those are also the fraction which are the most difficult to float. Historical, the total amount of coarse and fine particles in the tailings are around 70% but the distribution may vary. Monthly composite samples is preferred for control.

A comparison of the results obtained with the Widmatic sampler and the one from Heath & Sherwood showed that the particle size distribution was almost the same (in every second sample the H&S sampler collected slightly more -20 μm) while the assays had a slight, but acceptable variation. The gas hold-up value was consistently lower with the

Widmatic sampler, i.e. 2-5% air compared to 7-12 % air as measured with the H&S sampler. I.e., there is a need for additional sampling before conclusions can be drawn regarding the gas hold-up determined with the different samplers. The air hold-ups in the first rougher are shown in Figure 25, where it can be seen that there is a difference between the two samplers as well as variations inside the cell.

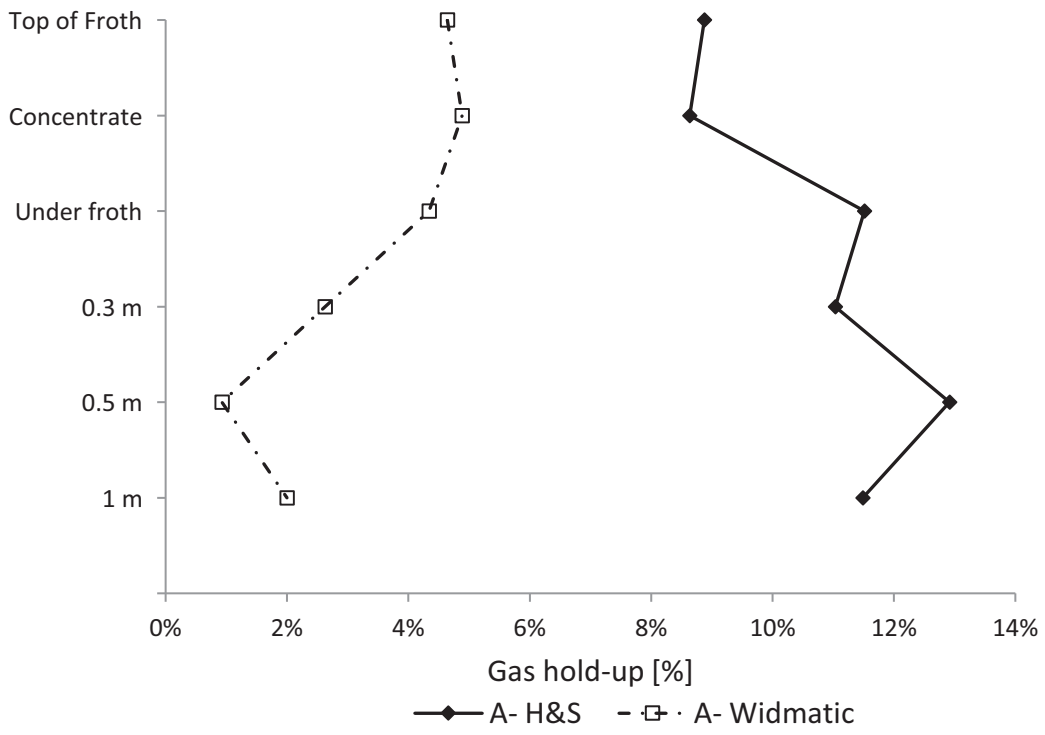

Figure 25 The gas hold-up for different samplers in first rougher

4.1.2 Cleaner cells

Spatial investigation in cleaner cells will contribute to the full understanding of the Aitik flotation process. A master thesis student has contributed to the thesis with this information. Further details on this work has been documented separately (Lappi, 2015).

The material to the cleaner cells passes a hydrocyclone where the coarser material is sent to a regrinding mill. This makes the feed to the cleaner

cell much finer compared to the rougher and scavenger cells. For instance, in April 2015, the feed to the first cleaner circuit had a P_{80} below 45 µm. From the investigation it was found that the feed solid content was around 10 wt.% in all cleaner cells.

The sampling survey was conducted from the top of froth, through the froth layer, and down to 2 m under the lip. The solid content increased from the slurry phase up through the froth phase. For all investigated cells the vertical profile looked like Figure 26, from which the froth phase can be detected by comparing the wt.%. For cell 2.1 the froth phase started between 140 and 160 cm below the lip level and for the other two cells it was between 80 and 100 cm below the lip level.

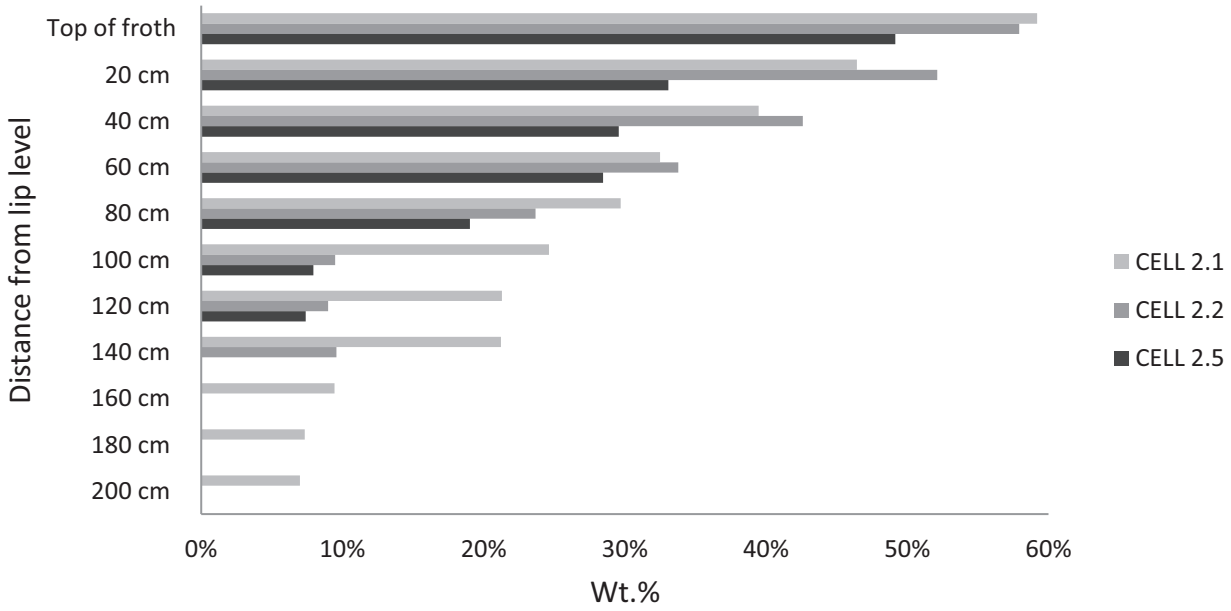

Figure 26. Second cleaner mass percentage of solids

The first cleaner cell, which floats the reground scavenger concentrate and where the purpose is to depress pyrite to the tailings, leaves about 1 % of the copper minerals in the tailings. The losses are found in the smallest fraction, -10 µm, which can be seen in Figure 27.

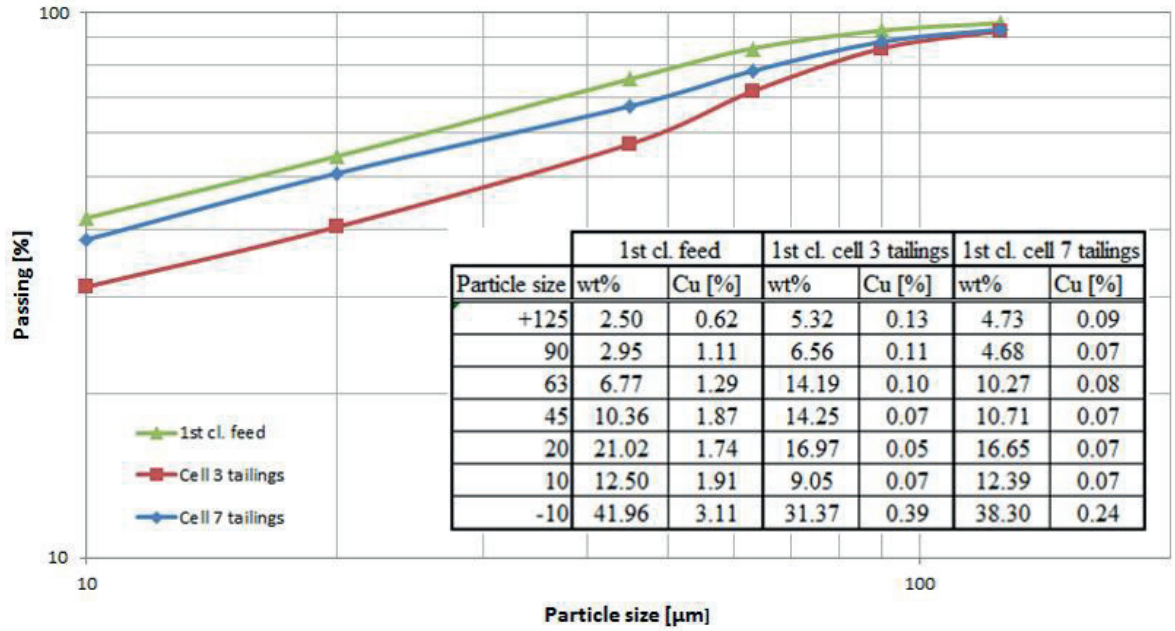

	1st cl. feed		1st cl. cell 3 tailings		1st cl. cell 7 tailings	
Particle size	wt%	Cu [%]	wt%	Cu [%]	wt%	Cu [%]
+125	2.50	0.62	5.32	0.13	4.73	0.09
90	2.95	1.11	6.56	0.11	4.68	0.07
63	6.77	1.29	14.19	0.10	10.27	0.08
45	10.36	1.87	14.25	0.07	10.71	0.07
20	21.02	1.74	16.97	0.05	16.65	0.07
10	12.50	1.91	9.05	0.07	12.39	0.07
-10	41.96	3.11	31.37	0.39	38.30	0.24

Figure 27. Size distribution from Aitik 1st cleaner bank

In the later cleaner stages, 2nd , 3rd and 4th , where the purpose is to increase the grade, a vertical distribution has been detected. For the cells 2.1 and 2.2, the feed is mostly the reground rougher concentrate with newly liberated minerals. Here, the upgrade in the froth is more distinct compared to the other investigated cells where the grade in the froth phase is more or less constant, see Figure 28.

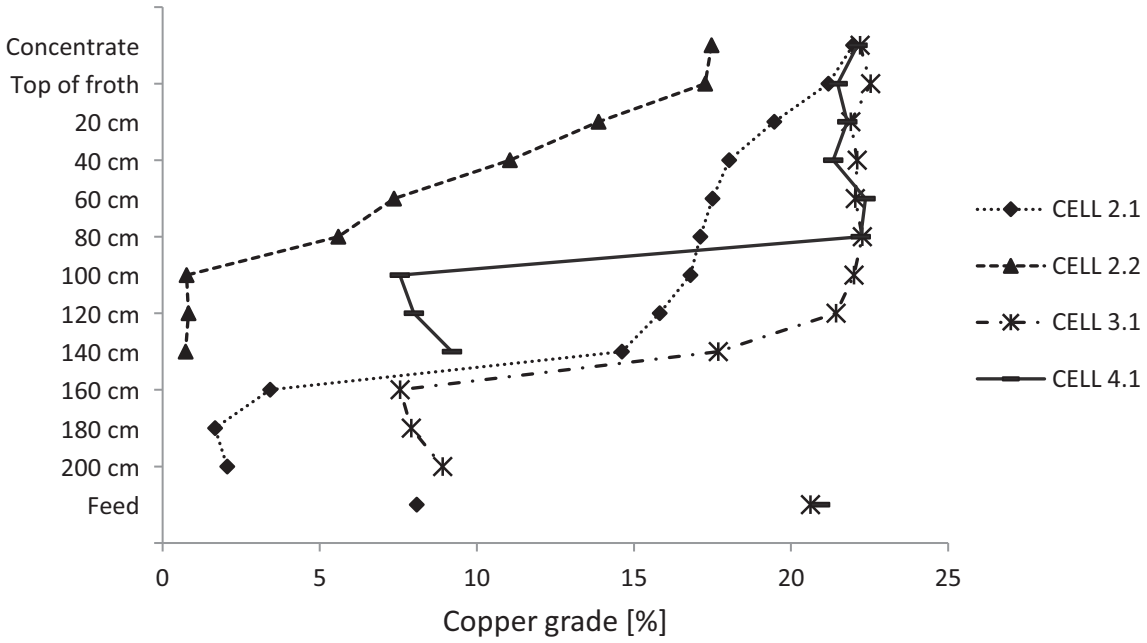

Figure 28. Copper grade as a profile for some cleaning cells at Aitik

Typical for the second, third and fourth cleaner stage is that the feed to the first cell in each stage has a higher grade compared to what is detected in the slurry in the mixing zone. This is an indication for fast floating copper particles with highly hydrophobic surfaces, which either are already carried by an air bubble or attach directly to a bubble and enter the froth phase.

In Figure 29, particle size results from the first cleaner cell in stage 2 are presented. The particle size distribution is constant throughout the froth zone for all size classes. The dotted horizontal lines indicate the area in-between where the pulp/ froth interface level lies.

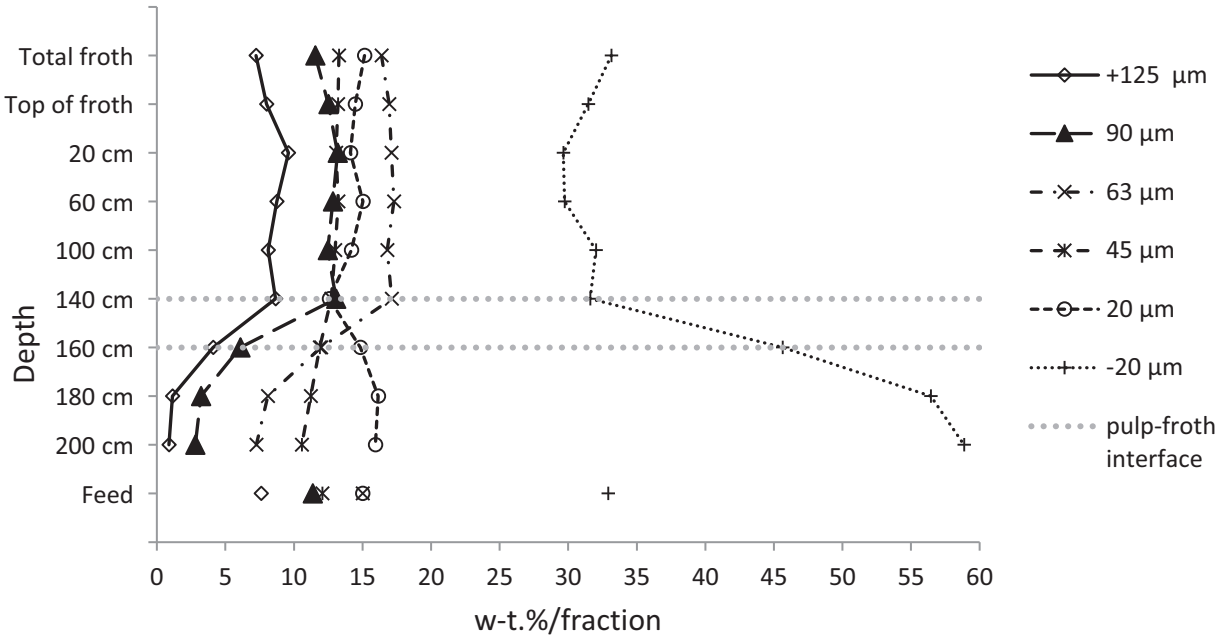

Figure 29. Cell 2.1- Particle size distribution at different depth

The difference between the feed and the samples from the slurry phase indicates a composition where between 50 to 60 % of the solid particles is of size smaller than 20 µm. Interestingly, the size distribution in the froth zone is similar to the feed. Another interesting observation is the grade in those fractions which is presented in Figure 30, compare Figure 28 where the total sample grade is presented. Even when the relationship between

the fraction is similar through the froth, seems the grade to increase between 5 to 10% Cu.

For instance, the amount of non-sulphuric gangue in the -20 µm fraction seems to stay in the mixing zone and/ or being depressed in the froth transport, probably mostly because of the water drainage.

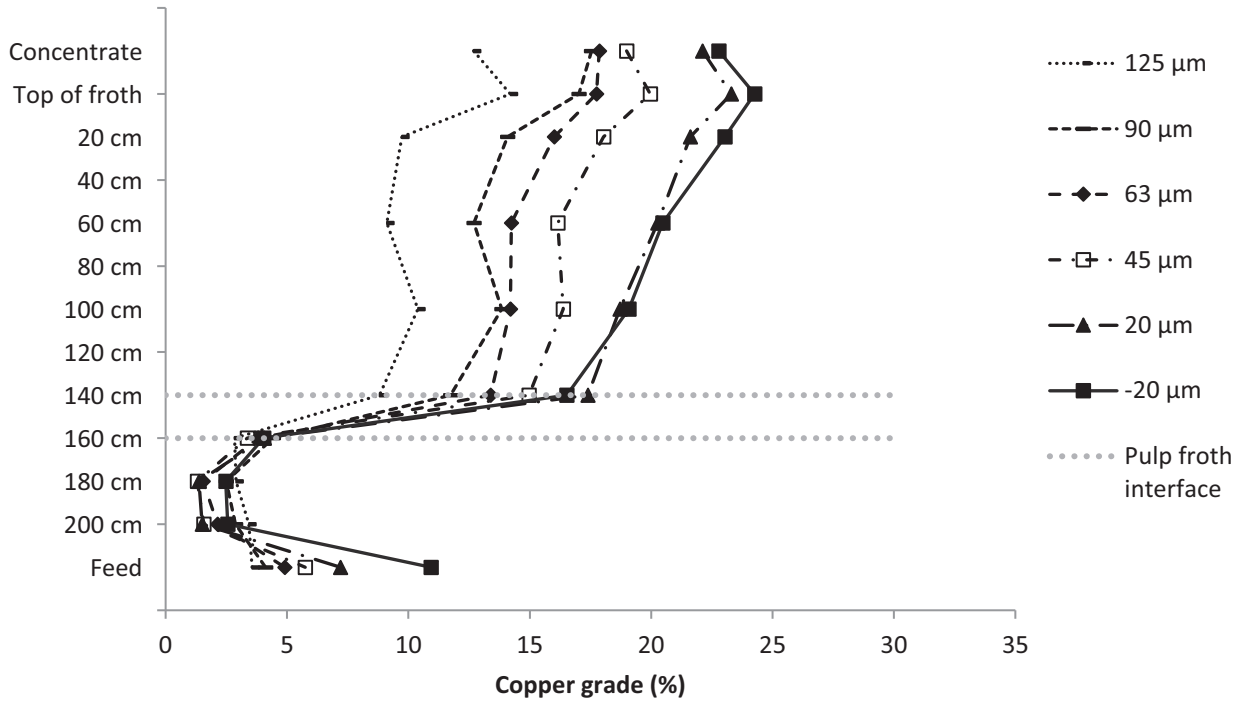

Figure 30. Cell 2.1- Copper grade for different size fraction at different depth

The particle distribution profile is similar in the third and fourth cleaning cells, where the slurry phase contains more slimes and where a constant profile is seen in the froth, as shown in Figure 31. The grade differs since no upgrading of the copper grade seems to take place for any of the fractions. Data from the first cell in the third cleaning cell is presented in Figure 32.

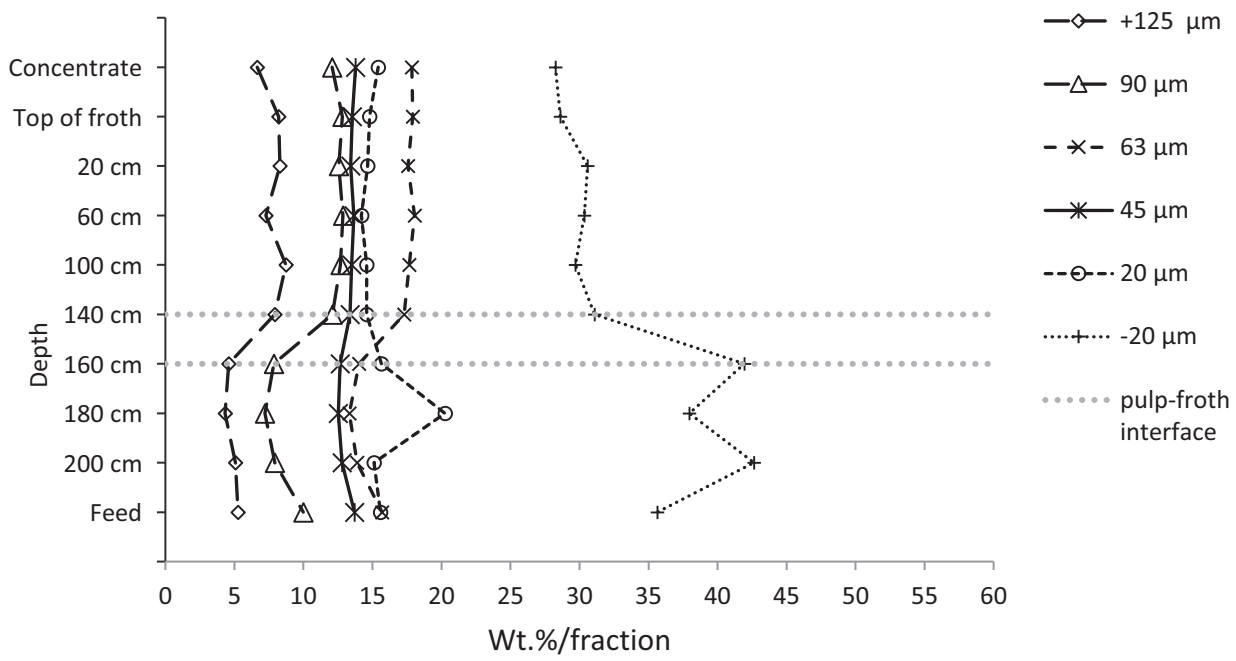

Figure 31. Cell 3.1- Particle size distribution at different depth

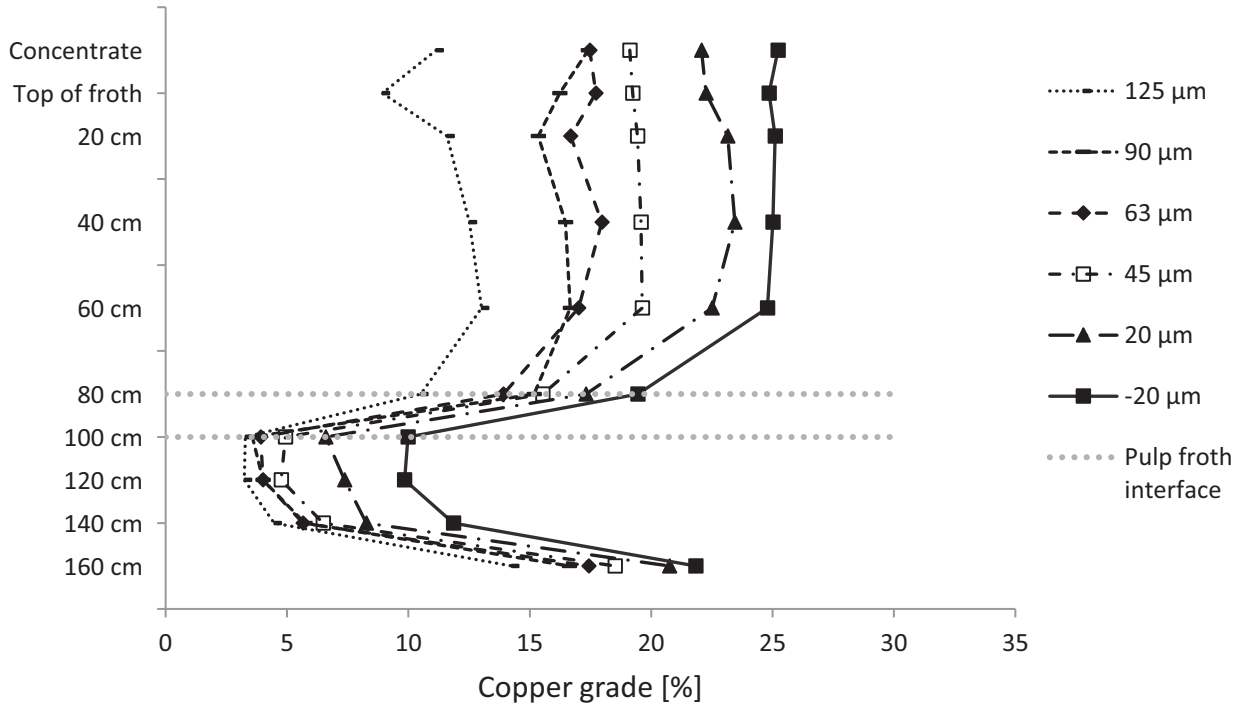

Figure 32. Cell 3.1- Copper grade for different size fraction at different depth

4.2 PRACTICAL IMPLICATIONS FROM THE SAMPLING PROCEDURE

In order to define a standard sampling procedure for further investigations, it is of interest to know that the sampling equipment is easily operated (with respect to sampling and transportation) and that a reliable sample can be taken.

The two supplementary samplers bought from Heath & Sherwood (2015) were fully mechanical samplers. It was not possible to dismantle them, which makes it more difficult to transport. The one liter sampler was bought with a 5 meter long rod to be able to sample in the lower part of the cell. This length of the rod did not fit in a regular car, i.e. a truck was needed for transportation. The samplers from Heath and Sherwood were also opened and closed on top of the rod. To be able to have the container in upright position for emptying, a lower platform was needed for the 5 meter long rod, see Figure 33.

Figure 33. Sampling solutions for emptying the 5 meter long H&S sampler

It has to be noted for such a huge investigation with over 100 samples, the sampling with a dip-sampler, like the Widmatic or H&S sampler, requires the sampler to be lifted up after every sample was obtained. This is labor intensive and physically demanding work.

If the gas hold-up is important, more investigation is needed for determining which sampling method is the most reliable. Until then, for future sampling campaigns, the slurry content may be sampled with a peristaltic pump connected to a pipe since it is the simplest way of sampling. A handheld peristaltic pump wheel is available, which can be operated by a battery powered drilling machine, see Figure 34.

Figure 34. Hand-held peristaltic pump wheel operated by a battery driven drilling machine

For froth investigation, it is important to know that there are grade variations in a radial profile and sampling at a single point has to be done at the same place all time for correct comparison. In this campaign no replicate was sampled, which should have been done to evaluate the sampling accuracy. The samples has on the other hand been collected fairly close to each other and a continuously curve from the bottom of the cell upwards is reasonable to achieve. Divergences would be easy to locate and question.

4.3 HYDROPHOBICITY MEASUREMENTS

4.3.1 Evaluation of DVS method

A comparative study was conducted where the Washburn technique was compared to DVS (Paper II).

The ore samples for the validation where obtained from a copper/ lead separation process in Garpenberg, another concentrator owned by Boliden. Four samples were chosen according to their expected differences in hydrophobicity.

The feed, the copper/ lead bulk floated concentrate (CuPb conc), the depressed lead (Pb conc) and the floated copper product (Cu conc) were included in the study. If the result follows the theory the feed is assumed to be the most hydrophilic since the content of gangue minerals is the highest and no collectors are added. The CuPb-concentrate should be more hydrophobic since it is a floated product. The depressed lead concentrate is assumed to be more hydrophilic compared to the CuPb-concentrate while the copper concentrate is assumed to have at least the same degree of hydrophobicity as the CuPb-concentrate.

The samples where extracted spring 2017 in Garpenberg, with each sample being divided into two equal parts. One part was sent to RISE laboratory for the DVS measurements and a BET surface analysis.

The other half of the sample was sent to Luleå University of Technology where the Washburn measurements were conducted.

The DVS result returned the highest water adsorption from the feed, as expected. The CuPb-concentrate adsorbed lower amount of moisture and the copper concentrate adsorbed very little moisture. The lead concentrate, which was depressed with dichromate, adsorbed more moisture, not as much as the feed but more than the CuPb concentrate. This can be see Figure 35 where the error bars is calculated based on a 95% confidence interval from five parallel measurements.

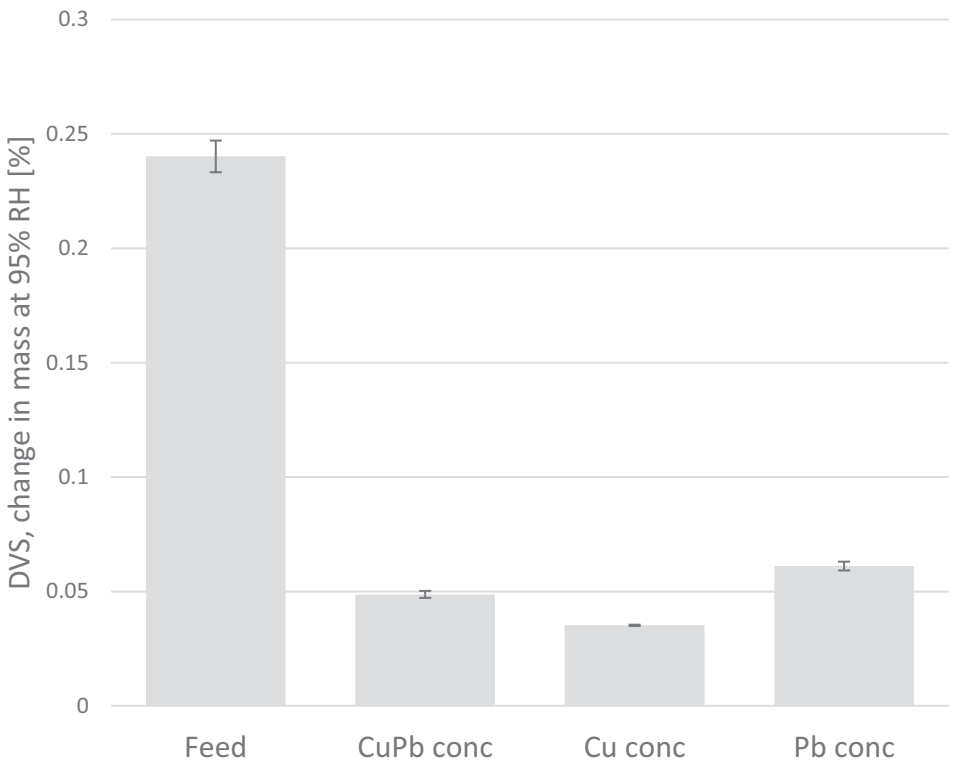

Figure 35. The DVS data for each sample with a 95% confidence interval

The DVS results showed in Figure 35 is similar as the earlier measurements on the same products (Paper II).

The Washburn measurements showed similar result in terms of the calculated contact angle, except that the feed had a much higher contact angle than expected.

The copper concentrate is not a pure copper mineral but the literature value of pure chalcopyrite covered with xanthates is 89°, which is close to what was measured (Klassen & Mokrousov, 1963). There was no measurement found in literature with galena covered with xanthates and depressed with dichromate, but the measured contact angle of the lead concentrate was lower than the one for the CuPb concentrate, which was expected. The results in Figure 36 present both the contact angle and the capillary constant.

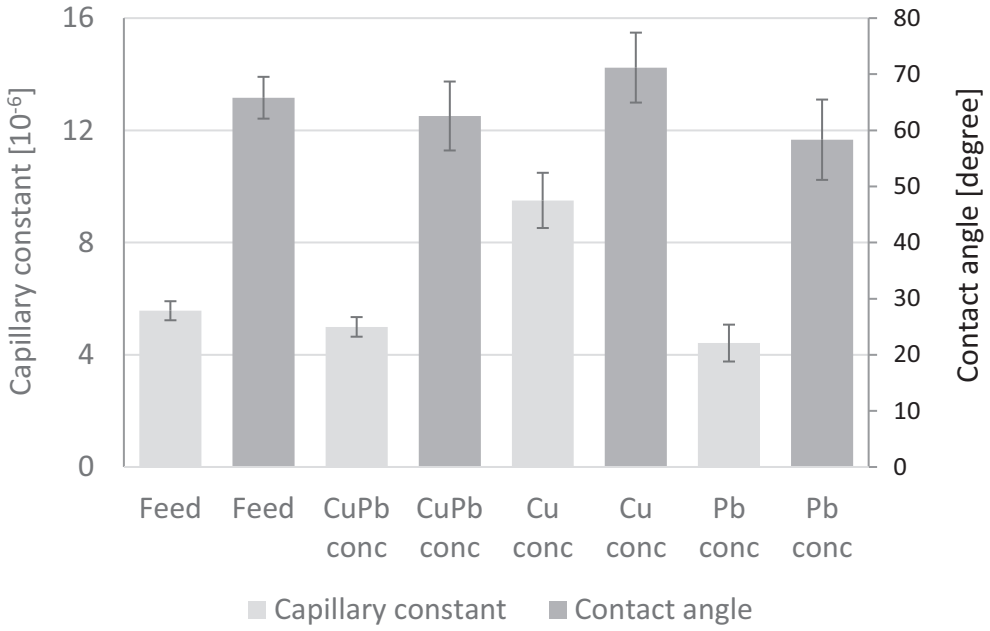

Figure 36. Mean values and a 95% confidence interval of the capillary constant and contact angle for each sample

The samples in this work have never been measured for contact angle before. Accordingly, no "expected" values were available. It is therefore difficult to speculate about how reliable the absolute values are. Instead the order of the values should be discussed.

It should also be noted that ore samples from different positions in a flotation circuit were used, which are each mixtures of both gangue- and valuable minerals, instead of pure minerals, which are usually used in publications of Washburn measurements. The contact angle and the ability to take up water will thus be an average value for all included minerals. Both techniques are affected by differences in particle density. A certain weight is used for each measurement which results in differences in the sample volume and number of particles depending on density of the sample. In Figure 37, the DVS value (change in mass) is plotted against the specific surface area measured by BET, resulting in a straight line correlation, achieved even though four different types of samples were used. If, on the other hand, the sample density is used to calculate the change in mass per volume and plotted against the specific

surface area the same straight line correlation is achieved but with two outliers. Both of them are related to the lead concentrate, which can be seen as more hydrophilic compared to the other samples.

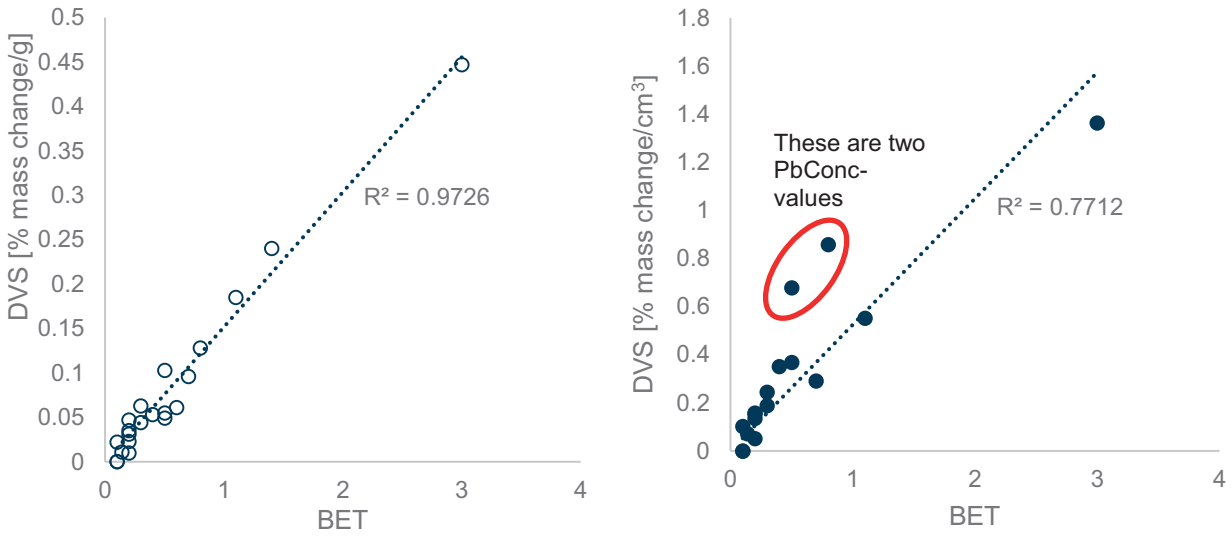

Figure 37. DVS data as %/g correlated to BET-data left and DVS-data as %/cm³ correlated to BET-data right

For all the investigations conducted (Paper II, III, IV), a correlation has been found between the DVS value and the specific surface area and also with the included minerals. Recommendations for using DVS as a measure for wettability are to (i) also measure the particle size distribution and to (ii) identify the included minerals.

4.3.2 DVS measurements for rougher cell samples

The samples selected for DVS measurements from the sampling campaign in Aitik are the ones from the first rougher, including the three radial positions according to Figure 13.

The mineral content, detected by XRPD, divided the samples in three different types, 1, 2 and 3. In general the Type 1 is the concentrate and froth samples which include more of chalcopyrite, pyrite and

molybdenite compared to type 2, which is the slurry sample and consists of more quartz for instance. Type 3 is the slurry samples but only the - 20 μm fraction. There was a difference between the total sample and the smallest fraction where the total sample contained more mica and the smaller fraction higher amounts of chalcopyrite and chamosite (which is a clay mineral).

The DVS measurements from the first rougher cells show a similar trend for the grade, as a function of sampling level. The DVS value of the total sample is presented in Figure 38 (Paper IV).

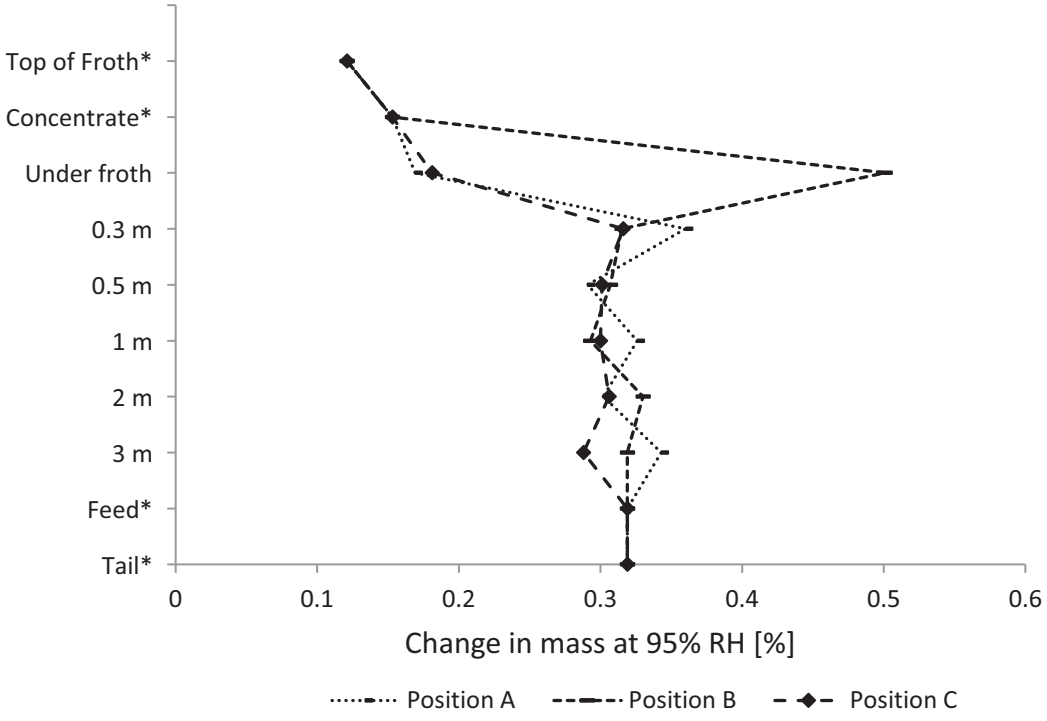

*Figure 38. DVS result, change in mass for total sample at 95% RH at different depth, where * is not position specific samples*

The sample collected from "under froth" in the B position deviates from the A and C position, see Figure 13. It must be taken into consideration that it is difficult to find the right sampling position just under the froth. There is a risk that particles from the froth phase become a part of the

"under froth" sample. In that case, the A and C position act more like the froth samples. The B sample could consist of more -20 µm particles compared to the other samples. Indications for that can be seen in Figure 39 where there is a high value measured for "under froth" at the B position.

When looking at Figure 39, where the DVS measurements for the -20 µm particles are plotted, it is apparent that the values vary considerably and shows a higher value compared to the total sample in Figure 38. This is with exception of the "top of froth" and "total froth" samples, which actually lie a bit lower than the total samples.

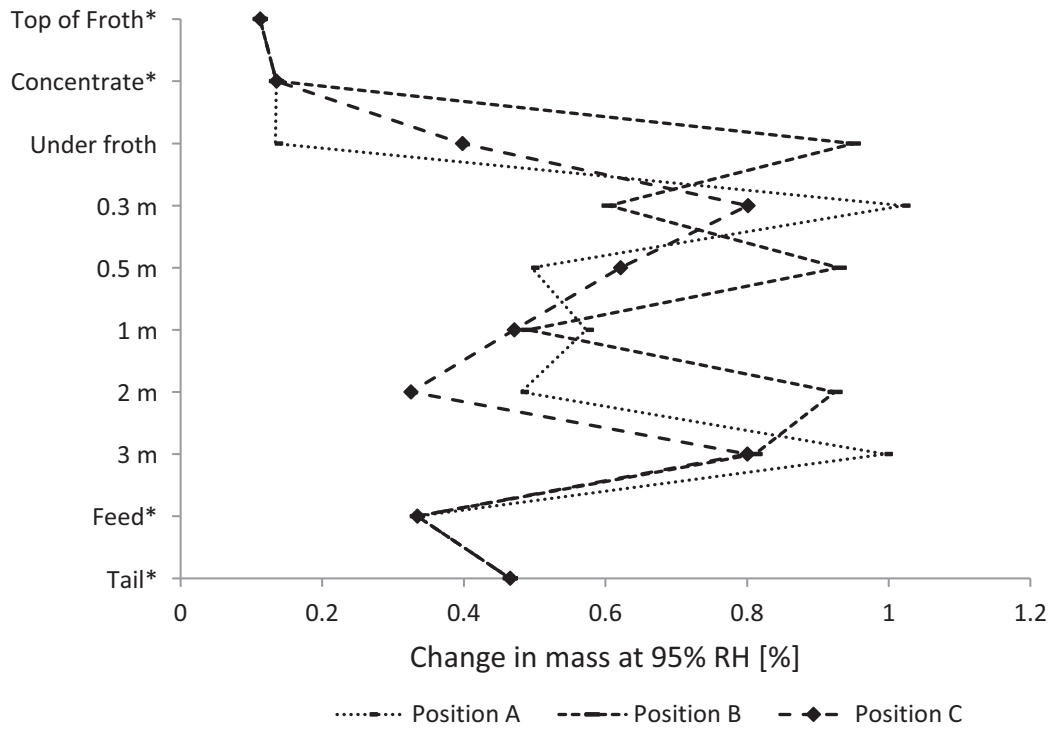

*Figure 39. DVS result, change in mass for -20 µm fraction at 95% RH at different depth, where * is not position specific samples*

In a comparative study the DVS results have shown to be affected by the surface area of the sample. The variation in Figure 39 may be a result of different amounts of smaller particles. The variation could also arise from the distribution of different minerals. From XRPD analysis, the -20 µm

samples from the slurry phase contain slightly more of chalcopyrite and pyrite than the total sample from the same level, less mica but more chamosite and actinolite. Chamosite is a clay mineral with a laminar shape with a sheet structure that could adsorb moisture. In Figure 40 the relationship between the content of chamosite and the DVS value is plotted with a straight line correlation at R^2 value at 0.6.

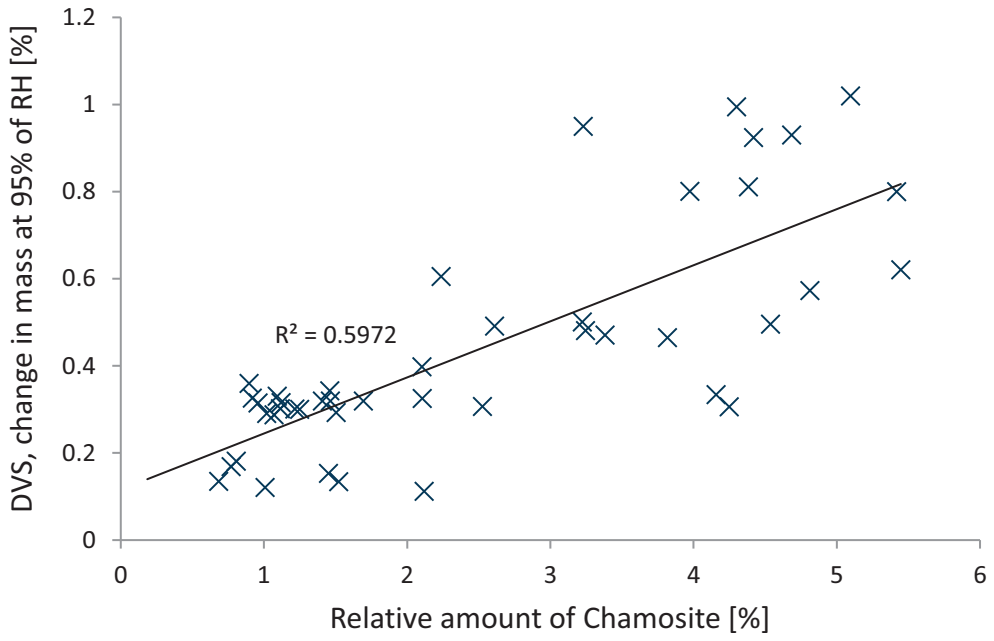

Figure 40. Water uptake with DVS as a function of the amount of chamosite

4.3.3 Concept development for using DVS in production

From a production point of view, it has always been of interest to know and measure the degree of hydrophobicity. Understanding of hydrophobicity is important for in-depth evaluation of flotation processes and mechanisms and for more detailed understanding of industrial process performance and troubleshooting. The DVS technique was used for characterization of the wettability properties of the minerals in this thesis. The results show a low relative standard deviation and reasonably low operator input, which is advantageous from a production point of view.

The DVS instrument is fairly expensive, but for daily use it can be a reasonable cost. The operator input is only needed for starting up the measurement, thereafter the measurement is conducted autonomously. At default, the analysis time is several hours. One measurement includes two cycles, this is because e.g. pharmaceutical samples may change when adsorbing moisture, which is detected if the second cycle diverges from the first. The ore samples will typically not be affected in the same way since it has been in a slurry phase already and the second cycle could therefore be excluded. The measurement starts with an absolute dry sample and then the first increase of % relative humidity is made and adsorption followed versus time until phase equilibrium has been reached. The number of steps required for the cycles strongly affects the time. For measuring on a daily basis it is possible to optimize the number of steps needed. For two cycles and with steps of 5% RH it is typically possible to complete at least two measurements per day. The samples have to be dried and divided into smaller portions, as only 0.5 grams are needed for one measurement.

Since there is a relative long lead time from sampling to analysis, it is for the time being difficult to use DVS data as a process control parameter. It is more likely that it could be used as an evaluation tool for a product stream on a daily basis.

5 SUMMARY OF MAIN FINDINGS

From the conducted sampling campaigns and sample analyses, the following findings have been obtained:

Rougher/ scavenger

- The quiescent zone starts from 1.5 and 2 meter depth and up to the interface level of the 160 m^3 TankCell® in Aitik.
- The quiescent phase is lower in solids density and the particle size distribution, P_{80}, decreases with distance from the mixing zone.
- The copper grade is more or less constant throughout the vertical profile even though the particle size distribution and weight % solid changes.
- The smaller particles/ slimes are to a higher extent represented by clay minerals. The coarser particles are most often quartz.

Cleaner cells

- Tailings from first cleaner bank have highest copper losses in the - 10 μm fraction.
- The first and second cleaning stage shows an upgrade in the froth zone even though the particle size distribution is stable.
- Third and fourth cleaning stage have no upgrade in the froth zone.
- The solids density is low inside the slurry phase, only 10 wt.% solids.
- The slurry phase contains a lot of slimes.

Measurement techniques

- The gas hold-up measurement needs more comparable studies to ensure the right equipment used for sampling.
- Sampling with a 5 meter long rod/sampler is not recommended if not necessarily needed.

DVS

- DVS, or wettability, result for the whole composite sample from Aitik first rougher shows a constant value throughout the cell that follows the copper grade.
- DVS, or wettability in the Aitik cell varies a lot in the -20 μm fraction, the copper grade in the smallest fraction is constant and the variation most likely originates from the content of clay minerals which can be hydrophilic.
- The DVS technique, as far as this research has shown, seems to be a reliable method for measuring the wettability of ore samples, but more research is needed.

6 CONCLUDING REMARKS

The Aitik concentration process has a lower copper feed grade (0.2 % Cu) and a coarser grind than most other copper operations. The physical parameters such as grade and particle size affect the flotation system, which makes it difficult to compare flotation research from other operations. Additionally, the fact that flotation cell sizes are increasing and how this is affects the total recovery requires its own research.

The decision to conduct a sampling investigation for characterization of the spatial variation in the Aitik flotation cell has resulted in useful information of the different zones inside the cells. The sampling method used gave reliable samples from the cells and contributed to the knowledge of suitable sampling procedures for large cells and how further sampling campaigns could be carried out. A sampling container with a 5 m long rod is not recommended with the handling problems that comes along, like transportation and conduct of the sampling procedure. The uncertainty of the gas hold-up measurement has to be further investigated to identify which kind of sampling method will give the

most reliable results. If the gas hold-up measurement is not of interest for a sampling investigation, pumping through a hollow pipe is recommended for sampling at different depth due to time saving.

In the Aitik flotation process selectivity problems are limited. The control strategy is to recover as much as possible in the rougher/ scavenger. The pyrite and gangue are assumed to be separated from the chalcopyrite in the first cleaner bank. Only 1 % loss overall from the plant feed arise here. In the scavenger tails (bulk tails) in Aitik, around 70 % of the copper losses in the scavenger tails were either +125 μm or -20 μm, particle sizes which are difficult to float.

From the spatial investigation, it was shown that there was a more or less stable copper grade throughout the whole cell height even though the solids density and the particle size distribution are different in the quiescent zone. The coarser particles are to a larger extent present in the lower part of the cells and in the concentrate. It seems that if floatable coarse copper particles are attached to air bubbles, they can report to the froth. However, the drop back effect is not investigated and there is no information on how the froth capture is behaving. It has to be recalled that the volume flow through the cell is high, around 5000 m^3/h which makes the residence time in each cell short. This holds especially for coarse particles that barely occur in the quiescent zone.

It was shown that the harder quartz minerals to a higher extent report to the coarser particles and that chamosite and other clay minerals are found in the fine fraction. Clay minerals like chamosite have a layered structure and are soft minerals that are easily ground to fine particle sizes and may therefore be overrepresented in the fine fractions, as was the case in Aitik. The test work with DVS showed a correlation between the chamosite content and the wettability for the -20 μm fraction. The layered structure means higher surface area where the hydrophilic surfaces can adsorb more water.

The DVS method investigated in this study for wettability test work has shown to be reliable for ore samples with only a small standard deviation when tested on 5 replicates. Since the instrument measures weight difference when adsorbing moisture on hydrophilic surfaces, the particle size is directly correlated to the moisture adsorbance. Combining surface area and mineral analysis is recommended to interpret the DVS result.

Boliden will continue using the DVS as an analytical tool for laboratory test work on collector or depressant research as well as continue with research of understanding the usefulness of the instrument for daily operation.

A general conclusion for the Aitik cleaner flotation stage is that the feed material to each cleaner stage contains fast floating particles since the froth phase corresponds to a higher extent to the feed than the slurry phase does. In the slurry phase, the smallest particles are predominant. An up-grading of the copper grade can be seen in the froth phase for the two first stages while the two later stages seem to conduct a plug flow through the froth. The two first stages have a feed material with higher content of pyrite and gangue and lies directly after a regrinding mill. To achieve a separation process in the flotation froth, a difference in wettability is required. The feed to the third and fourth step does not contain much gangue and non-liberated material, which could be the reason why the upgrading in froth phase is absent.

Using larger flotation cells in a flotation circuit requires fewer cells for reaching a certain residence time, less footprint area, simpler operational controls, lower maintenance cost, and less installed electrical power and lower power consumption per ton. The way forward in flotation research is not going back to smaller cells but trying to find solutions to the new problems that have occurred in the operation of larger tank cells. This involves new ways of widening the particle size distribution recovered in

the floated concentrate and continuing the research on how the hydrodynamic movement in a tank cell affects the recovery.

A sampling investigation like the one conducted in Aitik, where the different phases have been described by their mineral content, surface activity and physical parameters may be used for proper calibration of process models.

7 SUGGESTED FUTURE WORK

For the Aitik process the recovery is more important since the final concentrate grade can be achieved in the cleaning stage. From the investigation conducted the upper part of the cell doesn't seems to contribute to the result other than increasing the grade why further investigation regarding the significance of the cell height is suggested for further research. Changing a flotation cell height will change the hydrodynamic affects in the cell which can affect the results and further investigation at a smaller scale is recommended where different cell height is used. Another open issue is how Flowbooster® which increase the mixing energy higher up in the cell, affect flow and material distribution. This should be studied in a separate sampling campaign.

The gas hold-up measurement has to be further investigated, for example a comparative study where the Widmatic sampler and the JK Gas hold-up probe should be compared to validate the sampling technique.

Investigation of the cleaning cells regarding the low solid density in the bottom of the cell and how that is affecting the losses of fine particles is another recommendation for further test work. In the Aitik cleaner circuit, the froth is not pumped between cells, which is the more typical approach. It is not known if that may increase the bubble-gangue detachment for better separation and increase the intensity for smaller particles to attach to an air bubble.

This investigation was done with a coarse ground ore where the segregation inside the cell was detected. It should be studied further if this behavior is caused by the large particles in Aitik or if the same spatial variation will appear for finer ground copper ore.

Finally, the DVS results presented in this thesis can be seen as the starting point for a future systematic testing of different ore types and reagents in order to make full use of the instrument.

8 REFERENCES

Ahmed, M., Jameson, G.J., (1989). Flotation Kinetics, Mineral Processing and Extractive Metallurgy Review, 5, pp 77-99.

Akdemir, Ü., (1997). Shear flocculation of fine hematite particles and correlation between flocculation, flotation and contact angle. Powder Technology, 94 (1), pp 1-4.

Amini, E., Bradshaw, D.J., Xie, W., (2016). Influence of flotation cell hydrodynamics on the flotation kinetics and scale up, Part I: Hydrodynamic parameter measurements and ore property determination, Minerals Engineering, 99, pp. 40-51.

Ata. S., (2012). Phenomena in the froth phase of flotation- A review. International Journal of Mineral Processing, 102, pp. 1-12.

Bazin, C., Proulx, M., (2001). Distribution of reagents down a flotation bank to improve the recovery of coarse particles, International journal of mineral processing, 61, pp. 1-12.

Besagni, G., Inzoli, F., (2016). Bubble size distributions and shapes in annular gap bubble column. Experimental Thermal and Fluid Science, 74, pp. 27-48.

Brunauer, S., Emmett, P.H., Teller, E., (1938). Adsorption of Gases in Multimolecular Layers. Journal of the American Chemical Society, 60 (2), pp. 309-319.

Buckton, G., Darcy, P., (1995). The use of gravimetric studies to assess the degree of crystallinity of predominantly crystalline powders. International Journal of Pharmaceutics, 123 (2), pp 268-271.

Chau, T., (2009). A review of techniques for measurement of contact angles and their applicability on mineral surfaces. Minerals Engineering, 22 (3), pp 213-219.

Chegeni, M.H., Abdollahy, M., Reza Khalesi, M., (2015). Column flotation cell design by drift flux and axial dispersion models. International Journal of Mineral Processing, 145, pp.83-86.

Dube, R., Xia, J., Rinne, A., Lohilahti, J., Mattsson, T., (2015). CFD Analysis in Designing of Mixing Mechanism for a Mechanical Flotation Machine, AIChE Annual Meeting, November 8-13, Salt Lake City, UT.

DVS Adventure brochure, downloaded 2018-01-29. https://surfacemeasurementsystems.com/wp-content/uploads/2016/06/DVS_Adventure_Brochure_final_digital_updated_12July2016.pdf

Falutsu, M., Dobby, G.S., (1989). Direct measurement of froth drop back and collection zone recovery in a laboratory flotation column, Minerals Engineering, 2(3), pp. 377-386.

Farrokhpay, S., (2011). The significance of froth stability in mineral flotation — A review, Advances in Colloid and Interface Science, 166(1–2), pp. 1-7.

Finch, J.A., Dobby, G.S., (1990). The effects of frothers and particles on the characteristics of pulp and froth properties in flotation- A critical review. Journal of Minerals and Materials Characterization and Engineering, 4 (4), pp. 251-269.

Galet, L., Patry, S., Dodds, J., (2010). Determination of the wettability of powders by the Washburn capillary rise method with bed preparation by a centrifugal packing technique. Journal of Colloid and Interface Science, 346 (2), pp 470-475.

Gaudin, A.M., Schuhmann, R., Schlechten, A.W., (1942). Flotation kinetics. II. The effect of size on the behavior of Galena particles. Journal of Physical Chemistry, pp. 902-910.

Gorain, B.K., Franzidis, J.P., Manlapig, E.V., (1999). The empirical prediction of bubble surface area flux in mechanical flotation cells from cell design and operating data. Minerals Engineering, 12(3), pp. 309-322.

Gorain, B.K., Franzidis, J.P., Manlapig, E.V., (1997). Studies on impeller speed and air flow rate in an industrial scale flotation cell. Part 4: Effect of bubble surface area flux on flotation performance. Minerals Engineering, 10(4), pp. 367-379.

Gorain, B.K., Franzidis, J.P., Manlapig, E.V., (1995). Studies on impeller type, impeller speed and air flow rate in an industrial scale flotation cell Part 2: Effect on gas hold-up. Minerals Engineering, 8(12), pp. 1557-1570.

Hay, M.P., (2018). Personal communication with Martyn Hay of Eurus Mineral Consultants.

Hay, M.P., (2005). Using the SUPASIM flotation model to diagnose and understand flotation behaviour from laboratory through to plant. Minerals Engineering, 18(8), pp. 765-771.

Heath & Sherwood sample equipment, https://heathandsherwood64.com/products/mineral-processing-equipment/sampling/manual-probe-pd-samplers downloaded 2018-12-12.

Heng, J. Williams, D., (2011). Vapour Sorption and Surface Analysis in Solid State Characterization of Pharmaceuticals (eds R.A Storey and I. Ymén). John Wiley & sons, Ltd, Chichester.

Iveson, S., Holt, S, Biggs, S., (2004). Advancing Contact angle of iron ores as a function of their hematite and goethite content: Implications for pelletising and sintering. International Journal of Mineral Processing, 74 (1-4), pp 281-287.

Kawatra, S.K. (2011). Fundamental Principles of Froth Flotation, in SME Mining Engineering Handbook, 3rd Edition, Editor: Darling, P. ISBN 978-0-87335-264-2.

King, R., (2012). Modelling and Simulation of Mineral Processing Systems. Society for Mining, Metallurgy and exploration. Englewood, Colorado.

Kirdponpattara, S., Phisalaphong, M., Zhang Newby, B., (2013). Applicability of Washburn capillary rise for determining contact angles of powders/ porous materials. Journal of Colloid and Interface Science, 397, pp 169-176.

Klassen, V., Mokrousov, V., (1963). An introduction of the Theory of Flotation. Butterworth & Co. London.

Klimpel, R.R., Hansen, R.D., (1988). The interaction of Flotation chemistry and size reduction in the recovery of porphyry copper ore. International Journal of Mineral Processing, 22, pp. 169-181.

Koh, P., Schwarz M., (2006). CFD modelling of bubble-particle attachments in flotation cells, Minerals Engineering 19(6-8), pp. 619-626.

Kohmuench, J.N., Mankosa, M.J., Thanasekaran, H., Hobert, A., (2018). Improving coarse particle flotation using the HydroFloat™ (rising the trunk of the elephant curve). Minerals Engineering, 121, pp. 137-145.

Kruss. www.kruss-scientific.com/product/tensiometers/k100/force-tensiometer.k100

Lappi, S., (2015). A study of cleaner flotation in Aitik, Master thesis in Process Engineering, University of Oulu, Faculty of Technology.

Lynch, A.J., Johnsson, N.W., Manlapig, E.V., Thorne, C.G., (1981). Mineral and coal flotation circuits. Elsevier scientific publishing company, New York.

Mavros, P., Matis, K.A., (1991). Innovations in Flotation Technology, Kallithea, Chalkidiki, Greece.

Miettinen, T., Ralston, J., Fornasiero, D., (2010). The limits of fine particle flotation. Minerals Engineering, 23, pp. 420-437.

Nagaraj, D.R., Farinato, R.S., (2016). Evolution of flotation chemistry and chemicals: A century of innovations and the lingering challenges, Minerals Engineering, 96-97, pp. 2-14.

Norori-McCormac, A., Brito-Parada, P.R., Hadler, K., Cole, K., Cilliers, J.J., (2017). The effect of particle size distribution on froth stability in flotation. Separation and purification Technology, 184, pp. 240-247.

Nowak, E., Combes, G., Stitt, H., Pacet, A.W, (2013). A comparison of contact angle measurement techniques applied to highly porous catalyst supports. Powder Technology, 233(2013), pp 52-64.

Outotec, (2012). 100 Years of Flotation Technology, www.outotec.com. Downloaded 2015-12-09.

Panire, I., Vinnett, L., Yianatos, J., (2015). Flotation rate characterization using top of froth grades and froth discharge rates in rougher flotation circuits, Flotation 15, Minerals Engineering International, November 16-19, Cape Town, South Africa.

Pérez-Garibay, R. and De Villar, R., (1998). On line gas hold-up measurement in flotation columns. Canadian Metallurgical Quarterly 38(2), pp. 141-148.

Prakash, R., Kumar Majumder, S., Singh, A., (2018). Flotation technique: Its mechanisms and design parameters. Chemical Engineering & Processing: Processing Intensification, 127, pp. 249-270.

Qiu, G., Jiang, T., Fa, K., Zhu, D., Wang, D., (2004). Interfacial characterization of iron ore concentrates affected by binders. Powder Technology, 139 (1), pp 1-6.

Rahman, R., Ata, S., Jameson, G. J., (2013). Froth recovery measurements in an industrial flotation cell. Minerals Engineering, 53, pp. 193-202.

Shi, S., Zhang, M., Fan, X., Chen, D., (2015). Experimental and computational analysis of the impeller angle in a flotation cell by PIV and CFD, International Journal of Mineral Processing, 142, pp. 2-9.

Susana, L., Campaci, F., Santomaso, A.C., (2012). Wettability of mineral and metallic powders: Applicability and limitations of sessile drop method and Washburn´s technique. Powder Technology, 226, pp 68-77.

Schwarz, S., Grano, S., (2005). Effect of particle hydrophobicity on particles and water transport across a flotation froth. Colloids and Surfaces A, 256, pp. 157-164.

Tabosa, E., Runge, K., Holtham, P., Duffy, K., (2016). Improving flotation energy efficiency by optimizing cell hydrodynamics, Minerals Engineering, 96-97, pp. 194-202.

Tang, C., Heindel, T.J., (2006). Estimating gas hold-up via pressure difference measurements in a co-current bubble column. International Journal of Multiphase Flow, 32(7), pp. 850-863.

Teipel, U., Mikonsaari, I., (2004). Determining contact angles of powders by liquid penetration. Particle & Particle Systems Characterization, 21 (4), pp 255-260.

Trahar, W., Warren, L. (1976). The floatability of very fine particles – A review, International Journal of Mineral Processing, 3, pp. 103-131.

Van der Westhuizen, A., Deglon, D., (2007). Evaluation of solids suspension in a pilot-scale mechanical flotation cell: The critical impeller speed, Minerals Engineering 20(3), pp. 233-240.

Van Deventer, J.S.J., Van Dyk, W.A., Lorenzen, L., Feng, D., (2002). The dynamic behavior of coarse particles in flotation froths. Part III: ore particles. Minerals Engineering 15, pp. 659-665.

Vinnett, L., Ledezma, T., Alvarez-Silva, M., Waters, K., (2016). Gas hold-up estimation in flotation machines using image techniques and superficial gas velocity. Minerals Engineering, 96-97, pp. 26-32.

Wills. B.A., (1997). Mineral Processing Technology. Butterworth-Heinemann, Burlington.

Yianatos, J., Panire, L., Vinnett, L., (2016). A new method for flotation rate characterization using top-of-froth grades and the froth discharge velocity. Minerals Engineering, 92, pp. 242-247.

Yianatos, J., Bergh, L., Condori, P., Aguilera, J., (2001). Hydrodynamic and metallurgical characterization of industrial flotation banks for control purposes, Minerals engineering 14(9), pp.1033-1046.

Xiangning, B., Guangyuan, X., Yaoli, P., Linhan, G., Chao, N., (2017). Kinetics of flotation. Order of process, rate constant distribution and ultimate recovery. Physicochemical Problems of Mineral Processing .53(1), pp. 342-365.

Zheng, X., Franzidis, J-P., Manlapig, E., (2004). Modelling of froth transportation in industrial flotation cells Part I. Development of froth transportation models for attached particles. Minerals Engineering 17, pp. 981-988.

Zhu, X., Li, C., Yang, C., Wang, G., Geng, W., Li, T., (2013). Gas-solids flow structure and prediction of solids concentration distribution inside a novel multi-regime riser, Chemical Engineering Journal 232, pp. 290-301.

Paper I

SPATIAL VARIATIONS OF PULP PROPERTIES IN FLOTATION - IMPLICATIONS FOR OPTIMIZING CELL DESIGN AND PERFORMANCE

Paper 354

SPATIAL VARIATIONS OF PULP PROPERTIES IN FLOTATION - IMPLICATIONS FOR OPTIMIZING CELL DESIGN AND PERFORMANCE

*Lisa Malm[1], Anders Sand[2], Jan Rosenkranz[2], Nils-Johan Bolin[1]

[1]Boliden Mineral AB
93632 Boliden, Sweden
*(*Corresponding author: lisa.malm@boliden.com)*

[2]Luleå University of Technology, Mineral Processing
97187 Luleå, Sweden

ABSTRACT

Within flotation technology the general trend is towards very large cells. Scale-up is usually done by postulating geometrical similarity, which implies keeping the aspect ratio constant when increasing cell volume. Consequently, the design of flotation circuits typically involves several cells of identical geometry within a bank. Using a few standard sizes in a flotation plant simplifies design, manufacturing and maintenance of the cells, but does not necessarily guarantee optimal performance and selectivity of the flotation process. Geometry parameters for a given cell volume that influence flotation cell performance include cell height, which causes changes in the hydrostatic pressure and suspension hydrodynamics, and also influences the travel distance of particle-bubble agglomerates as well as the homogeneity of the mixing. Also the thickness of the froth layer depends on the aspect ratio of the cell. The objective of this work is to gain a better understanding of material distribution and properties within a flotation cell and, based on this information, elucidate how alterations of the cell geometry can influence separation efficiency. For this purpose systematic measurements and analyses of the spatial distribution of the different phases within a 160 m^3 flotation cell have been carried out with a particular focus on an industrial, low-grade copper ore beneficiation process. The concepts for sampling at different vertical and lateral positions of the flotation cell are introduced. The results from the experimental work give an understanding of internal material distribution within flotation cells. Based on the measured phase distribution and concentrations as well as particle properties at various positions within the cell, the implications for an optimized scaling and design of individual flotation cells within a flotation circuit are discussed.

KEYWORDS

Flotation, Pulp composition, Sampling, Cell dimensioning, Circuit design

INTRODUCTION

Froth flotation is one of the most important unit operations in mineral processing. It is based on different surface properties of materials, i.e. differences in the hydrophobicity, and how these can be utilized for physico-chemical selective separation of various mineral species by use of chemical additives. Within the flotation process a number of sub processes can be distinguished, including collision and attachment of hydrophobic particles to air bubbles, upwards transport of bubble-particle agglomerates to the froth layer, drainage of the froth, followed by detachment and entrainment of the solid material, which is finally transported to the launder and recovered as the concentrate (Wills and Napier-Munn, 2006; Kawatra, 2011). Particle size is known to play a significant role in flotation, with an optimal size range typically in the range of 10-100 µm. Small and light particles tend to follow the liquid phase while the insufficient adhesion of large and heavy particles to air bubbles can prevent them from being transported to the froth (Trahar and Warren, 1976; Espinosa-Gomez et al., 1988; Chipfunhu et al,. 2012).

In order to study the various mechanisms occurring in these sub processes, several directions of flotation research have evolved. From the chemistry viewpoint, interest has been devoted for instance towards the selection or tailoring of collectors, frothers and other reagents that influence the surface properties of particles, froth stability, etc. (Kawatra, 2011; Nagaraj and Farinato, 2015). Mechanical aspects, such as dispersion and mixing efficiency, bubble-particle collision rates, etc. have been extensively studied either experimentally or by e.g. Computational Fluid Dynamics (CFD) and other modeling approaches in order to optimize the process (e.g. Koh and Schwarz, 2006; Shi et al., 2015; Chegeni et al., 2015; Xia et al., 2015).

As capacity is increased and ever lower metal grades are treated in beneficiation plants, the current trend is towards increasingly large cells. While an industrial scale flotation cell in the 1980's was typically around 50 m^3 in size, the flotation cells sold today can be as large as 700 m^3 (Arbiter, 2000; Outotec, 2012). Large cells are typically scaled-up versions of their smaller counterparts, while maintaining a similar aspect ratio. Comparatively few publications have been directed towards systematically investigating the material distribution in different regions within the pulp and in the froth layer of flotation cells (Van der Westhuizen and Deglon, 2007; Zhu et al., 2013; Panire et al., 2015), this in contrast to that such work is highly relevant for proper dimensioning of flotation cells and for influencing the separation results.

This work aims at improving the understanding of the material distribution in flotation cells, which in turn can give important indications regarding the processes taking place within the tank. Material distribution can involve the distribution of phases, particle sizes and minerals as function of lateral and horizontal position in the cell. A better understanding of the material distribution can give useful guidelines for cell dimensioning and finding suitable cell aspect ratios in order to optimize separation performance depending on the cell position within the flotation circuit. In this work, results are presented from both trials conducted in industrial scale (sampling from 160 m^3 cells) and from using a laboratory scale flotation cell with variable height.

MATERIALS AND METHODS

Industrial Scale Sampling

Full scale sampling was carried out at the Boliden concentrator plant of the Aitik mine in Northern Sweden, located 20 km east of Gällivare. The plant was commissioned in 2010 and has since then processed over 36 million tons per year of a low-grade copper ore.

The flotation circuit of the plant has two parallel flotation lines of 160 m^3 cells, each with four rougher cells, five scavengers and four further cells for pyrite flotation. The 160 m^3 cells are supplied with Outotec's FloatForce 1500 agitator. The pyrite flotation cells were during the time of sampling supplied with the FlowBooster modification, but not the rougher and scavenger cells. The first two pyrite flotation cells can be used to prolong the scavenger process by redirecting the concentrate. The rougher concentrate from

both lines continues to a pebble mill for re-grinding and classification via hydrocyclones. The cyclone overflow is sent to the cleaner stage 2. The scavenger concentrate from both lines is pumped to a separate pebble mill for re-grinding and classification via hydrocyclones. The cyclone overflow is sent to the cleaner stage 1. The flowsheet is shown in Figure 1.

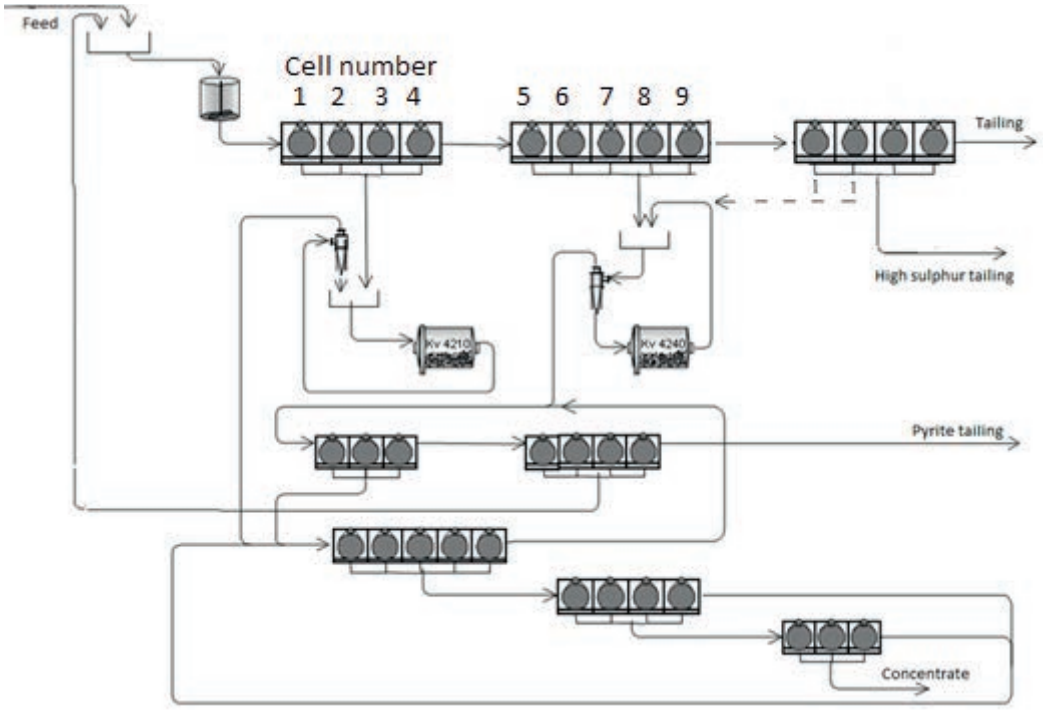

Figure 1 – Flowsheet of Aitik flotation circuit

To obtain an understanding of the material distribution inside the 160 m^3 cells, samples were collected inside the cells using a sealable sampler, which was lowered in closed position down to the desired depth where it was opened to collect a sample. The sampling campaign was conducted in April 2015 and covered the first and last rougher (cell 2 and 4 at the day of sampling, since the first rougher was by-passed due to maintenance work) and first and last scavenger cells of the plant (cell 5 and 9, compare Figure 1). This would probably give differences in results (e.g. Copper grade) in cell 4, 5 and 9 if the same sampling procedure was to be repeated at normal running conditions of the plant. However, it was not deemed critical for this study as the main focus was on internal material distribution within the cells at different positions of the flotation circuit. At the day of the sampling, the feed grade was 0.14 % Cu, which is lower than the average 0.2 % Cu. The flotation feed contained 44 wt-% of solids. Relevant process data from the plant are presented in Table 1. The collector reagent used in the plant is PAX (potassium amyl xanthate).

Table 1 Process data from the flotation cells

Cell number	Conditioning tank	2	4	5	6	8	9
Air addition [m^3/h]		11	10.7	10			15
Froth depth [cm]		21	23	35			30
PAX dosage [g/ton]	2	0.8	0.5	-	1	0.5	-

Three positions were sampled in the first rougher, in order to investigate the variations inside the cell. One position was close to the agitator (B), the second near the outlet (C) and a third closer to the inlet

and between the center and edge of the cell (A). A complementary investigation of the grade on the top of the froth layer was done. The froth layer was sampled by a simple cup with an extended handle, lowered down just far enough for the top of froth to pour into the cup. The samples were taken in 20 cm increments starting from the center and moving outwards to the edge of the cell. The sampling positions are illustrated in Figure 2.

The cells were sampled in sequence and all the samples were collected from one cell before the next cell was sampled. Only the first rougher was sampled in all three positions A-C, while the other cells were sampled in the A position. The top of froth samples were taken in all investigated cells. Samples were taken from a maximum depth of 3.5 meters and up to 0.5 meter from the interface level, with 0.5 m intervals. Complementary samples from 0.3 m depth and just under the froth were also taken. The top of froth and complete froth were also sampled.

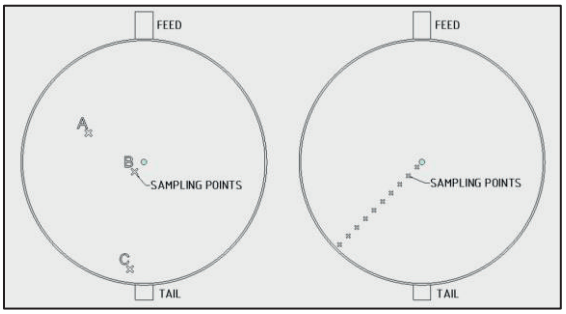

Figure 2 – Three sampling positions in first rougher (left), position of top of froth sampling (right)

There are no easily accessible sampling points for feed and tail for each cell in the Aitik flotation plant. Those streams were sampled with a pump connected to a 6 m long pipe placed as near as possible to the inlet or outlet, respectively. The sampler used for the full scale cells was designed and manufactured within Boliden and is referred to as the Widmatic sampler. A sketch is shown in Figure 3. While in use, the system can be oriented either vertically or laterally. In the present study it was used in the vertical position to allow measurement of the gas hold-up. The sampler has a capacity to sample one liter of pulp and the openings at each sides are closed simultaneously by compressed air. After sampling, the gas hold-up was calculated from collected sample weights and wt-% solids as input, and comparing it to the sampler maximum capacity.

Figure 3 – The Widmatic sampler

In order to evaluate the representativity of samples and whether the gas holdup and particle distribution data was reliable, a supplementary sampling was done with an alternative sampler from Heath

& Sherwood (2015), see Figure 4. A one liter sampler ("model 5105") was used for the deeper positions and a 3 dl sampler ("model 5033") for the positions 1 and 2 m down in the cell. Unlike the Widmatic sampler this device must be opened and closed from the top of the rod. The one liter sampler could not be used after the first cell due to a mechanical failure. At the highest positions in the cell, where the sampling points were more closely spaced, the samples were, therefore, additionally collected in a bottle with a lid that, triggered by a rod, could be opened and closed at a specific depth.

Approximately 100 samples were taken in total during the campaign. Due to the extensive sampling and later size fractionation, only single samples were taken from each position. Therefore, any variation in composition originating from the sampling or time-dependent variations in the cell has not been investigated in this case. All samples were weighed and analyzed for wt.% of solids, fractionated into five fractions by sieving and then analyzed on a table-top ED-XRF (energy dispersive X-ray fluorescence spectrometer). The samples were measured as powder in a cup using a pre-calibrated fundamental parameter model. Without extra sample preparation, such as fine grinding, pelletizing of glass borate smelting, the inaccuracy (expressed as one standard deviation) of XRF performed on different size fractions can be expected to be up to 20- 30 % relative. This inaccuracy is the probable deviation from the true value for ore powders independent of ore type and size fraction. Within a group of samples with the same ore type and size fraction the relative uncertainty inside the group will typically be smaller than 5- 10 % relative (one standard deviation).

Figure 4 – The Heath & Sherwood sampler (heathandsherwood.com)

Laboratory Scale Tests

As a complement to the full scale tests, a number of laboratory flotation tests were carried out to investigate how the flotation cell height as well as the air flow and rotor speed in relation to the cell volume will affect the result. For this purpose, a tailor-made Magotteaux lab-scale flotation cell with the agitator mounted from the bottom was used. The cell allows stepwise adjustment of the cell height by adding or removing rings. The material used for the laboratory tests was rougher feed from the plant. Dedicated sampling devices were developed for the lab flotation cell, one single-point sampler holding about 12 ml and another capable of simultaneously taking multiple samples of 20 ml each. The laboratory cell is illustrated in Figure 5.

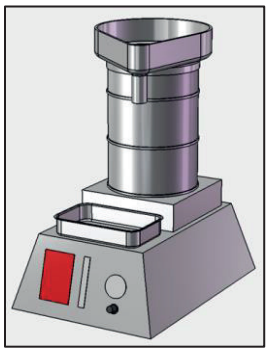

Figure 5 – Magotteaux lab flotation setup with a custom made cell

RESULTS AND DISCUSSION

Rougher and Scavenger Cells

The solids concentration inside the different flotation cells are shown in Figure 6. From the bottom and up to 2 meters height from the surface, there is almost a constant solids concentration of around 42 wt-%. In the quiescent zone, the solids concentration decreases stepwise and tendentially reaches its lowest value just under the pulp-froth interface line with differences in the absolute figures for the considered cells. The P80 is shown to the right in Figure 6. The trend is towards decreased values higher up in the cells. The first rougher deviates from the other investigated cells with a significant higher P80 value in the upper part of the cell. Note that the P80s in the concentrates have the same value as in the lower part of the cells.

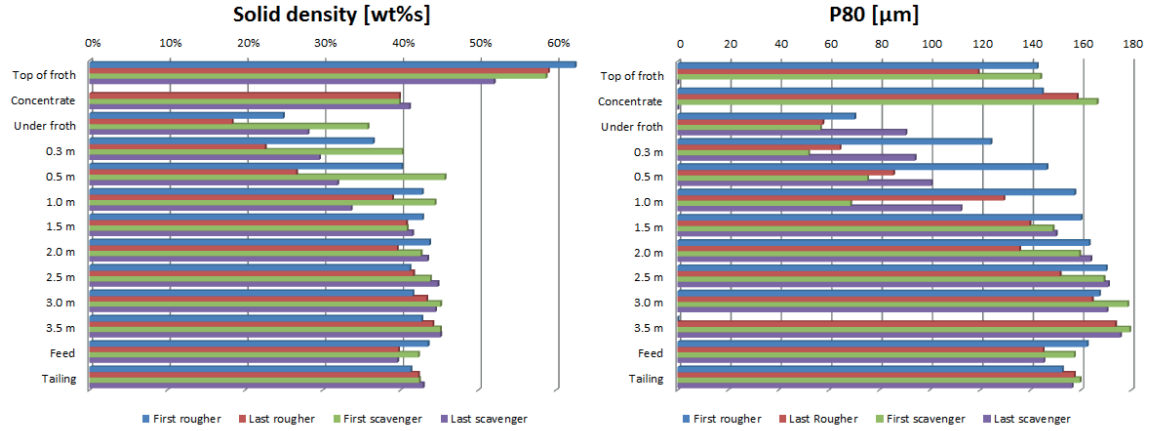

Figure 6 – Distribution of solids concentration inside the cells (left) and the P80 (right)

The mineral grades inside the flotation cells showed a similar trend in all cells, with only small variations. For example, Figure 7 shows the results from the first rougher cell for the size fraction of 20-45 µm particles as this was one of the most easily floatable particle sizes. The grade of quartz was more or less the same throughout the cell. Underneath the interface level, a decrease in quartz grade occurred while the grade of sulphides increased at the same time. It is notable that the composition of mineral content was the same even though the amount of solid particles was lower at the higher position.

Further, it has to be emphasized that the grade of chalcopyrite in the first scavenger was higher than in the last rougher in all fractions, which indicates better flotation in that cell, see figure 7 to the right. As mentioned earlier, the air feed rate was the same in both cells but it is possible that the differences in grade can be accounted to the conditioning time needed for the collector reagent (PAX). The reagent is added at the inlet of the last rougher, which might not allow sufficient conditioning time for it to be efficient in that cell. Reagent not following the concentrate in the last rougher will be carried forward to the first scavenger.

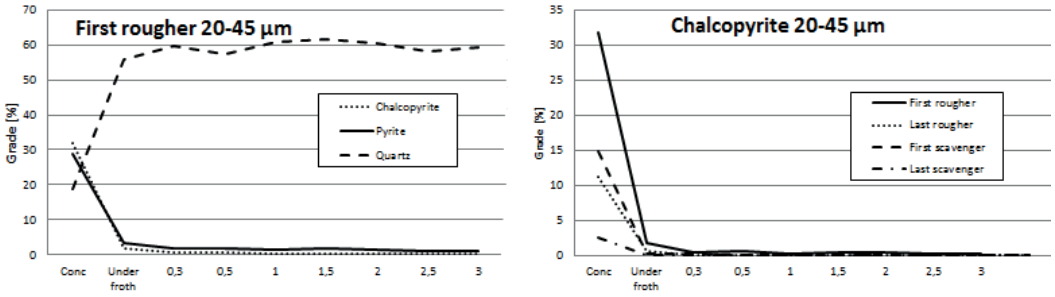

Figure 7 – Mineral grades of 20-45 µm particles inside the first rougher (left) and the chalcopyrite grade in all cells (right)

Samples taken from the top of the froth showed an increase in grade of chalcopyrite, from the centre and outwards, in all the cells investigated. The highest value of chalcopyrite was obtained ca 20 cm from the edge. In all the cells the grade went down close to the edge of the cell, see Figure 8. The grade was highest

in the first cell, with an increase from 30% chalcopyrite at the center point to 40% chalcopyrite just before the edge where it again went down to 35% chalcopyrite.

The last rougher and the first scavenger showed a similar trend, with an increase from 15-20 to 30% chalcopyrite and a small drop just at the edge. The last cell showed grades between 5 and 7% chalcopyrite, and also exhibited the typical grade drop at the edge of the cell.

Along with the increase in copper content at the top of the froth, quartz showed the opposite trend with the highest grade being found at the center of the cells, compare Figure 8.

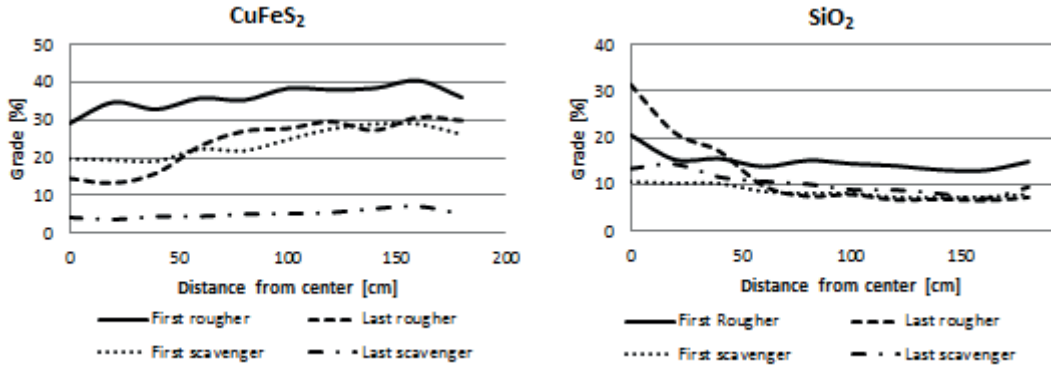

Figure 8 – Top of froth measurements, chalcopyrite (left) and quartz (right)

A comparison of the results obtained the Widmatic sampler and the one from Heath & Sherwood showed that the particle size distribution was almost the same (in every second sample the H&S sampler collected slightly more -20µm) but the gas hold up value was consistently lower with the Widmatic sampler, i.e. 2-5% air compared to 7-12 % air as measured with the H&S sampler. Therefore, there is a need for additional sampling before more detailed conclusions can be drawn regarding the gas hold-up calculation with different samplers. The air holdups in the first rougher are shown Figure 9, where it can be seen that there is a difference between the two samplers as well as variations inside the cell.

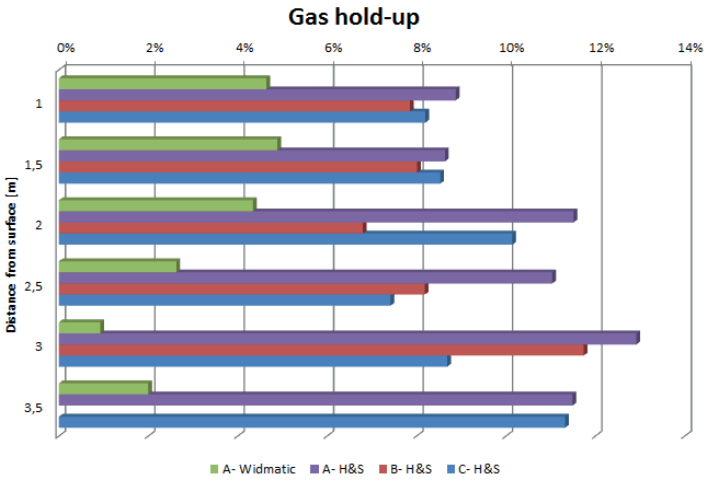

Figure 9 - The Gas hold-up for different position and samplers in first rougher

Cleaner Cells

The major finding from sampling the cleaner cells was that the cleaning process easily floated the coarser particles that were present in the feed to the cleaners. The material was, however, predominantly in the finer fractions, particularly in the first cleaning stage where the scavenger concentrate was processed. The scavenger survey also showed a higher percentage of smaller particles in the concentrate, as compared to the rougher cells. Just over 40 wt.% of the material in the first cleaning feed was finer than 10 µm and 75 wt.% were finer than 45 µm, compare Figure 10.

The recovery of particles below 20 µm decreased during the flotation process and particularly particles smaller than 10 µm were difficult to concentrate with an acceptable recovery. This survey showed a decrease of copper in the <10 µm fraction in the first cleaning bank from 3.11% Cu in the feed to 0.24% Cu in the tailings. The coarser fractions, however, had a copper grade between 0.07 and 0.09% Cu in the tailings. In the second cleaner stage 50 wt.% of the particles were finer than 20 µm in the feed, which implies a slightly coarser feed than in the first cleaner.

The trend of the solids concentration within the cleaning cells was opposite to that in the rougher. At the bottom of the cells, the solids concentration was around 10 wt.%. At a depth of one meter under the surface, the solids concentration started to increase and just underneath the surface interface the solids concentration was between 40 and 50 wt.%.

The cleaner cells typically have a one meter froth layer, and the froth samples showed that the last of the cleaner cells had the same copper grade throughout. This means that there was no upgrading of the concentrate in the froth of that cell. The particle size distribution was finer in the bottom of the last cleaning cell than inside the froth and in the final concentrate.

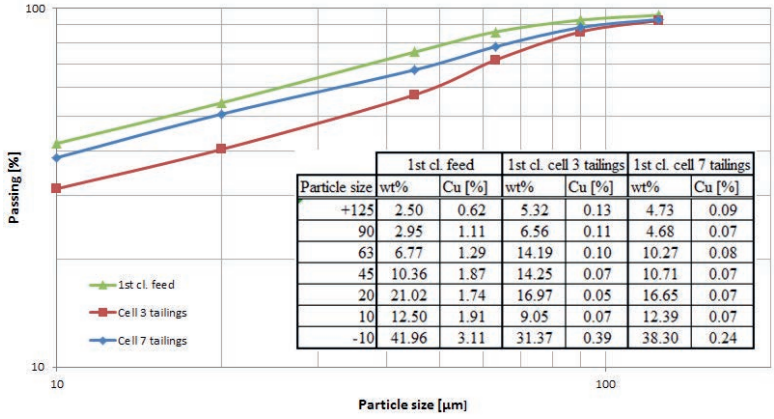

	1st cl. feed		1st cl. cell 3 tailings		1st cl. cell 7 tailings	
Particle size	wt%	Cu [%]	wt%	Cu [%]	wt%	Cu [%]
+125	2.50	0.62	5.32	0.13	4.73	0.09
90	2.95	1.11	6.56	0.11	4.68	0.07
63	6.77	1.29	14.19	0.10	10.27	0.08
45	10.36	1.87	14.25	0.07	10.71	0.07
20	21.02	1.74	16.97	0.05	16.65	0.07
10	12.50	1.91	9.05	0.07	12.39	0.07
-10	41.96	3.11	31.37	0.39	38.30	0.24

Figure 10 – Particle size distribution in first cleaner bank (Lappi, 2015)

Laboratory Flotation Tests

A number of early batch tests were carried out using the Magotteaux lab flotation cell with adjustable height and using the Aitik rougher feed directly collected from the plant. The purpose of these tests was to obtain first qualitative indications regarding the influence of cell height on flotation performance. With the taller cell design the copper grade increased but at the expense of recovery. The concentrate also had a higher percentage of finer particles compared to the concentrate from the lower cell. The flotation rate constant decreased when the cell height was increased, see Figure 11. In the tests, the rotor speed was increased accordingly when the cell height and consequently also cell volume was increased. This circumstance could probably have changed the bubble size.

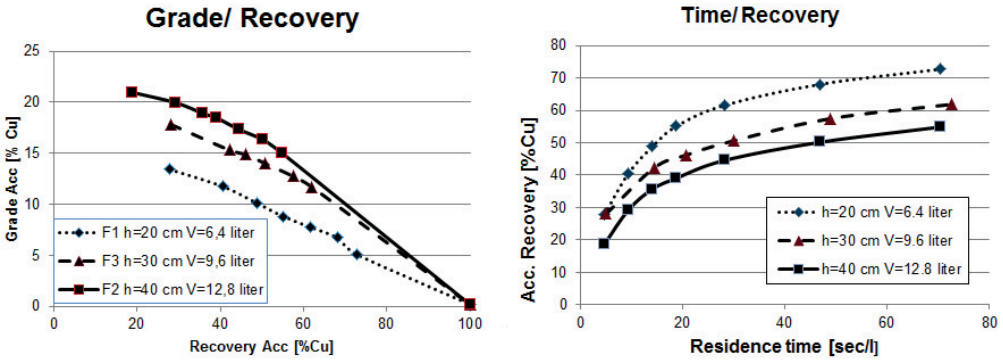

Figure 11 – Lab flotation results at varying cell height

The experience from the first lab tests, with significant variation in percentage solids inside the cell (measured by using a sampling device capable of taking samples from different positions simultaneously) and lower recovery than expected, indicates that several factors need to be further optimized. For instance, there is a need for higher mixing energy in the taller cell configuration, which will change the bubble size and this needs further investigation. No further reagents were added for the lab flotation tests, as the samples used already contained reagents added in the concentrator plant. This could explain the low recovery as shown in Figure 11. It is, however, possible that there is also a need to optimize e.g. the collector addition in order to achieve better recoveries in the lab tests. Further tests will be conducted with other streams as well, in order to compare the results and to find the optimal lab flotation height for each feed stream.

DISCUSSION

To summarize the findings in the tank cells, there is a big difference in the pulp density at different heights. The solid concentration inside the rougher/ scavenger cells have, during this survey, been well mixed up to 2 meters depth from the surface. Above that, in the quiescent zone, the mixing energy is waning and there is probably a combination of weaker mixing and flotation/ rising of air bubbles that make up the composition of the quiescent zone. Sedimentation effects likely also play a role.

It is of greatest interest to have spatial information about the particle size distribution in conjunction with the grades of the tailing and concentrate fraction in order to handle it in the right way in the next stage. This investigation showed that the scavenger cells were floating high amounts of smaller particles (< 60 µm) and larger particles (>125 µm). The reason may be that the most easily floated particles, with appropriate surface properties, have already floated in the previous cells. The measurements in the first cleaning cells (where the scavenger concentrate is floated) showed a feed of even smaller particles due to the use of a regrinding mill. Based on the findings from this work, it was tested to shut down the regrinding mill. However, when the feed contains higher amounts of sulphur, it has been found that there is still a need for regrinding with lime to depress pyrite.

The segregation observed in the scavenger cells could make it difficult for a part of the sulphur minerals to reach the froth phase. Better mixing could possibly increase the amount of coarse and non-liberated particles floating. Therefore, a FlowBooster will be tested with the expectation that the recovery of sulphur minerals can be increased. The FlowBooster mechanism is available for the Outotec tank cell for direct installation on the shaft. It is expected to increase the mixing within the upper parts of the cell. The FlowBooster mechanism in the pyrite cells was installed late spring 2015 within a Boliden project for increasing the pyrite recovery. The two parallel lines at Aitik should make it easy to evaluate whether the FlowBoosters have an effect or not.

The sampling of the first rougher verifies that there is a good recovery of all fractions, despite the same differences of solids distribution over height as in the scavenger cells. This suggests that the dimensions (heights) could be of secondary importance in the first rougher cells.

The results from the lab scale flotation test show a decrease in the flotation kinetic rate constant when using a higher cell. They also indicated a higher copper grade and a lower recovery. A more complete study is intended for the future, but if the full scale flotation cells exhibit the same behaviour as the initial test results with the lab cell, it needs to be investigated at which height-diameter ratio the full scale cells start to lose recovery and increase grade. The mineral composition and size of particles lost should also be explored further. If the results mainly are caused by weaker agitation in a higher lab cell with an increased quiescent zone, it would be possible to alter the flow dynamics in the cell by using a FlowBooster mechanism that increases the mixing energy.

As to the sampling equipment, no remarkable differences in particle size distribution between the different sampling systems were noted. However, the gas hold up was consistently higher in the H&S sampler compared to the Widmatic. This could perhaps be explained by leaking of air from the Widmatic lids combined with slurry coming in to the sampler on the way up through the cell even though no such problems were noticed during sampling. The H&S sampler has lids on both sides of the container which may affect the flow into the sampler. Therefore, another reason may be that the H&S sampler is not shutting both lids simultaneously, i.e. that the upper lid is closed slightly sooner allowing for some extra air to enter from the bottom. The gas hold-up results will have to be evaluated further and perhaps completed by additional tests before any conclusions can be drawn. For further sampling inside the full scale flotation cell, a new sampler will be designed at Boliden.

CONCLUDING REMARKS

The internal mineral distribution in both the rougher and the cleaner flotation cells have been mapped. The findings have provided, first of all, knowledge on the mineral distribution inside the cell as well as on the differences in pulp solid content. This resulted in several actions for improvement. For instance, for the scavenger flotation circuit, which was designed for floating non-liberated particles, the investigation showed that not many of the coarse mixed grain particles were floated but a greater proportion of fine particles. A new survey needs to be done after an installation of the FlowBooster in the scavenger cells to see whether a better mixing will result in better flotation of the coarser particles.

The height/ diameter ratio of the first rougher in a plant does not appear to be that significant since it floats the easiest floatable minerals in all particle sizes. The aspect ratio and function of subsequent cells is more important, since these are dealing with particles that are more difficult to float in a regular flotation tank cell. Therefore, the FlowBooster mechanism will not be installed in the first roughers and for dimensioning a flotation circuit, the focus should lie on the scavenger cells.

As part of the further work, more systematic studies will be conducted using the laboratory cell with variable height. This work will include variation of air addition and agitator speed, in order to closer evaluate the influence of cell height at various conditions. There are also plans to conduct pilot scale tests with different ratios between diameter and height. The tests in pilot scale will be carried out with two pilot cells in parallel. The first tests will be done with Aitik's rougher feed in order to study how the aspect ratio is affecting the results. Studies will also be carried out on the feed to the copper cleaners where the effect of residence time and the carrying capacity limitations will be studied. The influence of the FlowBooster on flow dynamics inside the cell will be further evaluated through CFD simulation.

ACKNOWLEDGMENTS

The authors gratefully acknowledge that the work has been performed with financial support from the Swedish Governmental Agency for Innovation Systems (VINNOVA). The study presented here would not have been possible without the support from Boliden Mineral AB and the personnel at the Aitik mine.

REFERENCES

Arbiter, N. (2000). Development and scale-up of large flotation cells, Mining Engineering 52(3):28-33.
Chegeni, M., Abdollahy, M., Khalesi, M. (2015). Column flotation cell design by drift flux and axial dispersion models, International Journal of Mineral Processing, in press.
Chipfunhu, D., Zanin, M., Grano, S. (2012). Chemical Engineering Research and Design 90(1): 26-32.
Espinosa-Gomez, R., Finch, J., Yianatos, J., Dobby, G. (1988). Flotation column carrying capacity: Particle size and density effects, Minerals Engineering 1(1):77-79.
Heath & Sherwood (2015). Manual for Probe PD Sampler, http://heathandsherwood64.com/products/sampling/manual_probe_pd, Downloaded 2015-12-02.
Kawatra, S.K. (2011). Fundamental Principles of Froth Flotation, in SME Mining Engineering Handbook, 3rd Edition, Editor: Darling, P. ISBN 978-0-87335-264-2.
Lappi, S. (2015). Study of the cleaner flotation in Aitik, Master's thesis, University of Oulu, Oulu, Finland.
Outotec (2012). 100 Years of Flotation Technology, www.outotec.com. Downloaded 2015-12-09.
Koh, P., Schwarz M. (2006). CFD modelling of bubble-particle attachments in flotation cells, Minerals Engineering 19(6-8):619-626.
Nagaraj, D., Farinato, R. (2015). Evolution of flotation chemistry research: a century of innovations and the emerging challenges, Flotation 2015, Minerals Engineering International, November 16-19, Cape Town, South Africa.
Panire, I., Vinnett, L., Yianatos, J. (2015). Flotation rate characterization using top of froth grades and froth discharge rates in rougher flotation circuits, Flotation 2015, Minerals Engineering International, November 16-19, Cape Town, South Africa.
Shi, S., Zhang, M., Fan, X., Chen, D. (2015). Experimental and computational analysis of the impeller angle in a flotation cell by PIV and CFD, International Journal of Mineral Processing 142:2-9.
Trahar, W., Warren, L. (1976). The floatability of very fine particles – A review, International Journal of Mineral Processing 3:103-131.
Van der Westhuizen, A., Deglon, D. (2007). Evaluation of solids suspension in a pilot-scale mechanical flotation cell: The critical impeller speed, Minerals Engineering 20(3): 233-240.
Wills, B. and Napier-Munn, T. (2006). Mineral Processing Technology – An Introduction to the Practical Aspects of Ore Treatment and Mineral Recovery, 7th Ed., Butterworth-Heinemann, ISBN 978-0-7506-4450-1.
Xia, J., Rinne, A., Lohilahti, J., Dube, R., Mattsson, T. (2015). CFD Analysis in Designing of Mixing Mechanism for a Mechanical Flotation Machine, AIChE Annual Meeting, November 8-13, Salt Lake City, UT.
Zhu, X., Li, C., Yang, C., Wang, G., Geng, W., Li, T. (2013). Gas-solids flow structure and prediction of solids concentration distribution inside a novel multi-regime riser, Chemical Engineering Journal 232: 290-301.

Paper II

APPLICATION OF DYNAMIC VAPOR SORPTION FOR EVALUATION OF HYDROPHOBICITY IN INDUSTRIAL-SCALE FROTH FLOTATION

Minerals Engineering 127 (2018) 305–311

Contents lists available at ScienceDirect

Minerals Engineering

journal homepage: www.elsevier.com/locate/mineng

Application of Dynamic Vapor Sorption for evaluation of hydrophobicity in industrial-scale froth flotation

Lisa Malm[a,*], Ann-Sofi Kindstedt Danielsson[b], Anders Sand[c], Jan Rosenkranz[c], Ingvar Ymén[b]

[a] Boliden Mineral, Dept. of Process Technology, SE-936 81 Boliden, Sweden
[b] RISE – Research Institutes of Sweden AB, Surface, Process and Pharmaceutical Development, SE-151 36 Södertälje, Sweden
[c] Minerals and Metallurgical Engineering, Dept. of Civil, Environmental and Natural Resources Engineering, Luleå University of Technology, SE-971 87 Luleå, Sweden

ARTICLE INFO

Keywords:
Dynamic Vapor Sorption
Hydrophobicity
Dichromate
Froth flotation
Industrial scale

ABSTRACT

The particle surface properties are essential for understanding froth flotation, particularly for the evaluation of various chemical or reagent effects.

Dynamic Vapor Sorption (DVS) is used in the pharmaceutical industry for the evaluation of surface properties and has to the knowledge of the authors not been used for applications in mineral processing. This paper describes an evaluation of industrial ore samples using DVS.

Four samples (feed, CuPb concentrate, Cu concentrate and Pb concentrate) from each of the Cu – Pb flotation processes in the Boliden and Garpenberg concentrators, Sweden, were analyzed by DVS in order to investigate if this technique could be used to estimate differences in their hydrophilicity. The DVS measures the water uptake as a function of the relative humidity (%RH) at constant temperature.

For both series of four samples, it was found that the DVS-data are in precise agreement with the flotation theory on hydrophobicity (indicated by differences in water uptake). The feed material, without any collectors, adsorbed more water compared to the CuPb bulk concentrate, which in turn adsorbed more water than the Cu concentrate. The lead concentrate on the other hand, which had been depressed by dichromate and should be more hydrophilic, showed a higher adsorbance of water than that of the CuPb concentrate.

The repeated measurements of three sub samples from one of the ore samples gave a mean value and an estimated standard deviation of 0.13 ± 0.01%. This shows that the method gives highly reproducible results and that the differences between the samples had high significance. This also shows that the DVS method can serve as a useful complement to traditionally used contact angle or capillary absorption-based measurement methods, especially when screening for new flotation reagents on industrial ore samples.

1. Introduction

In froth flotation crushed and ground mineral particles in aqueous suspension are mixed with one or more collectors. These are typically amphiphilic molecules with polar and non-polar end groups. Under the right conditions, the polar ends of the collector molecules can selectively bind to the surface of certain minerals, thus leaving them with a surface more or less covered with non-polar molecular tails. This renders these mineral particles more hydrophobic than mineral particles where no collector has attached. These differences in hydrophobicity between the different minerals forms the basis of the flotation process. The choice of collector reagent, together with the chemical conditions in the pulp, affects the degree of hydrophobicity on selected minerals (Wills, 1997).

In a flotation process, a number of flotation steps are utilized and in the case where several valuable minerals have been floated and are to be separated from each other, a so-called depressant may be used. A depressant can act in two ways, first to selectively inhibit the adsorption of collector to ascertain mineral, or secondly to restore the hydrophilicity of particles which have floated in a previous step. Consequently, the depressed minerals will either go to the middling product for further processing or end up as a final concentrate. Both the action of the collector and depressant is strongly pH dependent. In this way, different minerals may be separated by manipulating their surface properties (Wills, 1997; Kawatra, 2011).

Dichromate is one of those depressant reagents, which can be used for the separation of copper and lead. The depressant is still used in the Garpenberg and Boliden concentrators, both owned by Boliden Mineral. The process employs bulk flotation of copper and lead with PAX (potassium amyl xanthate) and in a second stage galena is depressed by

* Corresponding author.
E-mail address: lisa.malm@boliden.com (L. Malm).

https://doi.org/10.1016/j.mineng.2017.11.004
Received 7 June 2017; Received in revised form 2 November 2017; Accepted 8 November 2017
Available online 21 November 2017
0892-6875/

using sodium dichromate (Bolin et al., 2003; Bulatovic, 2007)

The problem with using dichromate is that it is both carcinogenic and an environmental hazard. Since ECHA (echa.europa.eu) has put dichromate on the authorization list, the ongoing research for finding a suitable alternative reagent has been intensified (Laskowski et al., 1991; Bolin and Laskowski, 1991; Javadi and Rao, 2016). The work described in this paper is a part of a larger research program included in studying the reason why dichromate is successful as a depressant of galena, which might aid in the selection of a similar reagent that works in the same way (Lundmark and Ymén, 2017).

In order to identify new suitable depressants for the inhomogeneous mineral samples collected in the concentrators, one way is to compare the hydrophobicity between two identical ore samples treated with different reagents. In practice, there are several ways to compare the hydrophobicity of related materials. Such methods typically entail measuring the contact angle either on a flat surface of a mineral or as capillary methods e.g. the capillary rise method on a compacted powder or the capillary pressure method, (Akdemir, 1997; Qiu et al., 2004; Chau, 2009; Iveson et al., 2000; Alghunaim et al., 2016; Iveson et al., 2004). However, these methods suffer from serious drawbacks, e. g. that the direct contact angle measurement must be made on a large, reasonably flat and preferably non-permeable surface. This is not possible on a mineral sample taken directly from a flotation process (Susana et al., 2012). The capillary methods on the other hand are sensitive to particle properties, such as size and shape distributions and surface properties. In addition, the methods require the use of packed mineral powder samples where the packing procedure is of importance and has been shown to affect the reproducibility (Susana et al., 2012; Teipel and Mikonsaari, 2004).

Other factors that affect the contact angle measurements could be the surface roughness, particle size or shape and the heterogeneity of the ore sample. The selection of liquids has also been shown to be sensitive to the equipment design (Teipel and Mikonsaari, 2004; Kirdponpattara et al., 2013).

In this work Dynamic Vapor Sorption, DVS (sometimes also referred to as Gravimetric Vapor Sorption, GVS) was used for characterization of wettability properties of minerals. The DVS method is an analytical method where the adsorption of water (or solvent) onto the particles, in the form of a powder, is measured as a function of the relative humidity (or the solvent partial pressure) at a constant temperature. In the pharmaceutical industry this technique has been used for a long time to measure the moisture sensitivity of active pharmaceutical ingredients, but has to the knowledge of the authors not been used for applications in mineral processing (Buckton and Darcy, 1995; Heng and Williams, 2011).

The purpose of this work was to investigate the effect of the depressant collector system on the surface properties of mineral samples. Four samples from different locations of the Cu/ Pb- flotation circuits of two concentrators were evaluated with the DVS method and compared with each other. The samples were also analyzed with XRPD and the particle size analyzed by laser diffraction for obtaining a better understanding of the results from the DVS measurement.

2. Materials and methods

2.1. Materials

Four pulp samples were collected from each of the flotation processes in Garpenberg and in Boliden. The samples were (a) ore feed to the 1st flotation step, (b) the CuPb concentrate, before Cu- Pb separation, (c) the Cu-concentrate, which floated in the Cu-Pb separation step and (d) the Pb concentrate, which was depressed with dichromate in the Cu-Pb separation step.

The samples were filtered and dried in an oven at 80 °C.

2.2. Methods

2.2.1. Dynamic Vapor Sorption

A DVS-instrument is basically a very sensitive balance, with a sample cup and an empty reference cup, which are both flushed with an extremely well controlled moist gas stream. The %RH of the gas stream is obtained by careful mixing of two gas streams, one with 0 %RH and one with 100 %RH. The mass flow control meters of the two gases are extremely accurate giving very exact %RH-values. The %RH obtained is also checked with a dew-point sensor.

The instrument used in this paper is a Surface Measurement Systems DVS Advantage instrument, in which the balance can operate at a constant temperature between 5 and 60 °C. The temperature is controlled by keeping the whole assembly in a closed cabinet with very sensitive temperature sensors and heaters/coolers. It uses a sample amount between 1 and 150 mg (5–70 mg in this work) with a sensitivity of 0.1 μg and, if water is used, with a percent relative humidity between 0 and 98 %RH and an accuracy of ± 0.5 %RH.

The instrument was used to measure the water uptake as a function of the relative humidity at 25.0 °C. A % Partial Pressure Method was used. The sample weight was monitored while the sample was exposed to different relative humidities (%RH). The sample was first dried with dry nitrogen gas for 1 hour before the 1st cycle. The sample was then allowed to adsorb water in the 1st sorption/desorption cycle, where the %RH was increased stepwise up to 95 %RH (10, 20, 30, 40, 50, 60, 70, 80, 90 and 95 %RH) and then down to 0 %RH again. The sample was once again dried for 1 hour at 0 %RH, before another identical cycle, the 2nd sorption/desorption cycle, was run. In both sorption/desorption cycles, at each step, the sample was kept at the set relative humidity until $dm/dt < 0.002\%$, over a period of 5 min (a lower value of dm/dt will increase accuracy and lower the sample hysteresis, at the expense of increased measuring time).

2.2.2. Particle size measurements by laser diffraction

The particle size distribution data for the collected ore sample were obtained with a Malvern Mastersizer 2000, equipped with a Hydro 2000S presentation unit. A sample RI of 2.000 was used as well as a dispersant Miglyol, with an RI of 1.449 and an absorption value of 0.05. Measurements were performed by adding each sample directly to the presentation unit, which was stirred at 2500 rpm. Three measurements were performed on each sampling and each ore sample was sampled four times, two with and two without prior ultrasonication. Each ore sample was thus measured 12 times. From the analyses mean values of different particle size parameters were calculated with and without ultrasonication.

2.2.3. X-Ray powder diffraction (XRPD)

XRPD-analyses were performed at 22 °C on a PANalytical X'Pert PRO instrument, equipped with a Cu, long fine focus X-ray tube and a PIXcel detector. Automatic divergence and anti-scatter slits were used together with 0.02 rad Soller slits and a Ni-filter. Samples prepared at 22 °C were ground in an agate mortar and were then smeared out on cut Silicon Zero Background Holders (ZBH). In order to increase the randomness of the samples they were spun during the analysis. All samples were analyzed between 2 and 80° in 2θ. The full detector capacity of 256 channels was used and all samples were scanned continuously with a 2θ step size of 0.007° and a measuring time of 39.27 s per step.

3. Results and discussion

The XRPD-data for the ore samples are given in Figs. 1 and 2.

The data were matched against the JCPDS-database (PANalytical ICDD PDF-2 database). The minerals in Table 1 were found to match with the diffraction data. It should be noted that pyrite and sphalerite have X-ray peaks at very similar positions and are therefore difficult to separate, even when they are present in significant amounts. When

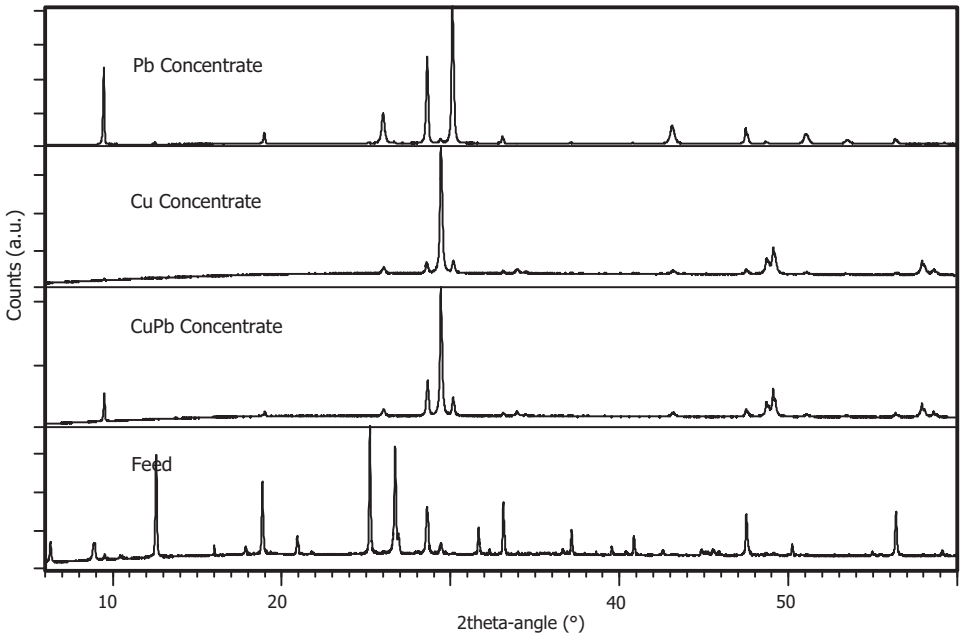

Fig. 1. XRPD-data for the Boliden ore.

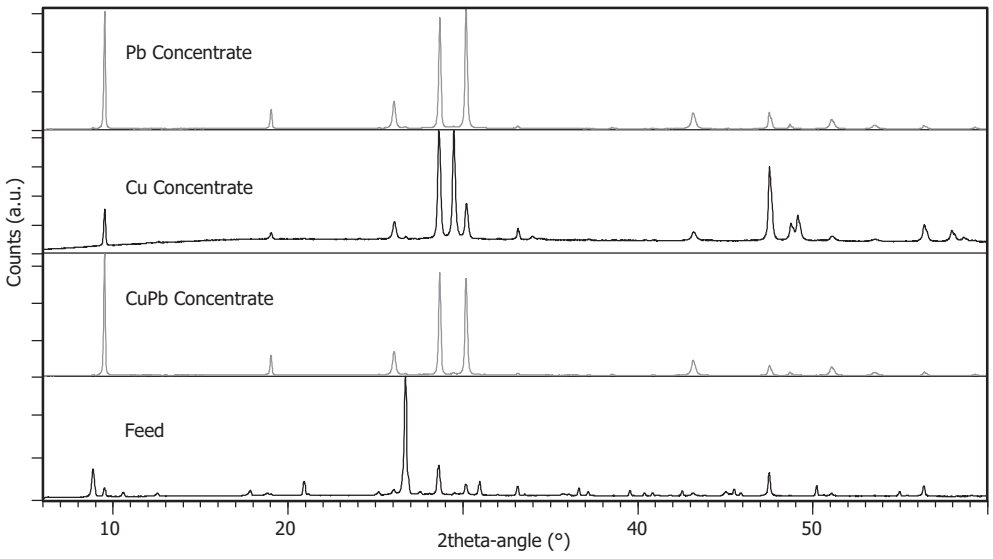

Fig. 2. XRPD-data for the Garpenberg ore.

Table 1
Minerals identified by XRPD in the ore samples. X = present in significant amounts, M = present in minor amounts, 1 = includes calcite and chalcopyrite, 2 = includes muscovite and biotite type, 3 = includes pyrite and sphalerite. B and G denote Boliden and Garpenberg, respectively.

Ore sample	Actinolite	Chalcopyrite[1]	Chamosite	Dolomite	Galena	Muscovite[2]	Pyrite[3]	Quartz	Talc
Feed (B)	M	M	X	–	–	M	X	X	–
CuPbK (B)	–	X	M	–	M	–	M	–	X
CuK (B)	–	X	–	–	M	–	M	–	–
PbK (B)	–	M	M	–	X	–	X	–	X
Feed (G)	M	M	X	X	X	X	X	X	X
CuPbK (G)	X	X	M	–	X	–	X	M	X
CuK (G)	X	X	–	–	X	–	X	M	X
PbK (G)	X	X	M	–	X	–	X	M	X

present in small amounts similar situations exist for calcite and chalcopyrite and for biotite and muscovite. Dolomite is only found in the Garpenberg ore, making this ore naturally alkaline.

In Figs. 3 and 4 the results from the eight DVS-analyses of the ore samples are shown. The figures show the %RH on the abscissa and the moisture uptake on the ordinate (as the % change in mass of the sample). The figures show the different sorption- and desorption cycles and observe the differences in scale. In Fig. 5 the kinetics for the DVS-measurement of the Boliden feed material is shown. The top, stair-shaped curve refers to the right y-axis, ie it shows how the %RH is

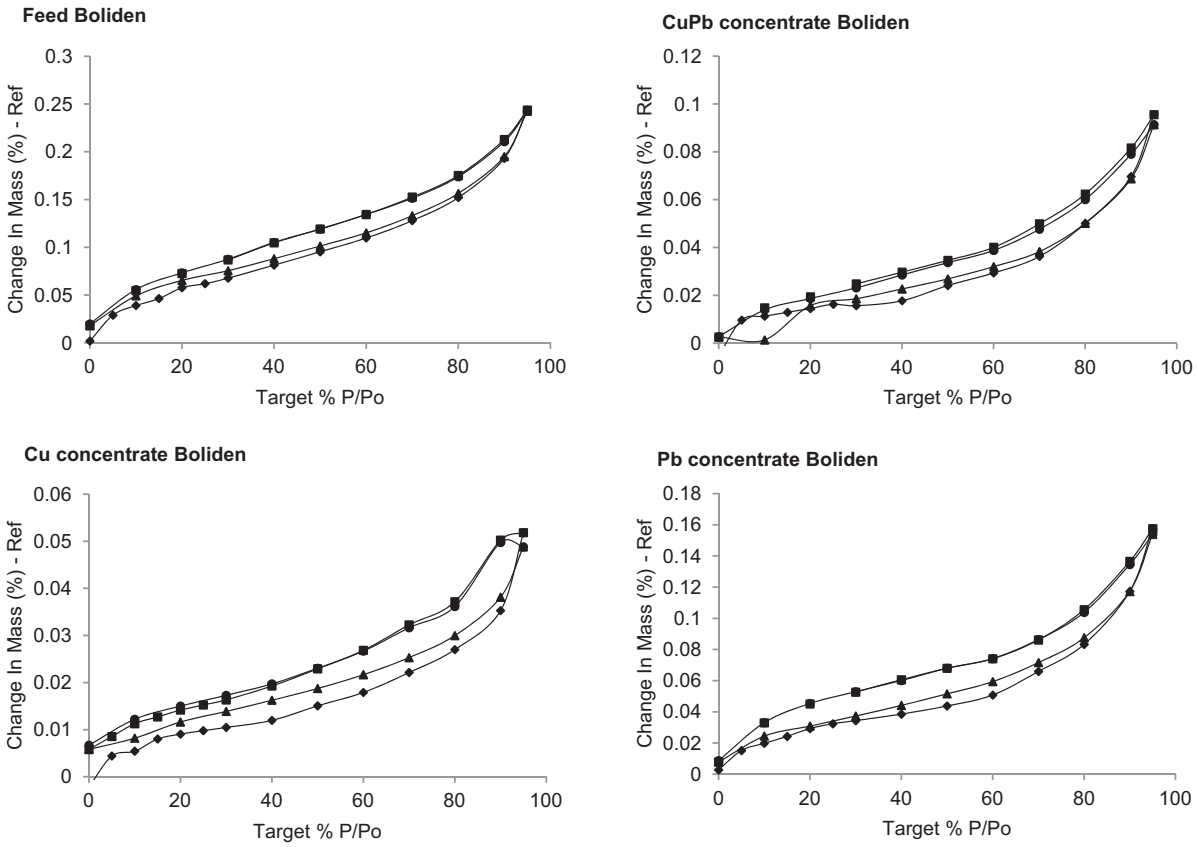

Fig. 3. DVS- data for Boliden ore, Diamonds = 1st sorption cycle, squares = 1st desorption cycle, triangles = 2nd sorption cycle and circles = 2nd desorption cycle.

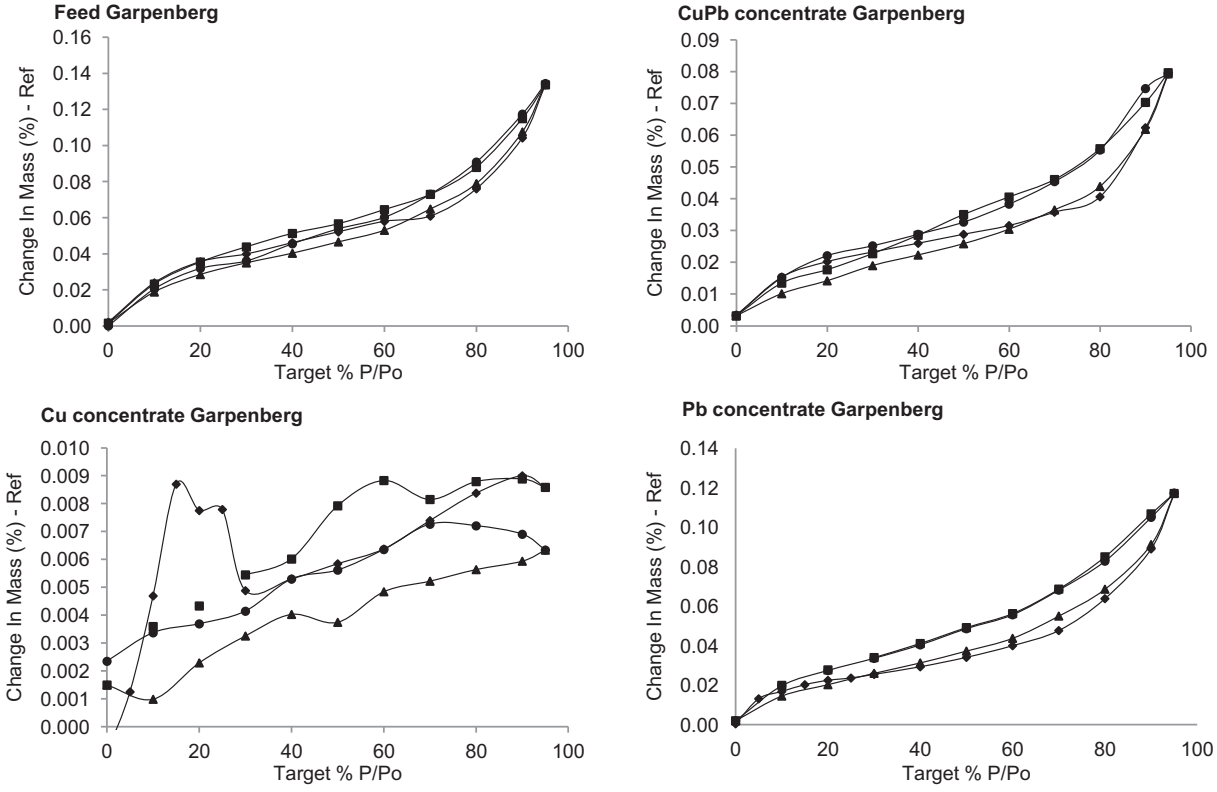

Fig. 4. DVS- data for Garpenberg ore, Diamonds = 1st sorption cycle, squares = 1st desorption cycle, triangles = 2nd sorption cycle and circles = 2nd desorption cycle.

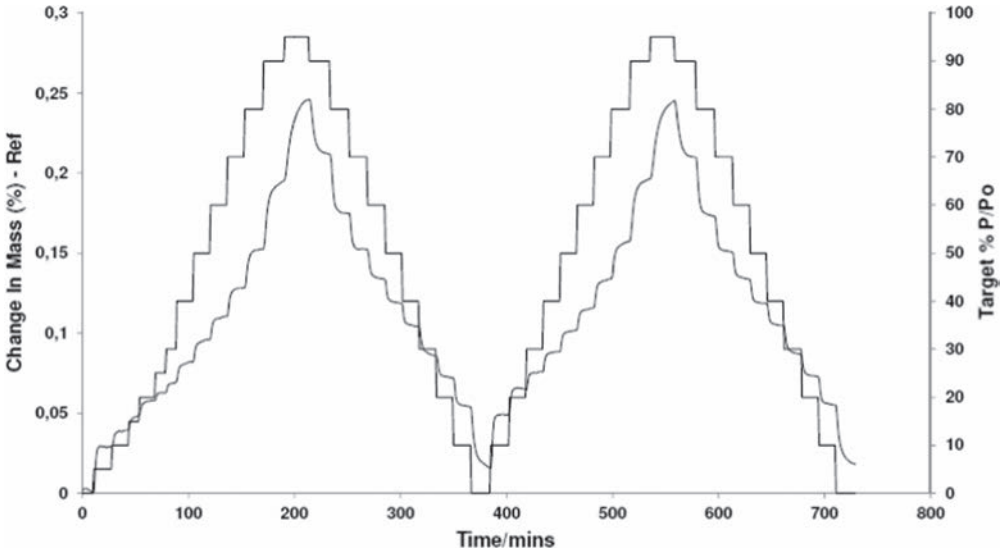

Fig. 5. The kinetics for the DVS measurement of the Boliden feed ore.

Table 2
DVS-data for the eight ore samples. The water uptakes at 95 %RH in sorption cycles 1 and 2 are given.

Ore sample	95 %RH sorption cycle 1 [% mass change]	95 %RH sorption cycle 2 [% mass change]	95 %RH mean [% mass change]
Feed (B)	0.2437	0.2425	0.243
CuPbK (B)	0.0955	0.0913	0.094
CuK (B)	0.0518	0.0488	0.050
PbK (B)	0.1575	0.1538	0.156
Feed (G)	0.1337	0.1344	0.134
CuPbK (G)	0.0797	0.0793	0.079
CuK (G)	0.008	0.006	0.007
PbK (G)	0.1172	0.1174	0.117

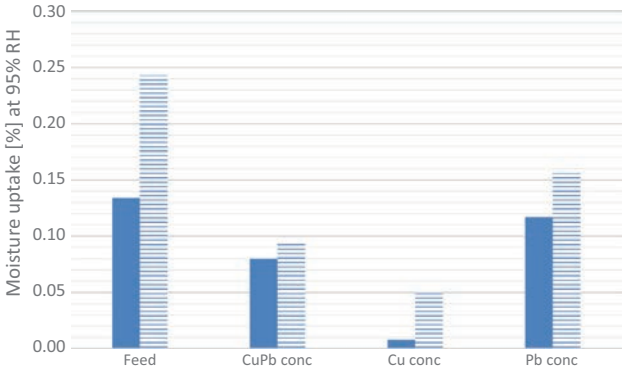

Fig. 6. The moisture uptake at 95 %RH for the ore samples. The filled columns are from Garpenberg and the striped ones from Boliden.

changed. The lower curve refers to the left y-axis and shows the sample response to the %RH-change.

When the water uptake levels of the different ore samples are compared, it is obvious that there are significant differences between them. In fact, one ore sample (the Garpenberg Cu concentrate in Fig. 4 – bottom left) is so hydrophobic that the DVS instrument is struggling to obtain an equilibrium. This is seen as a fairly random water uptake as a function of %RH. Therefore, the reproducibility can also be expected to be adversely affected for samples with very low hydrophobicity.

One way of comparing the data is by simply listing the amounts of water taken up at 95 %RH, as is presented in Table 2. These data have been plotted in Fig. 6. The trend is the same for samples from Garpenberg and Boliden; for both ores the incoming material is most hydrophilic, the CuPb-concentrate is significantly more hydrophobic, the Cu-concentrate is even more hydrophobic, whereas the depressed Pb-concentrate has again become more hydrophilic.

The results are in precise agreement with flotation theory considering that Potassium Amyl Xanthate (PAX) modifies the surface properties to be more hydrophobic and consequently the floated product should be more hydrophobic compared to the non-treated feed material. For each cleaning step in a flotation plant the expected results is to have an incrementally higher grade at the expense of recovery. Therefore, it is logical that Cu- concentrate is more hydrophobic than the CuPb- concentrate. Also, a concentrate containing a mixture of galena and chalcopyrite is expected to have different hydrophobicity than any of the pure constituent. The addition of potassium dichromate to the Cu-Pb separation step renders the Pb-fraction more hydrophilic, thus depressing it successfully.

In order to obtain information about the significance of these data the Garpenberg feed ore was analyzed several times; first five consecutive analyses were performed on the same sample placed in the DVS-balance and then two new samples were analyzed, one twice and the other one three times. Since each analysis consists of two cycles, this altogether constitute 20 analyses to compare. The moisture uptakes at 95 %RH for all of these analyses are compiled in Table 3, together with calculated mean values and standard deviations. The mean value and standard deviation for one sample, analyzed 10 times in its position is very similar to that for all the data. For both the relative standard deviation is just below 6%. This shows that the differences between the four ore samples, both from Garpenberg as well as from Boliden, are highly significant. See Table 2 and Figs. 3 and 4.

It is noted that the moisture uptakes are generally higher for the ore from Boliden than for the one from Garpenberg. This can be explained by the smaller particle size of the ore from Boliden (see Table 4 below), because the moisture adsorption onto a material is strongly correlated to its specific surface area, with a finer particulate matter having a higher specific surface area.

Even though the discussion above is straightforward and the results logical for industrial minerals, it is important for anyone performing DVS-analyses to have some knowledge about the moisture uptake processes, which may occur. These include:

1. Surface adsorption and pore filling,
2. Dissolution/Deliquescence,
3. Hydrate formation,
4. Crystallization of glass.

Table 3
DVS-data for repeated analyses on the Garpenberg feed. Three samples were analyzed; sample 1 five times, sample 2 twice and sample 3 three times.

Sample	1st cycle	2nd cycle	Mean	Standard Deviation
1:1	0.1433	0.1451		
1:2	0.1208	0.1244		
1:3	0.1317	0.1330		
1:4	0.1300	0.1320		
1:5	0.1239	0.1261	**Samples 1:1–1:5:** 0.1310	**Samples 1:1–5:** 0.0076
2:1	0.1279	0.1281		
2:2	0.1405	0.1431		
3:1	0.1340	0.1331		
3:2	0.1444	0.1448		
3:3	0.1410	0.1421	**All data:** 0.1345	**All data:** 0.0077

Table 4
Particle size results from laser diffraction measurements on the eight ore samples. Average values of the 6 analyses of each ore sample are given, with the standard deviation in bracket. The specific surface area was calculated from the particle size measurements.

Sample	d(0.1) [μm]	d(0.5) [μm]	d(0.9) [μm]	Specific surface area [m^2/g]
Feed (B) no ultrasound	12.0 (2)	59 (2)	179 (6)	0.23 (1)
Feed (B) ultrasound	11.0 (3)	45 (7)	135 (20)	0.28 (3)
CuPb (B), no ultrasound	5.40 (2)	27.2 (4)	75.2 (8)	0.47 (1)
CuPb (B), ultrasound	4.76 (8)	22.9 (2)	59.6 (8)	0.54 (1)
Cu (B), no ultrasound	6.6 (2)	36.1 (6)	100 (4)	0.38 (1)
Cu (B), ultrasound	5.4 (1)	27.4 (1)	73 (1)	0.47 (1)
Pb (B), no ultrasound	14.5 (2)	46.8 (4)	108 (2)	0.22 (1)
Pb (B), ultrasound	12.5 (2)	40.5 (1)	89 (1)	0.25 (1)
Feed (G) no ultrasound	9.1 (1)	58.0 (5)	200 (5)	0.28 (1)
Feed (G) ultrasound	8.0 (2)	50 (1)	184 (6)	0.32 (1)
CuPb (G), no ultrasound	12.5 (1)	46 (1)	125 (8)	0.23 (1)
CuPb (G), ultrasound	12.2 (1)	46 (1)	133 (5)	0.23 (1)
Cu (G), no ultrasound	21.2 (2)	58 (1)	134 (5)	0.15 (1)
Cu (G), ultrasound	17.3 (2)	47.4 (3)	117 (9)	0.19 (1)
Pb (G), no ultrasound	11.5 (3)	40 (1)	102 (2)	0.25 (1)
Pb (G), ultrasound	11.0 (3)	37 (1)	89 (2)	0.27 (1)

Surface adsorption correlates strongly with the specific area of similar samples and normally corresponds to a small water uptake, unless for very fine particulate samples. For a non-micronized sample it is usually much less than 1%. If a material is porous, water may also be taken up into pores. One reason for the generally larger moisture uptake in the Boliden ore samples compared to those from Garpenberg is that they are ground finer, as was shown by laser diffraction (see Table 4). The copper concentrate in Garpenberg turned out to lack the fine fractions, which is not normal, but can explain the low DVS value.

As expected, ultrasonication gives slightly more fines and correspondingly a slightly larger surface area. The samples were measured with and without ultrasonication, to reduce loose (mainly electrostatic) agglomeration. Such agglomeration will decrease the particle size but has no effect on surface area. However, if ultrasonication breaks up more strongly bonded agglomerates, the specific surface area will also increase. Mild ultrasonication should not be able to break up strong agglomerates of such hard materials as ore particles, so the higher surface areas obtained after ultrasonication is likely to be an artifact because the specific surface area is calculated from the particle size distribution. Hence, the standard deviations given for the specific surface areas are likely to be underestimated.

If a sample is highly soluble in water it will at some point during the DVS-analysis start to take up large amounts of water and start to dissolve. This is usually referred to as deliquescence. If a sample, which is not soluble in water, shows large uptakes of water from a certain %RH and upward, one should suspect that it either becomes hydrated, or that it contains an impurity, which is deliquescent or forms one or more hydrates.

Sulphide ore samples will rarely contain salts, being more than slightly soluble in water. This is clearly shown by the XRPD-analyses of the samples in this investigation. Samples which have been processed through flotation cells will contain even less water-soluble salts, since they have been processed in water, which will already have dissolved most of these salts. Ore samples may however contain minerals, which may give off and take up water, such as zeolites or clay-type minerals. This may also be a reason for the generally larger moisture uptake in the Boliden ore samples compared to those from Garpenberg. The Boliden feed ore contains much more chamosite (a clay mineral) than the Garpenberg feed ore.

The standard procedure for performing DVS-analyses is to run two consecutive sorption – desorption cycles. The reason for this is that some samples may exhibit phase transitions (e.g. hydrate formation) during the analysis and if this occurs during the first cycle, the second cycle will usually looks different. This can be a neat way of identifying metastable crystal modifications, but is observed most frequently when a sample is water soluble and partly amorphous. When such a sample is analyzed it will take up water, but at some point during the first cycle, it may suddenly give off some of its water. This is the point at which the amorphous material softens and crystallizes. In the second cycle this phenomenon will usually not be seen (unless in cases where a hydrate is formed, which during desorption becomes amorphous when dehydrated).

When the sorption and desorption curves for a cycle are compared, there is always various degrees of hysteresis effects, meaning that water which has been taken up in the sorption cycle is given off at lower %RH than it was taken up. This is due to the dynamic nature of the DVS-analyses. If one allows the analysis to take a much longer time to be completed (lower dm/dt), the hysteresis effects would become much less apparent.

4. Concluding remarks

The results of the study clearly show the usefulness of using the DVS technique for detecting the differences in wettability between samples collected from an industrial flotation circuit. The main benefits of the method are that it is suitable for inhomogeneous powders, which are common in industry, while still allowing reliable measurements with low sample amounts. This is especially useful for screening of new flotation reagents, evaluating their performance and impact on surface properties of minerals.

The samples in this investigation were also analyzed by XRPD for constituent minerals. Furthermore, the particle size distribution of the systems was analyzed by laser diffraction to evaluate possible differences arising from the particle sizes of the ore samples. It was found that the samples from the Boliden concentrator had higher wettability compared to the samples from Garpenberg. The Boliden samples were shown to have a higher specific surface (Malvern) and to contain a clay mineral, which also affects the DVS results in the same direction as a higher wettability does. Knowing that different minerals and particle sizes have influence on the results of wettability tests, one should exercise caution with drawing conclusions, when comparing samples from different mines.

The high accuracy and reproducibility of the DVS analysis, however, makes the technique a good complement to commonly used methods based on direct or indirect contact angle measurement, such as the Washburn capillary rise test or the sessile drop test method.

The main drawback of using the instrument in comparison with the Washburn or similar techniques is the operating time, approximately one or two samples a day can be processed. The result is also only an indirect measure of the contact angle, and therefore a comparative study is recommended. In this work, the particle size distribution was measured by laser diffraction, but for further investigations one should also conduct evaluations using other techniques such as the BET surface area method and compare and correlate these with the DVS

measurement results.

The DVS instrument is a relatively costly investment, which possibly should not be made unless the instrument is used on a daily basis. Due to its benefits, however, it is an interesting tool for in-depth evaluation of flotation processes and mechanisms, either for research and academic purposes, or for more detailed understanding of industrial process performance and troubleshooting.

Since the results are repeatable with small amounts of industrial materials, the method is particularly well-suited for screening of new flotation reagents, including both depressants and collectors.

Acknowledgements

The authors would like to acknowledge Dr. Nils- Johan Bolin, Mr. Jan- Eric Sundkvist, Mr. Paul Kruger and Dr. David Degerfeldt for their help during preparation of this manuscript. The authors also wish to acknowledge Boliden Mineral and RISE for permission to publish this paper, as well as VINNOVA, the Swedish Governmental Agency for Innovation Systems for financial support.

References

Akdemir, U., 1997. Shear flocculation of fine hematite particles and correlation between flocculation, flotation and contact angle. Powder Technol. 1–4.

Alghunaim, A., Kirdponpattara, S., Zhang Newby, B.-M., 2016. Techniques for determining contact angle and wettability or powders. Powder Technol. 201–215.

Bolin, N., Laskowski, J., 1991. Polysaccharides in flotation of sulphides. Part II. Copper lead separation with dextrine and sodium hydroxide. Int. J. Miner. Process. 235–241.

Bolin, N., Brodin, P., Lampinen, P., 2003. Garpenberg - an old concentrator at peak performance. Miner. Eng. 1225–1229.

Buckton, G., Darcy, P., 1995. The use of gravimetric studies to assess the degree of crystallinity of predominantly crystalline powders. Int. J. Pharm. 268–271.

Bulatovic, S.M., 2007. Handbook of Flotation Reagents. Elsevier Science & Technology Books.

Chau, T., 2009. A review of techniques for measurement of contact angles and their applicability on mineral surfaces. Miner. Eng. 213–219.

Heng, J., Williams, D., 2011. Vapour sorption and surface analysis. In: Storey, R.A., Ymén, I. (Eds.), Solid State Characterization of Pharmaceuticals. John Wiley & Sons Ltd, Chichester, UK.

Iveson, S., Holt, S., Biggs, S., 2000. Contact angle measurements of iron ore powders. Physicochem. Eng. Aspects Colloids Surf. 203–214.

Iveson, S., Holt, S., Biggs, S., 2004. Advancing contact angle of iron ores as a function of their hematite and geothite content: implications for pelletising and sintering. Int. J. Miner. Process. 281–287.

Javadi, A., Rao, K., 2016. Complex sulphide ore flotation: Effect of depressants additioon during grinding on H_2O_2 formation and its influences on flotation. Int. J. Miner. Process. 89–97.

Kawatra, 2011. Fundamental principles of froth flotation. In: Darling, P. (Ed.), SME Mining Engineering Handbook, 3rd ed. (ISBN 978-0-87335-264-2. PANalytical ICDD PDF-2 database, Release 2000, version 2.1).

Kirdponpattara, S., Phisalaphong, M., Zhang Newby, B.-M., 2013. Applicability of Washburn capillary rise for determining contact angles of powders/porous materials. J. Colloid Interface Sci. 169–176.

Laskowski, J.-S., Liu, Q., Bolin, N.-J., 1991. Polysaccharides in flotation of sulphides. Part I. Adsorption of polysaccharides onto mineral surfaces. Int. J. Miner. Process. 223–234.

Lundmark, A., Ymén, I., 2017. Depression of galena with phosphate, a substitute for dichromate? In: Conference in Mineral Processing. Luleå.

Qiu, G., Jiang, T., Fa, K., Zhu, D., Wang, D., 2004. Interfacial characterizations of iron ore concentrates affected by binders. Powder Technol. 1–6.

Susana, L., Campaci, F., Santomaso, A.C., 2012. Wettability of mineral and metallic powders: applicability and limitations of sessile drop method and Washburn's technique. Powder Technol. 68–77.

Teipel, U., Mikonsaari, I., 2004. Determining contact angles of powders by liquid penetration. Part. Part. Syst. Charact. 255–260.

Wills, B.A., 1997. Mineral Processing Technology. In: B.A. Wills, Mineral Processing Technology (p. Chapter 12).

Paper III

DYNAMIC VAPOR SORPTION – A NOVEL METHOD FOR MEASURING THE HYDROPHOBICITY IN INDUSTRIAL-SCALE FROTH FLOTATION

Paper 431

DYNAMIC VAPOR SORPTION – A NOVEL METHOD FOR MEASURING THE HYDROPHOBICITY IN INDUSTRIAL-SCALE FROTH FLOTATION

Lisa Malm[a*], Ann-Sofi Kindstedt Danielsson[b], Anders Sand[c], Jan Rosenkranz[c] and Ingvar Ymén[b]

[a] *Boliden Mineral, Dept. of Process Technology, SE-936 81 Boliden, Sweden*
[b] *RISE- Research Institutes of Sweden AB, Surface, Process and Pharmaceutical Development, SE-151 36 Södertälje, Sweden*
[c] *Minerals and Metallurgical Engineering, Dept. of Civil, Environmental and Natural Resources Engineering, Luleå University of Technology, SE-971 87 Luleå, Sweden*
[*] *Corresponding author, email address: lisa.malm@boliden.com*

ABSTRACT

The understanding of particle surface properties is essential for the study and evaluation of froth flotation phenomena, particularly in the investigation of various chemical or reagent effects. Dynamic Vapor Sorption (DVS) is a method used for the analysis of surface properties of powders for instance in the pharmaceutical industry. To the knowledge of the authors, it has however not been used before in applications related to mineral processing. The DVS technique involves measurement of the water uptake of a relatively small amount of sample as a function of the relative humidity (% RH) in a temperature-controlled environment. The purpose of this work was to evaluate the method and investigate how it can complement existing techniques for surface characterization in mineral processing. Four samples (feed, CuPb concentrate, Cu concentrate and Pb concentrate) from the Cu – Pb flotation process in the Garpenberg concentrator, Sweden, were analyzed by DVS and the traditional capillary absorption technique (Washburn capillary rise). This enabled comparison between the two methods and evaluation of their respective advantages and disadvantages. Both methods give the expected ranking of the hydrophobicity for CuPb concentrate, Cu concentrate and Pb concentrate, but a discrepancy was observed for the feed. Washburn gave a value for the contact angle which was in the same range as for the CuPb concentrate, whereas DVS gave a value for the moisture uptake which was much higher than for the CuPb concentrate. Thus, DVS ranks all samples correctly, but with an unexpectedly high value for the feed whereas Washburn gives good ranking for three samples out of four. Potential reasons for the discrepancies are discussed.

KEYWORDS

Wettability, Dynamic Vapor Sorption, DVS, Washburn capillary rise, hydrophobicity, flotation

INTRODUCTION

The flotation process utilizes the differences in surface properties between minerals. In order to achieve the suitable surface properties, the chemical conditions in the pulp need to be changed by adding collectors and other reagents (Wills, 1997).

To be able to predict the floatability of a certain mineral, it is of interest to measure its degree of hydrophobicity or wettability. One way of characterizing the wettability is to measure the contact angle, θ, which is defined as the intersection of the liquid-solid and liquid-vapor interface for a liquid drop on top of a flat surface of a material. By definition, a contact angle less than 90° indicates a hydrophilic surface where the droplet will spread out over the surface. A contact angle above 90° is formed when the surface is hydrophobic and thus more water repellant, see Figure 1 (Erbil, 2014).

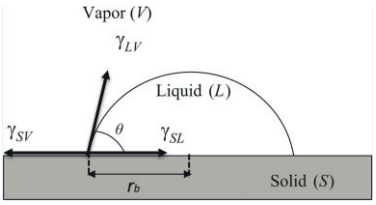

Figure 1 - Profile of a droplet on a flat solid surface. The contact angle, θ, formed between the solid surface and the droplet of the liquid.

There are several methods of measuring the contact angle. It can be done either by applying a droplet on a flat surface of a mineral (sessile drop method) or as a capillary method. The capillary rise test is performed on a compacted powder and measures liquid absorption by monitoring weight increase or capillary pressure (Nowak et al., 2013; Akdemir, 1997; Qiu et al., 2004; Chau, 2009; Iveson et al., 2004). The sessile drop method suffers from serious drawbacks, e.g. the direct contact angle measurement must be made on a large, reasonably flat and preferably non-permeable surface. This is not possible on a mineral sample taken directly from a flotation process. The capillary methods, e.g. Washburn capillary rise, on the other hand are sensitive to particle properties, such as size and shape distributions and heterogeneities in the surface properties. In addition, this method require the use of packed mineral powders samples where the packing procedure has been shown to affect the reproducibility (Susana et al., 2012; Teipel & Mikonsaari, 2004).

Dynamic vapor sorption, DVS, is an analytical method where the amount of water adsorbed by the particles is measured as a function of the relative humidity. The technique has successfully been used by the pharmaceutical industry for many years (Buckton & Darcy, 1995; Heng & Williams, 2011).

In an earlier work, the DVS was used to describe the hydrophobicity of mineral samples, with the purpose of finding a new depressant reagent (Malm et al., 2017). Even though the results of that study were in line with the expectations, the question arose how the DVS measurement correlated with more commonly used methods in mineral processing such as the Washburn capillary rise method (in this paper referred to as Washburn).

The aim of this work was therefore to compare the two methods and evaluate their respective advantages and disadvantages, when studying the surface properties of industrial ore samples.

MATERIAL AND METHODS

Material

The ore samples for this investigation were obtained from the CuPb flotation circuit of Boliden´s Garpenberg concentrator. Four samples were chosen according to their expected differences in hydrophobicity. The untreated feed material was expected to be hydrophilic while the CuPb concentrate was expected to be more hydrophobic since it contained floated material. In the copper - lead separation process dichromate was added to depress the lead. The Cu concentrate should be very hydrophobic since it has undergone more cleaning steps where gangue material and lead-containing particles have been depressed. The lead concentrate is the sink product and should be hydrophilic. The wettability is thus expected to vary as follows, where a higher value means more hydrophilic surface or a lower contact angle:

$$Feed > CuPb\ conc > Cu\ conc$$

$$Pb\ conc > Cu\ conc$$

The four samples were dried in an oven at 80°C for 8 hours and were then split in a Jones splitter into two fractions. One fraction was sent for Washburn tests and the other for DVS tests.

Washburn tests

The Washburn method (Washburn, E.W., 1921) is an established technique in the mineral industry for determining the wettability of powders, expressed by a contact angle. It uses the capillary forces in the capillaries formed between particles that are packed in a cylindrical tube with a permeable filter at the bottom. When liquid is transported into the sample, the increased weight is measured with time. The Washburn equation is presented below:

$$w^2 = kt\frac{\rho\gamma_{LG}cos\theta}{2\eta} \quad (1)$$

where w is the weight of the liquid that is taken up by the sample, γ_{LG}, ρ and η are the surface tension, density and viscosity of the liquid, respectively, θ is the contact angle, k is a material constant and t is the time required for the penetration.

The instrument used was a Krüss tensiometer K100 (Krüss, 2018). Ten glass cylinders and one ring, used as a filter base, were available for the test.

At least 1 cm height of packed samples has to be used and due to the high bulk density of the lead ore, 3 g of material was used for each test. The material was weighed on a calibrated scale to reach 3 ± 0.01g and then transported to the glass cylinder where a filter was mounted between the ring and the glass cylinder.

The material was packed manually by a piston with a 2 kg weight from the top, also supplied by Krüss. The packing procedure involved manually lowering the piston through the top of the glass tube and slowly letting the piston compress the material, so that the whole weight of the piston was finally placed on top of the sample before it was slowly removed. This procedure was carried out

carefully since the packing procedure, as well as the roughness or pores in the particles, have been shown to have an impact on the result (Galet et al., 2010; Kirdponpattara et al., 2013).

Five measurements with n-hexane were carried out on each sample, in a random order, to calculate an average capillary constant for each sample. The constant was then utilized in equation (1) to calculate the contact angle based on the results from the corresponding Milli-Q water measurement.

DVS

Basically, the DVS-instrument is a very sensitive balance, with a sample cup and an empty reference cup, which are both flushed with an extremely well controlled moist gas stream. The instrument used was a Surface Measurement Systems DVS Advantage instrument, in which the balance can operate at a constant temperature between 5 and 60 °C. It uses a sample amount between 1 – 150 mg with a sensitivity of 0.1 μg and, if water is used, with a percent relative humidity between 0 and 98 %RH and an accuracy of ±0.5 %RH.

The DVS instrument was used to measure the water uptake as a function of the relative humidity at 25.0 °C. In continuation a % Partial Pressure Method was used. A sample of 50 – 150 mg was placed into a weighting pan and its weight was monitored while the sample was exposed to different relative humidities (%RH). The sample was first dried with dry nitrogen gas for 1 hour before the 1st cycle. The sample was then allowed to adsorb/desorb water in the first sorption/desorption cycle, where the %RH was increased stepwise up to 95 %RH and then stepwise down to 0 %RH again. The sample was now once again dried for 1 hour at 0 % RH, before another identical cycle, the second sorption/desorption cycle, was run. In both sorption/desorption cycles, at each step, the sample was kept at the set relative humidity until dm/dt <0.002%, over a period of 5 minutes.

Surface analysis and density measurement

Both the Washburn and DVS techniques are sensitive to differences in the specific surface area. Therefore, a BET (Brunauer-Emmett-Teller) surface area test was conducted to support the evaluation of results. The BET surface method uses nitrogen gas to adsorb on the mineral surfaces at the temperature of liquid nitrogen, and the amount of adsorbed gas correlates with the specific surface area of the particles (Brunauer et al. 1938). The density measurements were conducted by a pycnometer, Micrometrics AccuPyc II 1340, with helium as the analysis gas.

RESULTS

Material Characterization

In Table 1, the results from the online XRF analysis during the sampling from the Garpenberg mill are presented together with the results from BET surface analysis and particle density analysis.

Table 1 - XRF analysis of the four sampled materials

Sample	Cu [%]	Pb [%]	Zn [%]	Fe [%]	BET [m^2/g]	Particle density [g/cm^3]
Feed	0.06	2.2	5.8	6.3	1.36	3.1
CuPb conc	1.8	68.1	6.5	3.7	0.46	6.2
Cu conc	19.4	13.8	9.2	18.6	0.25	4.6
Pb conc	0.4	72.7	6.4	2.9	0.58	6.4

Washburn test

A summary of the experimental data of the capillary constants and contact angle for the four Garpenberg samples can be seen in Table 2 and Figure 2, where SD the standard deviation and Rel. SD the relative standard deviation.

Table 2 - Measured values of the constant and the contact angle for each sample.

	Capillary constant				Contact Angle			
#	Feed	CuPb conc	Cu conc	Pb conc	Feed	CuPb conc	Cu conc	Pb conc
1	$5.1x10^{-6}$	$5.1x10^{-6}$	$7.4x10^{-6}$	$3.7x10^{-6}$	63.9	65.6	78.9	54.7
2	$5.0x10^{-6}$	$5.1x10^{-6}$	$8.9x10^{-6}$	$4.1x10^{-6}$	70.1	72.1	81.4	55.7
3	$5.2x10^{-6}$	$4.9x10^{-6}$	$8.0x10^{-6}$	$4.2x10^{-6}$	67.4	68.7	82.6	52.0
4	$5.0x10^{-6}$	$5.1x10^{-6}$	$9.2x10^{-6}$	$3.9x10^{-6}$	73.4	64.3	81.1	54.6
5	$5.7x10^{-6}$	$5.2x10^{-6}$	$7.7x10^{-6}$	$4.3x10^{-6}$	69.1	62.1	85.5	57.5
Mean value	**$5.2x10^{-6}$**	**$1x10^{-6}$**	**$8.2x10^{-6}$**	**$4.0x10^{-6}$**	**68.8**	**66.5**	**81.9**	**54.9**
SD	**$2.7x10^{-6}$**	**$1.3x10^{-6}$**	**$7.5x10^{-6}$**	**$2.4x10^{-6}$**	**3.5**	**3.9**	**2.4**	**2.0**
Rel. SD	**5.2%**	**2.6%**	**9.2%**	**6.1%**	**5.1%**	**5.9%**	**2.9%**	**3.6%**

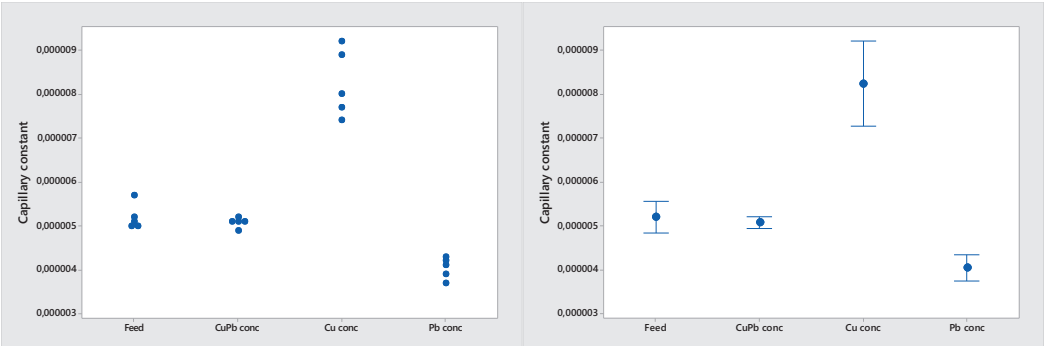

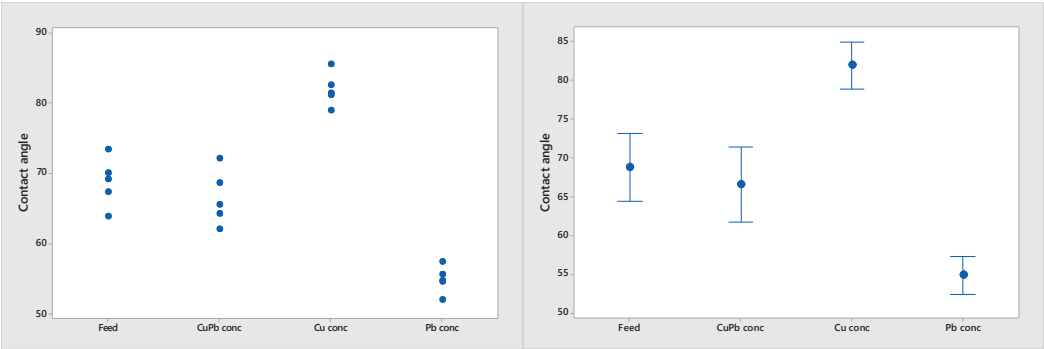

Figure 2 - Individual values and a 95% confidence interval of the capillary constant (above) and capillary constant (below) for each sample

Some measurements had to be excluded from the test work with both n-hexane and with ultrapure Milli-Q water due to various failures during measurement.

DVS

The DVS-data was evaluated only as the amount of water taken up at 95 % RH and the five values for each of the sub- samples are presented in Table 3 and in Figure 3 below. The reproducibility was in the same order as expected, as well as the hydrophilicity of the samples, but the mean values were significantly different from the previous investigation, which gave: feed = 0.13, CuPb conc = 0.08, Cu conc = 0.01 and Pb conc = 0.12 % (Malm et al, 2017).

Table 2 - DVS data for the Garpenberg samples

#	Feed	CuPb conc	Cu conc	Pb conc
1	0.256	0.047	0.036	0.062
2	0.234	0.047	0.035	0.064
3	0.237	0.048	0.035	0.062
4	0.247	0.053	0.035	0.056
5	0.228	0.048	0.035	0.061
Mean value	**0.240**	**0.049**	**0.035**	**0.061**
St dev	**0.011**	**0.002**	**0.0004**	**0.003**
Rel. St dev	**4.6%**	**5.1%**	**1.3%**	**5.1%**

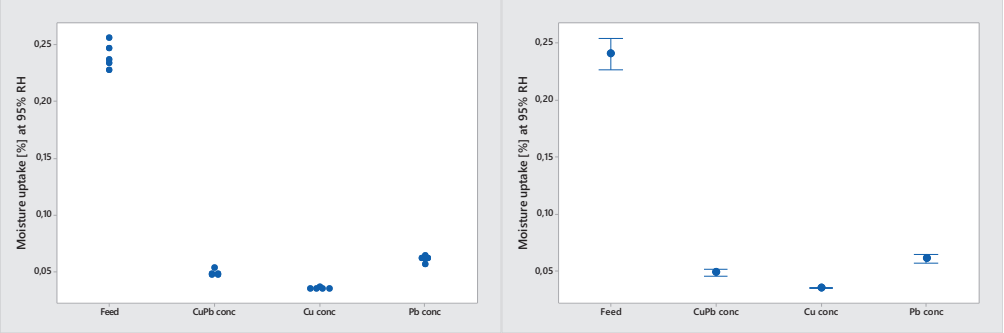

Figure 3 - The DVS data for each sample (left) and with a 95% confidence interval (right). Individual standard deviations are used to calculate the intervals.

DISCUSSION

To characterize the wettability of processed ore samples two different analytical methods were tested. The Washburn method is a sensitive and simple method that requires two measurements (hexane and Milli-Q water) with identical samples and packing procedures. The DVS method on the other hand, which requires far less material, has a long measuring time, but requires no operator during measurement and can perform up to two measurements per day.

The DVS results show a relative standard deviation between 1 and 5% and when five approved Washburn measurements with n-hexane were achieved, the relative standard deviation was 3-9%. There were also a significant number of measurements that had to be discarded due to various problems during the tests. It should be noted that the spread of the capillary constants was not included in the standard deviation calculations for the contact angle. If it had been, the relative standard deviation on the four samples would be much higher than the 3 to 6 % range the test work showed. These results are fairly reasonable compared to other published studies (Marín et al., 2017; Blankson Abaka- Wood et al. 2017). None of these authors has, however, mentioned how many tests they have conducted to receive the presented results.

The samples in this work have never been measured for contact angle before, accordingly, no “expected” values were available. It is therefore difficult to speculate about how reliable the absolute values are. Instead the order of the values should be discussed.

It should also be noted that ore samples from different positions in a flotation circuit were used, which are each mixtures of both gangue- and valuable minerals, instead of pure minerals, which are usually used in publications of Washburn measurements. The contact angle and the ability to take up water will thus be an average value for all included minerals. In addition to mineral properties, different conditions and chemicals in the process have also affected the samples.

The Garpenberg ore also contains some talc and clay minerals, which are layered minerals. I.e. these hese minerals have important properties, which may have an impact on the measurements, namely a) they form plate-like crystals and b) clay minerals can incorporate water into their crystal lattices.

The surfaces of talc can either be hydrophilic or hydrophobic, depending on the relative humidity (Rotenberg et al., 2011). It is believed that the surprisingly low contact angle for the feed material, to some extent, may be due to plate-like crystals, orientating themselves to give rise to a potentially hydrophobic barrier against water diffusion. On the other hand, the DVS-value for the feed material is much higher than in the earlier measurements and also compared to the other three materials. This is probably, at least to some extent, due to the presence of very hydrophilic clay particles too.

The Washburn- and DVS-methods are also affected by the presence of small particles, presenting a large area for water adsorption. This is clearly the case for the feed material, which can additionally explain its high moisture uptake with DVS. The fact that the DVS-data in the earlier study is so different from those presented here, shows that the hydrophilicity of the samples taken varies a lot on a day-to-day or maybe even hour-to-hour basis. This is not surprising, given what is known about variations in mineral composition in different parts of a lode. Still, in both DVS-studies the expected order of hydrophilicity of the samples is the same. This indicates that as long as different samples from the process are taken at the same time, it should be possible to rank them according to their hydrophilicity measured using DVS.

The results from both methods were also affected by differences in particle density. The Washburn test work was conducted with 3 g/ test, giving approximately twice the volume for the feed sample compared to the lead concentrate. This affects the packing procedure, which in turn affects the results (Marín et al., 2017). Similar packing is important to avoid the occurrence of local channeling (Prestidge & Ralston, 1996; Alghunaim et al., 2016). The DVS data was achieved from approximately the same amount of material, 0.05 – 0.07 g for the feed samples and 0.09 – 0.14 g for the other samples. Since the particle density is 3.1 g/cm^3 for the feed and 6.2 g/cm^3 for the CuPb-concentrate, the feed volume is doubled for the same mass and it can be expected that 1 g of feed sample will have a much higher surface area available for moisture uptake. This further explains the high moisture uptake with DVS, since it is expressed in % (grams per gram sample). Similarly, the specific surface area analysis is given as surface area per gram of sample.

Contact angles for water on galena and chalcopyrite have previously been measured (to 89° and 90°, respectively) for the individual minerals, treated with huge amounts of xanthate collector (Klassen & Mokrousov, 1963). In the tests within the present work, the copper concentrate with the chemical composition as listed in Table 1, gives a contact angle of 81.9° (mean value). Except for the xanthate collector, process water and other reagents (such as $ZnSO_4$, Nasfroth 240 and dextrin) also affect the mineral surfaces. No measurements on galena depressed with dichromate have been found in the literature, but the actual measurements on the lead concentrate did show a lower value than for the copper concentrate, which indicates more hydrophilic surfaces.

To exclude the fact that the DVS instrument it not only measuring differences in surface area, the four samples were dry sieved and the same size fraction of the four samples was analyzed. The results showed a similar trend as before, but the lead concentrate returned a comparably low value. This might be explained by depressed galena surfaces being worn off during sieving. A more elaborate study of this is planned.

CONCLUDING REMARKS

Flotation is a complex process, which is affected by physical, chemical and mechanical aspects. Consequently, comprehensive process understanding is therefore often still lacking. One step on the way would be to be able to measure the wettability of samples from the different process steps. The Washburn results from this investigation are reasonable except for the feed material, the wettability of which is the same as for the CuPb concentrate. This seems unlikely, considering that collector has been added to the latter sample. The DVS data, on the other hand, rank the samples correctly, but show a drastic drop from the feed to the CuPb concentrate. BET measurements indicate that part of this may be due to specific surface area effects (from the fine particles) or sample volume effects due to large differences in ore density. These aspects need to be further investigated.

ACKNOWLEDGMENTS

The authors would like to thank Dr. Tommy Karlkvist, Dr. Nils- Johan Bolin and Dr. Peder Lundqvist for their help during preparation of this manuscript. Boliden and RISE are recognized for granting permission to publish this paper. The financial support from the Swedish governmental agency for innovation systems (VINNOVA), through the Strategic Innovation Program for the Swedish Mining and Metal Producing Industry (SIP STRIM), is gratefully acknowledged.

REFERENCES

Akdemir, Ü. 1997. Shear flocculation of fine hematite particles and correlation between flocculation, flotation and contact angle. Powder Technology, 94 (1), pp 1-4.

Alghunaim, A., Kirdponpattara, S., Zhang Newby, Bi-min, 2016. Techniques for determining contact angle and wettability of powders. Powder Technology, 287, pp 201-215.

Blankson Abaka-Wood, G., Addai- Mensah, J., Skinner, W., 2017. A study of flotation characteristics of monazite, hematite and quartz using anaionic collectors. International Journal of Mineral Processing, 169 (10) pp 55-62.

Brunauer, S., Emmett, P.H., Teller, E., 1938. Adsorption of Gases in Multimolecular Layers. Journal of the American Chemical Society 60 (2), 309-319.

Buckton, G., Darcy, P., 1995. The use of gravimetric studies to assess the degree of crystallinity of predominantly crystalline powders. International Journal of Pharmaceutics, 123 (2) pp 268-271.

Chau, T., 2009. A review of techniques for measurement of contact angles and their applicability on mineral surfaces. Minerals Engineering, 22 (3) pp 213-219.

Erbil, H., 2014. The debate on the dependence of apparent contact angles on drop contact area or three-phase contact line: A review. Surface Science Reports, 69 (4), pp 325-365.

Galet, L., Patry, S., Dodds, J., 2010. Determination of the wettability of powders by the Washburn capillary rise method with bed preparation by a centrifugal packing technique. Journal of Colloid and Interface Science, 346 (2), pp 470-475.

Heng, J. Williams, D., 2011. Vapour Sorption and Surface Analysis in Solid State Characterization of Pharmaceuticals (eds R.A Storey and I. Ymén). John Wiley & sons, Ltd, Chichester.

Iveson, S., Holt, S, Biggs, S., 2004. Advancing Contact angle of iron ores as a function of their hematite and goethite content: Implications for pelletising and sintering. International Journal of Mineral Processing, 74 (1-4), pp 281-287.

Kirdponpattara, S., Phisalaphong, M., Shang Newby, Bi-min, 2013. Applicability of Washburn capillary rise for determining contact angles of powders/ porous materials. Journal of Colloid and Interface Science, 397, pp 169-176.

Klassen, V., Mokrousov, V., 1963. An introduction of the Theory of Flotation. Butterworth & Co. London.

Kruss. https://www.kruss-scientific.com/product/tensiometers/k100/force-tensiometer.k100/.

Malm, L., Kindstedt,.A-S., Sand, A., Rosenkrantz, J., Ymén, I., 2017. Application of Dynamic Vapor Sorption for evaluation of hydrophobicity in industrial-scale froth flotation. Minerals Engineering.

Marín Rivera, R., Koltsov, A., Araya Laxvano, B., Douce, J.,2017. Wettability in water/ iron ore powders systems: To the universality of the Cassie model. International Journal of Mineral Processing, 162, pp 36-47.

Nowak, E., Combes, G., Hugh Stitt, E., Pacet, A., 2013. A comparison of contact angle measurement techniques applied to highly porous catalyst supports. Powder Technology, 233, pp 52-64.

Prestidge, C.A., Ralston, J., 1996. Contact angle studies of particulate sulphide minerals. Minerals Engineering, 9 (1), pp 85-102.

Qiu, G., Jiang, T., Fa, K., Zhu, D.,Wang, D., 2004. Interfacial characterization of iron ore concentrates affected by binders. Powder Technology, 139 (1) pp 1-6.

Rotenberg, B., Patel, A., Chandler, D., 2011. Molecular explanation for why talc surfaces can be both hydrophilic and hydrophobic. Journal of the American Chemical Society, 133 (50), 20521-20527.

Susana, L., Campaci, F., Santomasso, A.C., 2012. Wettability of mineral and metallic powders: Applicability and limitations of sessile drop method and Washburn´s technique. Powder Technology, 226, pp 68-77.

Teipel, U., Mikonsaari, I., 2004. Determining Contact Angles of Powders by Liquid Penetration. Particle & Particle Systems Characterization, 21 (4) pp 255-260.

Wills. B.A., 1997. Mineral Processing Technology. Butterworth-Heinemann, Burlington.

Washburn, E.W., 1921. The Dynamics of Capillary Flow. Physical Review Journals Archive

Paper IV

DYNAMIC VAPOR SORPTION MEASUREMENT AND IDENTIFICATION OF MINERAL SPECIES IN INDUSTRIAL-SCALE FLOTATION CELL SAMPLES

Dynamic Vapor Sorption measurement and identification of mineral species in industrial-scale flotation cell samples

Lisa Malm[a*], Anders Sand[a], Nils-Johan Bolin[a], Jan Rosenkranz[c] and Ingvar Ymén[b]

[a] Boliden Mineral, Dept. of Process Technology, SE-936 81 Boliden, Sweden

[b] RISE- Research Institutes of Sweden AB, Bioscience and Materials / Surface, Process and Formulation, SE-151 36 Södertälje, Sweden

[c] Minerals and Metallurgical Engineering, Dept. of Civil, Environmental and Natural Resources Engineering, Luleå University of Technology, SE-971 87 Luleå, Sweden

[*]Corresponding author, email address: lisa.malm@boliden.com

Keywords: Froth flotation, Dynamic vapor sorption, Industrial scale, wettability, mineral processing

ABSTRACT

In order to understand flotation performance in industrial-scale, it is of relevance to understand the surface properties and mineral species of materials contained in the various parts of the cell, such as the mixing, quiescent and froth zones. In this work, sampling was made at different depths, the mineral composition and wettability being characterized by XRPD (X-Ray Powder Diffraction), and DVS (Dynamic Vapor Sorption). DVS is a novel technique for wettability measurement in mineral processing, of higher robustness and reproducibility compared to the Washburn technique. Furthermore, particle size distribution and specific surface area were obtained from laser diffraction analyses.

In the turbulent zone of the cell, the wettability properties are relatively similar, and decreases in the froth and concentrate. This finding could be correlated with mineral composition and particle size distribution. Differences in radial position were only found near the froth phase close to the shaft of the agitator may be a result of unstable hydrodynamics at the pulp/froth interface.

1 INTRODUCTION

Froth flotation is a technique for separating valuable minerals from gangue, based on differences in their surface properties. These differences are typically achieved by adding chemicals, i.e. collectors, which render the wanted minerals more hydrophobic and enable attachment to an air bubble.

Parameters affecting the flotation process include cell geometry, launder configuration, mixing energies and cell hydrodynamics (Kawatra, 2011; Wills, 1997).
As the flotation cell size increases it affects the hydrodynamic environment inside the cell but the effect on the flotation performance is still poorly understood. A way forward is to understand the spatial distribution of material inside flotation cells. Relatively comprehensive sampling investigations have been carried out to elucidate how different minerals and particle size fractions are distributed inside industrial scale flotation cells. Methods for characterization of samples collected from various cell positions are XRF, weight % solids, density, particle size analysis and XRD (Malm et. al., 2016; Tabosa et. al., 2016; Xia et. al., 2009).
Another parameter of interest is the wettability of particles which is often measured with Washburn or Sessile drop techniques (Susana et. al., 2012; Teipel and Mikonsaari, 2004). Due to the low reproducibility and the properties of the samples, this type of measurement techniques have often not been included in sampling campaigns such as in this paper. In order to fill this gap, alternative methods of higher accuracy are required for wettability characterization. One such method could be Dynamic Vapor Sorption, DVS. This is an analytical technique where the adsorption of water (or solvent) onto a powder sample. The adsorption is measured gravimetrically as a function of the relative humidity at a constant temperature. This technique has been used for a long time in the pharmaceutical industry to measure the moisture sensitivity of active pharmaceutical ingredients (Buckton and Darcy, 1995, Heng and Williams, 2011). For mineral powders, the only DVS-investigation known to the authors, is their own (Malm et al., 2018a, Malm et al., 2018b).

The objective of this work is to gain a better understanding of material distribution and properties within a flotation cell, focussing on the mineral composition and the wettability at different levels in an industrial scale flotation cell.
As part of the analysis procedure, the wettability was measured with DVS (Dynamic Vapor Sorption) instead of traditional contact angle measurement.

2 MATERIALS AND METHODS

2.1 SAMPLING AND SAMPLE PREPARATION

The material used in this investigation originates from a sampling campaign conducted in Boliden's copper plant, Aitik, which is situated 20 km south west of Gällivare, in the north of Sweden. Several flotation cells were sampled. The first rougher cell was sampled in three different positions A, B and C, see Figure

1. A detailed report of the sampling campaign is given in a previous paper (Malm et al., 2016).
To compliment the previous investigation, which included grade analysis and physical parameters, like solid density and particle size distribution, the samples were in this work also characterized in terms of wettability and mineral composition.

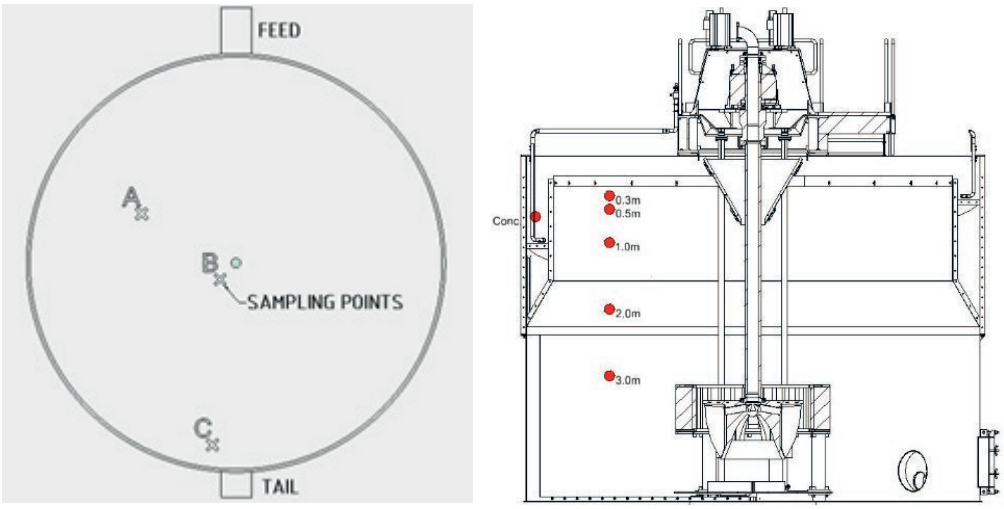

Figure 1. Left: The top of the flotation cell with sampling positions indicated. Right: Samplings position inside the 160 m^3 flotation cell

At each sampling point, A, B and C, six samples were chosen - 0.3; 0.5; 1; 2 and 3 meters down and one sample just under the froth. Additionally, one sample each of the feed, tail, total concentrate and top of the froth were taken - in total 22 samples. However, earlier research has indicated a correlation between DVS-results and particle size / specific surface area (Malm et. al., 2018a). Therefore, an additional 22 samples, corresponding to the -20 fraction, of the above samples were prepared. The bulk samples were dried at 60 – 65 °C and divided into two parts, where one part was sent as is. The other part was wet sieved on a 45 µm sieve for 10 minutes, filtered and dried at 60 – 65 °C and then sieved with ultrasound on a 20 µm sieve giving a -20 µm sample. In total 44 samples were prepared.

2.2 XRPD-ANALYSIS

The analyses were performed at 22ºC on a PANalytical X'Pert PRO instrument, equipped with a Cu X-ray tube and a PIXcel detector. Automatic divergence- and anti-scatter slits were used together with 0.02 rad Soller slits and a Ni-filter. Samples prepared at 22ºC were ground in an agate mortar and were then smeared out on cut Silicon Zero Background Holders.

The samples were spun during the analysis to increase the randomness. All samples were analyzed between 2 – 80º in 2-theta. The full detector capacity of 256 channels was used and all samples were scanned continuously with a 2θ step size of 0.007° and a measuring time of 39.27 s per step.

2.3 XRPD-DATA EVALUATION

Using the PANalytical High Score software each XRPD-data set was treated in the following way:

a) The K-alpha radiation was stripped off,
b) A peak search was performed,
c) The peak data was scrutinized by manually deleting some peaks and adding others,
d) All peaks were profile fitted in small 2θ-window using the default setting (Pseudo Voigt),
e) All peaks in the whole 2θ-range were profile fitted in order to get a correct baseline.

All fitted peaks were checked and if necessary, bullet points d) – e) were repeated.
A Search-Match was performed against the PDS database of inorganic substances. A multiphase scoring scheme matching both intensity and 2θ-positions and allowing for pattern shift was applied.
Initially, the search-match hits with the highest scores were accepted, but as scores were declining new reference data was added manually, using the reference codes as can be found in Table 2 of the Results section and only accepting data with reasonably good fitting. The procedure was stopped when no more significant peaks were left unexplained.
Peak positions in XRPD-data are best discussed using d-values, since such values are independent of the X-ray radiation used. However, when XRPD-data is presented graphically, θ- or 2θ-values are normally used. The relationship between d-values and θ-values is given by Bragg's law in equation 1.

$$n\lambda = 2dsin\theta \qquad (1)$$

where λ represents the x-ray wavelength (in Ångströms), d is the distance between layers in the crystal structure (in Ångströms), θ is the diffraction angle and n is the diffraction order of the peak.
In the discussion below both d-values and 2θ-values will be used.
In the search-match procedure the XRPD-data has been compared to reference data for the minerals or mineral groups presented in Table 1.

Table 1. Mineral identification by database search

Mineral group	Identified by peak
Mica group	9.9 - 10.1 Å
Chlorite group	14.3 and 7.1 – 7.2 Å
Talc	9.4 Å
Amphibole group	9.1 and 8.4 Å
Alkali feldspars	6.5 Å
Plagioclase feldspars	6.4 Å
Tourmaline group	2.56 - 2.58, 4.20 – 4.23 and 3.97 – 4.0 Å
Garnet group	difficult to identify by single peaks, must be identified by high score
Quartz	4.25, 3.34 and 1.82 Å
Pyrite	2.71, 2.41 and 1.63 Å
Chalcopyrite	3.03 Å
Galena	3.43 and 2.97 Å
Pyrrhotite	2.64, 2.06 and 1.72 Å
Magnetite	2.53, 1.48 and 1.10 Å
Barite	3.45, 3.10 and 2.10 Å
Molybdenite	6.1 Å

When all minerals in Table 1 had been fitted, or had failed to fit, to each XRPD-dataset, the peak areas for a few significant peaks of each mineral were extracted from the peak lists and tabulated. For each XRPD-dataset the peak areas where then normalized by dividing each peak area with the sum of the areas of all the used peaks. The values thus obtained were then converted to per cent values by multiplying them with 100. This way, per cent amounts of each mineral were obtained for each sample. It should be noted that these per cent values are by no means absolute representations of the exact mineral content in each sample, but rather relative values, representing how the amounts of different minerals vary within this specific group of samples.

2.4 DVS-ANALYSIS

Dynamic Vapor Sorption, DVS (sometimes also referred to as Gravimetric Vapor Sorption, GVS) was used to determine the wettability of minerals.

The DVS-instrument is basically a very sensitive balance with a sample cup and an empty reference cup, which are both flushed with an extremely well controlled moist gas stream. The instrument used in this paper is a Surface Measurement Systems DVS Advantage, in which the balance can operate at a constant temperature between 5– 60 °C, with a sample size between 1– 150 mg with a sensitivity of 0.1 μg and, if water is used, with a relative humidity between 0 - 98 % and an accuracy of ±0.5 %.

The instrument was used to measure the water uptake as a function of the relative humidity at 25.0 °C. A % Partial Pressure Method was used. Prior to any analysis

the measuring pans were exposed to 95 %RH for 30 minutes to remove static electricity. The balance was zeroed and then a sample was then weighted into the sample pan and its weight was monitored while the sample was exposed to different relative humidity (%RH). The sample was first dried with dry nitrogen gas for 1 hour before the 1st cycle. The sample was then allowed to adsorb water in the 1st sorption/desorption cycle, where the relative humidity was increased stepwise up to 95 %RH (10, 30, 50, 70 and 95 %RH) and then down to 0 %RH again. The sample was now once again dried for 1 hour at 0 %RH, before another identical cycle, the 2nd sorption/ desorption cycle, was run. In both sorption/desorption cycles, at each step, the sample was kept at the set relative humidity until dm/dt <0.002% over a period of 5 minutes.
As this method is not a standard method in mineral processing, a comparative study has been conducted as part of previous work. The DVS was compared to the more traditional Washburn (Malm et. al., 2018a) and the results followed the expected values.

2.5 PARTICLE SIZE DISTRIBUTION ANALYSIS

Particle size distribution data for the ten -20 μm samples from sample position A were obtained with a Malvern Mastersizer 2000, equipped with a Hydro 2000S presentation unit. A sample RI of 2.000 was set and the dispersant Miglyol, with an RI of 1.449 and an absorption value of 0.05, was used. Measurements were performed with and without ultra-sonication prior to measurement. Three measurements were performed on each sample and the results were averaged.

3 RESULTS AND DISCUSSIONS

3.1 XRPD-ANALYSIS

Some of the minerals listed in the database came out with a top score in the search-match fitting. They were without doubt present in the sample and were thus accepted. These minerals were quartz and albite for the high-silicate samples and chalcopyrite and pyrite for the low-silicate samples.
For the residual fitting, reference patterns for different minerals of each mineral group were inserted manually, using their codes. Minerals with sufficiently high scores were accepted.
Finally, all single minerals in Table 1, which had so far not been accepted, were tested by inserting their reference patterns. If the scores were high enough and all important peaks were present, they were accepted. For some minerals, which were not accepted with this procedure, only the presence of its strongest peak was investigated. If there was such a peak the mineral was accepted, but with low significance.
In this way, all peaks in the diffractograms could be explained by a mixture of all, or some of the following minerals:

- Actinolite
- Albite
- Biotite
- Chalcopyrite
- Chamosite
- Molybdenite
- Muscovite
- Orthoclase
- Pyrite
- Quartz

The possible presence of Magnetite could only be suggested by the presence of peaks at 2.53 and 1.48 Å. Unfortunately, these are not unique peaks, because several of the other minerals also have peaks there. The definite presence of Magnetite could thus not be proven in any sample with the XRPD instrument.

Calculation of relative amounts
In Table 2 the d-values for the XRPD-peaks, which have been used to calculate the relative amounts of the different minerals, are given. In the table the codes to the reference patterns, obtained from the search-match calculations, are also given. It should be noted that these calculations were made to obtain a) rough

information about the amounts of the minerals in each samples and b) information about how the amounts of each mineral varies between the samples.

Table 2. XRPD-peaks for each mineral, used to make relative quantifications between samples, together with codes to mineral reference patterns obtained from the search-match procedures.

Mineral	d-value 1	d-value 2	d-value 3	d-value 4	Reference pattern code
Actinolite	9.1	8.4	-	-	41-1366
Albite	6.4	4.04	3.20	3.18	41-1480, 20-554
Biotite + Muscovite	10.1	3.36	3.32	1.99	42-1437, 46-1409
Chalcopyrite	3.03	-	-	-	1-71-507, 37-507
Chamosite	14.3	7.1	4.73		13-29
Magnetite	2.53	-	-	-	3-863
Molybdenite	6.1	-	-	-	24-513
Orthoclase	6.5	3.76	3.24	-	19-931
Pyrite	2.71	2.21	1.63	-	24-76
Quartz	3.34	1.82	1.54	-	1-85-335

When the XRPD-data for the different samples were compared, it was observed that the diffractograms could be divided into three groups:

Type 1: These samples contain large amounts of chalcopyrite and pyrite and smaller amounts of silicate minerals. A typical diffractogram is shown in Figure 2, where chalcopyrite and pyrite peak positions are inserted. The high background level is due to the fact that the data was collected with an X-ray tube with a copper anode. In samples containing much iron this will cause X-ray fluorescence in the sample.

Type 2: This is typical of samples with large amounts of silicates, especially with high amounts of mica (both biotite and muscovite). An example of this is given in Figure 3 and 4 (upper, black diffractogram).

Type 3: This is also a sample with large amounts of silicates, but with comparably low amounts of mica (both biotite and muscovite). An example of this is given in Figure 3 and 4 (lower, blue diffractogram).

With few exceptions the samples taken from the froth belong to Type 1, the non-sieved samples belong to Type 2 and the -20 μm samples belong to Type 3. The only obvious deviations are the two samples (total sample and -20μm) from the B position, collected just under the froth, which both belong to the "wrong" type. They also have high water uptakes with DVS as can be seen in Figure 9 and 10.

It seems that these have not been sampled in the correct position, but rather a bit below it.
It is obvious that Type 1 samples contain low amounts of silicate minerals and large amounts of chalcopyrite, pyrite and significant amounts of molybdenite. Type 2 samples contain no molybdenite, very low amounts of chalcopyrite and pyrite, but high amounts of mica. Type 3 samples contain slightly more chalcopyrite and Pyrite than Type 2, less mica than Type 2, but more chamosite and actinolite than Type 2. Figures 5-7 shows some of the mineral relations between the different sample types.

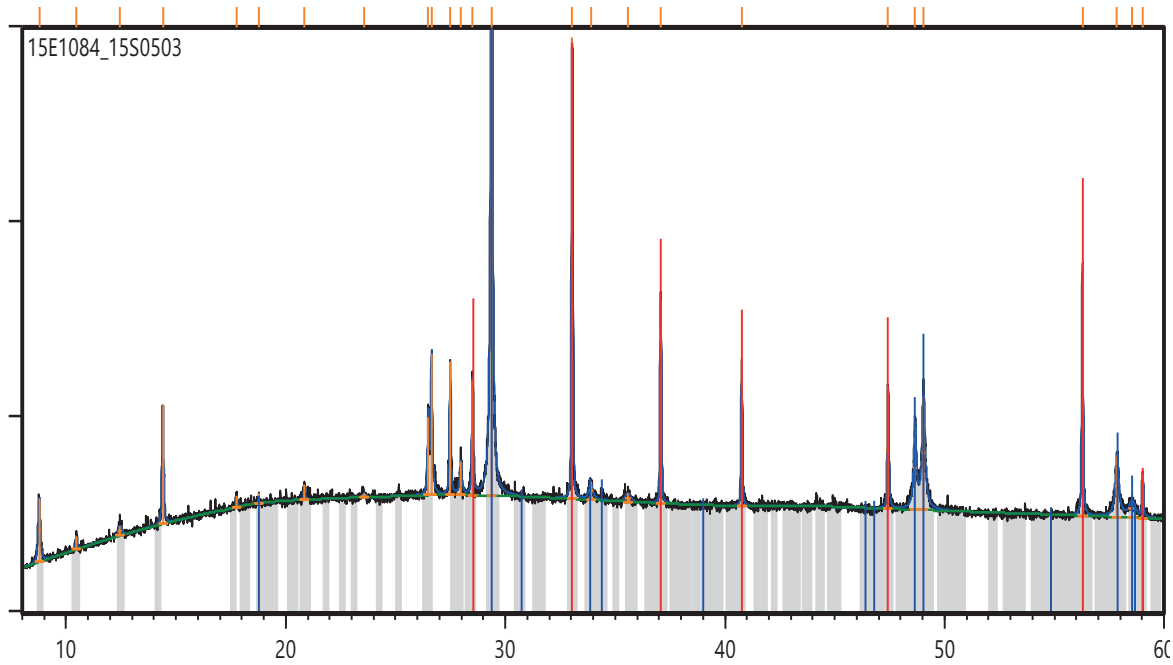

Figure 2. A typical Type 1 diffractogram with large amounts of chalcopyrite (blue vertical peaks) and pyrite (red vertical peaks) and a high background due to X-ray fluorescence from iron.

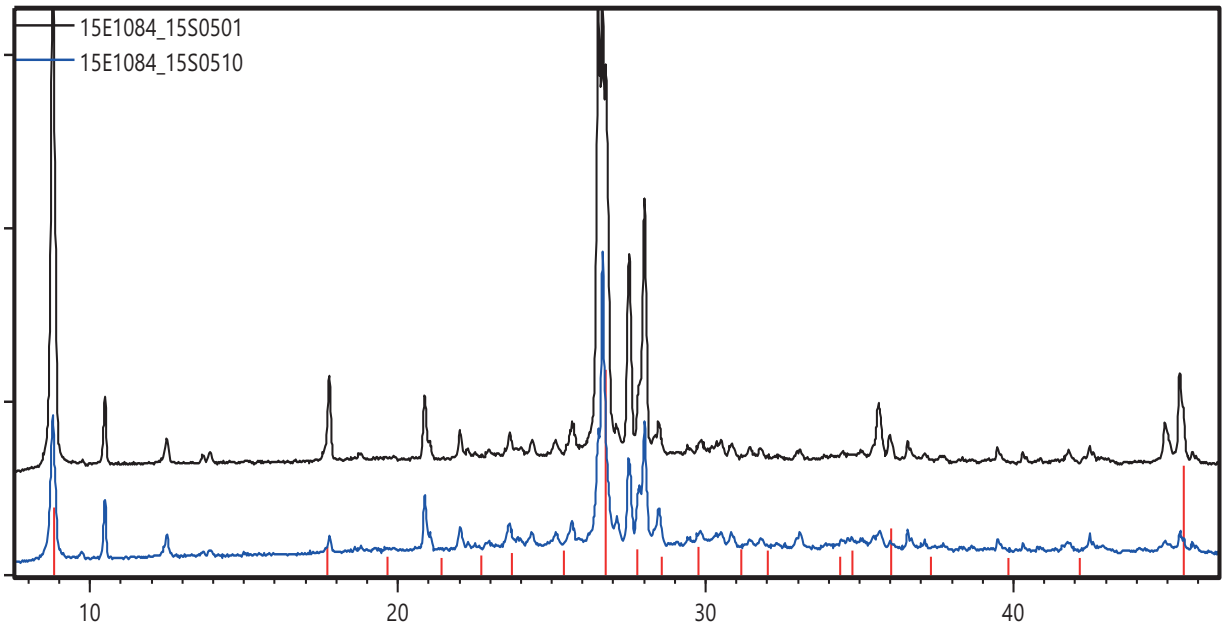

Figure 3. XRPD-data for the Type 3 (blue, bottom) and Type 2 (black, top) of diffractograms, differing mainly with larger amounts of biotite and muscovite.

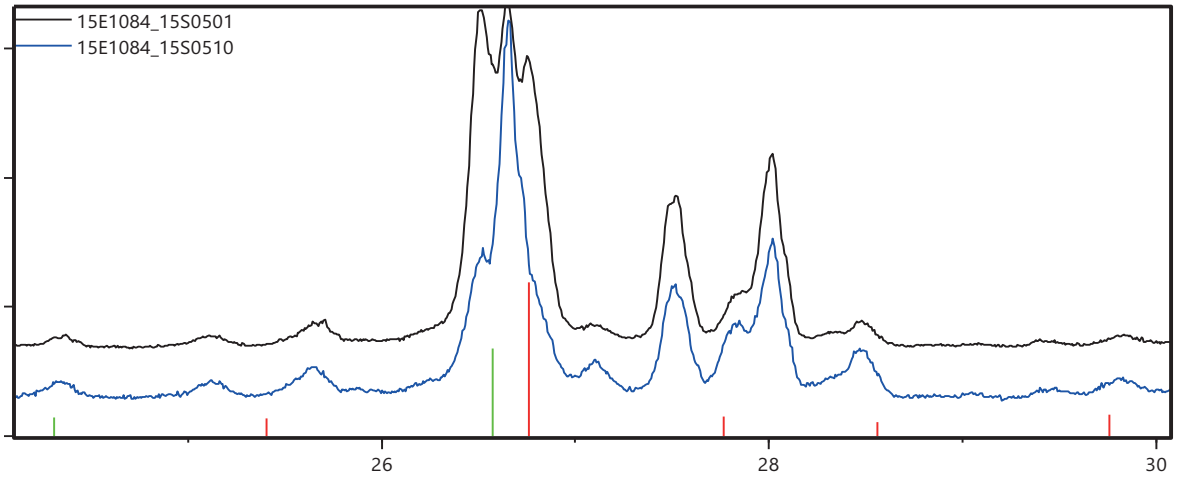

Figure 4. A zoom in for one of the diffractogram of Type 2 and 3, showing the influence of the strong muscovite (red) and biotite (green) peaks surrounding the strongest quartz peak.

In Figure 5 the grade of chalcopyrite is plotted against the grade of quartz where the different types are marked. There is also a zoom-in showing the type 2 and 3 samples more clearly.
In Figure 6 and Figure 7 mica is plotted against quartz and chamosite with type 2 and 3 marked, were the difference between the two types can be seen.

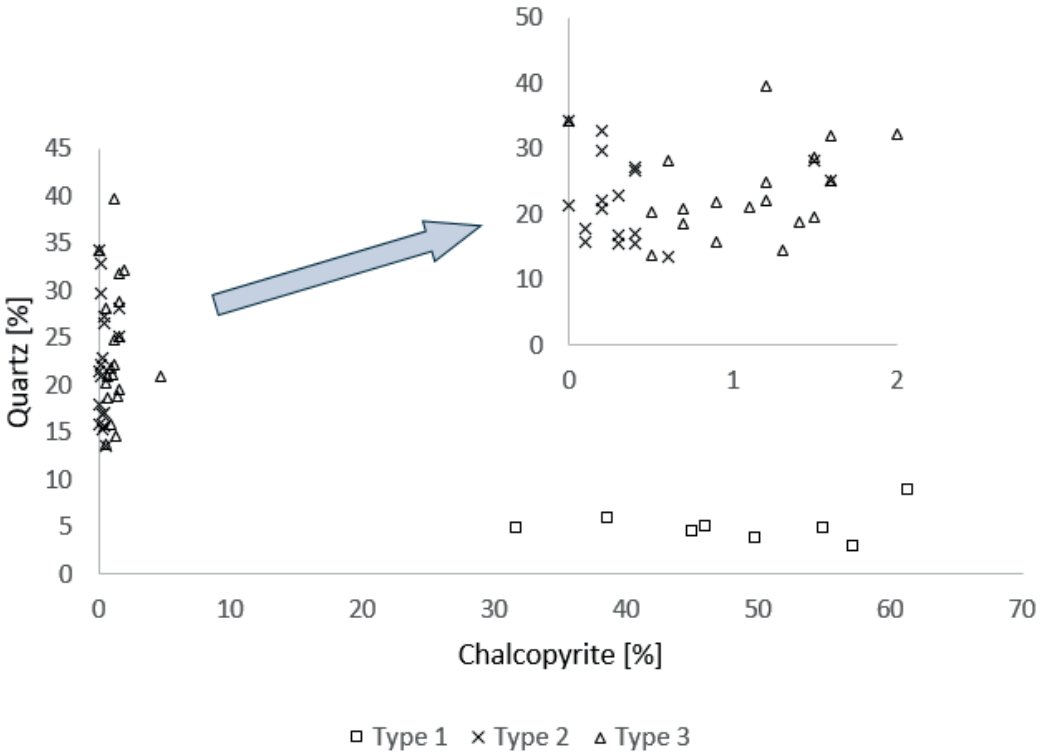

Figure 5. Relative amounts of chalcopyrite plotted against quartz

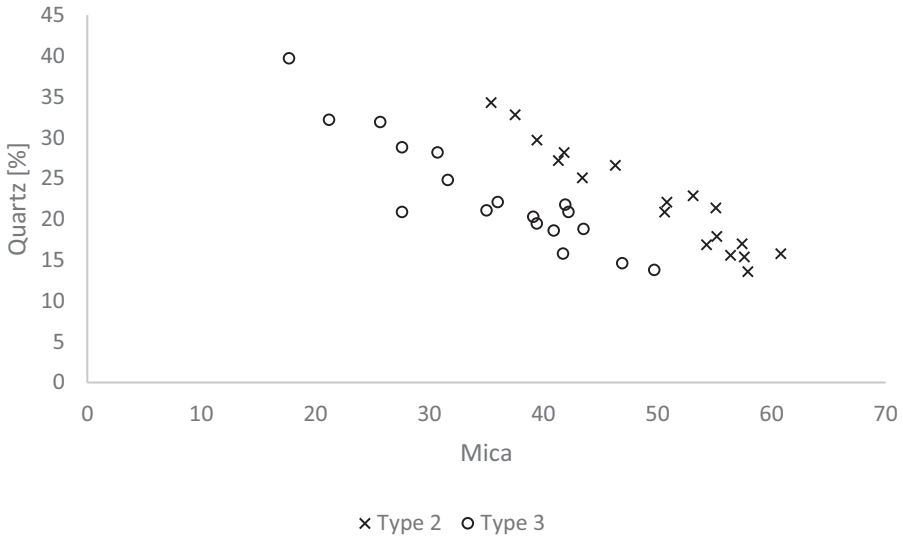

Figure 6. Relative amounts of mica plotted against quartz

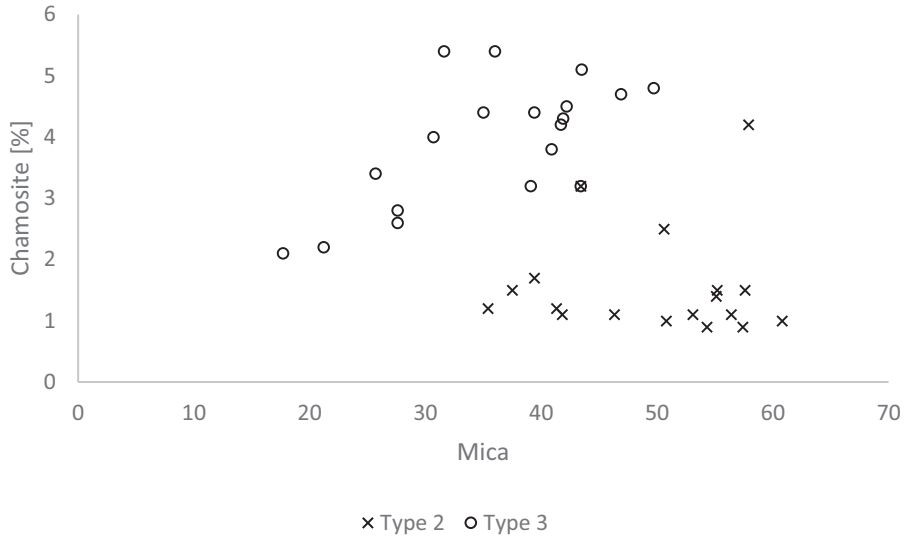

Figure 7. Relative amounts of mica plotted against chamosite

3.2 DVS AND PARTICLE SIZE ANALYSIS

For all samples the first and second DVS-cycles were very similar, indicating that no changes to the samples in terms of phase transitions or hydrate formation occurred during the cycles. In Figure 8 the moisture uptakes at 95 % RH for the 1st cycle sorption curves are shown for ten of the -20 µm samples. The same diagrams for the 1st desorption and the 2nd sorption and desorption curves are very close to identical. It is seen that the big leap for the most hydrophilic samples occurs between 70 and 95 % relative humidity.

Two samples with high values (A 3m -20µm and A 0.3m -20µm) were checked a second time by reanalysing the first sample and then resampling and analysing the new samples. No significant differences could be seen between the three analyses of the same samples.

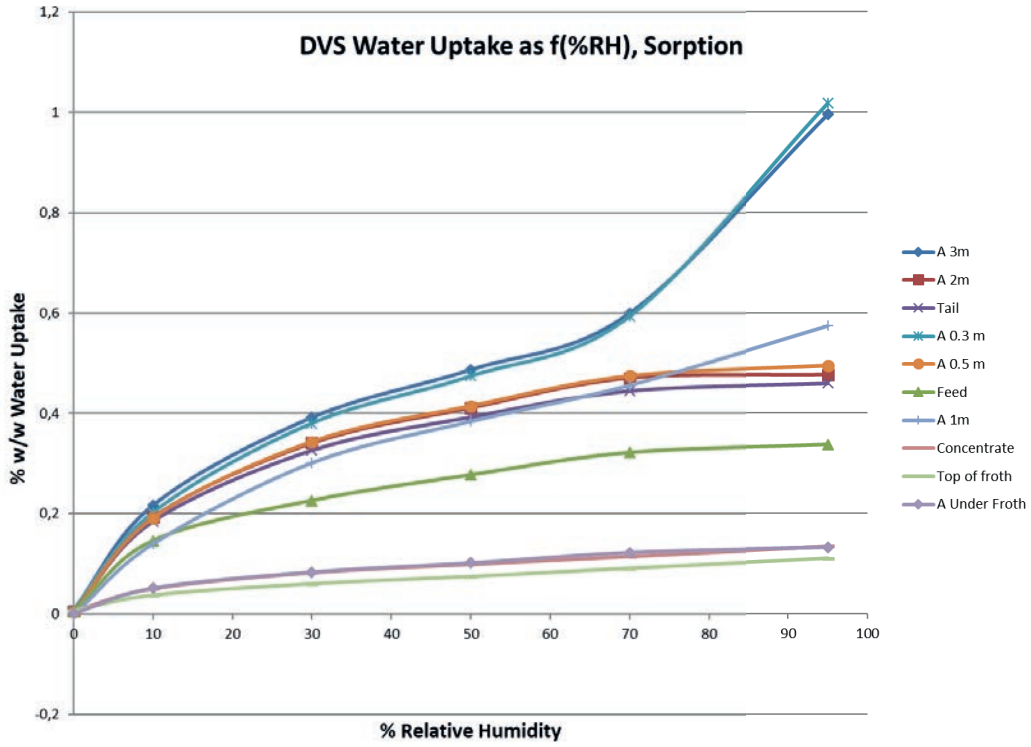

Figure 8. DVS water uptake as a function of %RH for the 1st sorption cycle

In Figure 9 and Figure 10, the DVS results are plotted against the sampling point in the flotation cell. In Figure 9 the non-sieved samples have a constant hydrophobicity level throughout the cell, but as one enters the froth face a decrease of the DVS value occurs and this material is thus more hydrophobic.

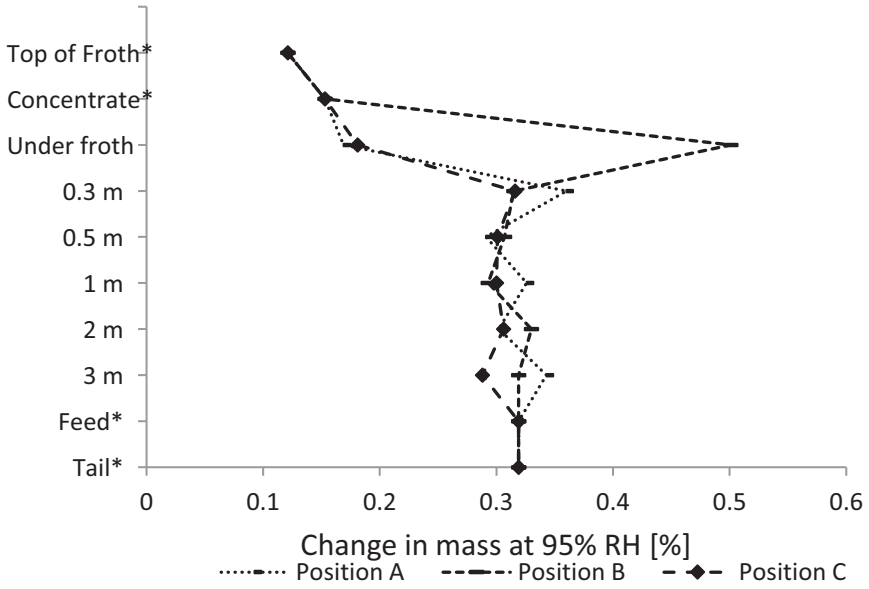

*Figure 9. DVS water uptake at 95 %RH for the non-sieved samples, where * is not position specific samples*

The sample collected from “under froth” in the B position however departs from the A and C positions. It must be taken into consideration that it is difficult to find the right sampling spot under the froth. There is a risk that particles from the froth phase become a part of the “under froth” sample. In this case, the A and C positions act more like the froth samples, but the B sample deviate both from the froth and the deeper positions.
The DVS values for the -20µm particles are given in Figure 10 and most values vary considerably and have higher values than the corresponding total samples. Several froth samples however, have values significantly lower than the corresponding total samples.

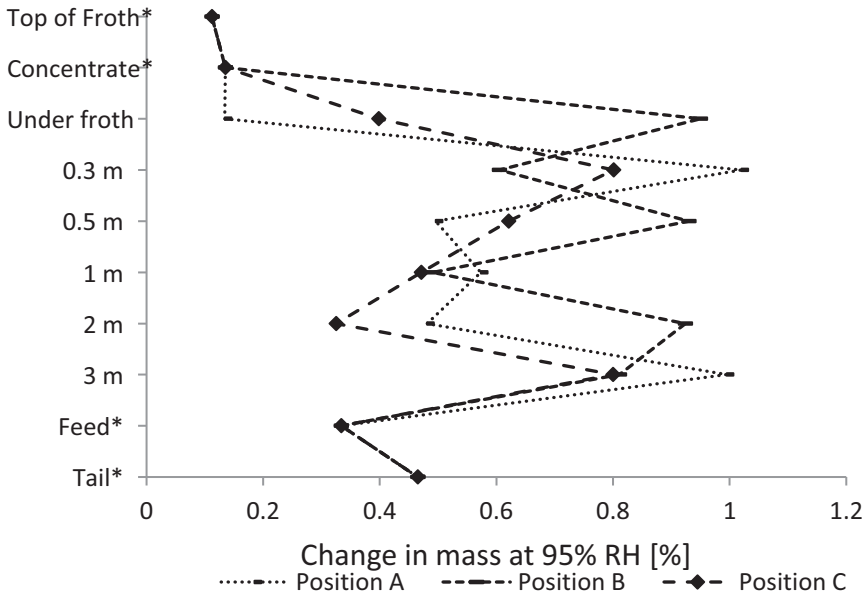

*Figure 10. DVS water uptake at 95 %RH for the -20µm fractions, where * is not position specific samples*

Correlations were investigated for mineral contents and DVS-values and in Figure 11 the chamosite content is plotted against the DVS values. This was the

strongest correlation found. Chamosite is a clay mineral that can exchange water in its layers.

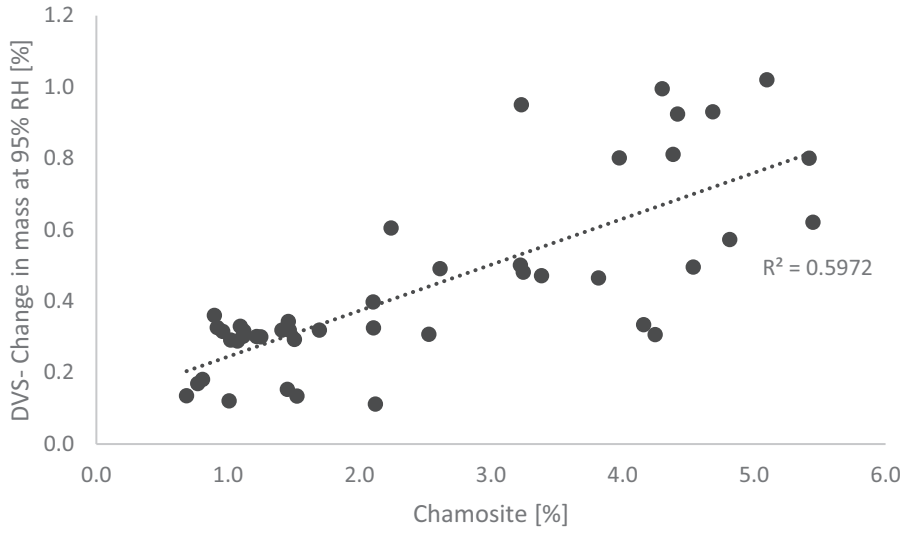

Figure 11. Correlation between relative amount chamosite and the DVS value

As expected, the DVS-data for the ten -20 µm samples of the A-series also correlates to the particle size distribution. The correlations to the Malvern d_{10}-values and to the calculated specific surface area for the not ultrasonicated samples, are presented in Figure 12 and Figure 13. They show that the moisture uptake increases with the amount of small particles, even though the composition of minerals vary between the samples. The error bars shown are estimated from the standard deviation of two measurements, with three replicates each. This can be expected, since a larger amount of small particles gives a larger specific surface area and a larger specific surface area means a larger area for water adsorption. It should also be noted, however, that the specific surface area was estimated from laser diffraction measurement, which induces some error to the estimation.

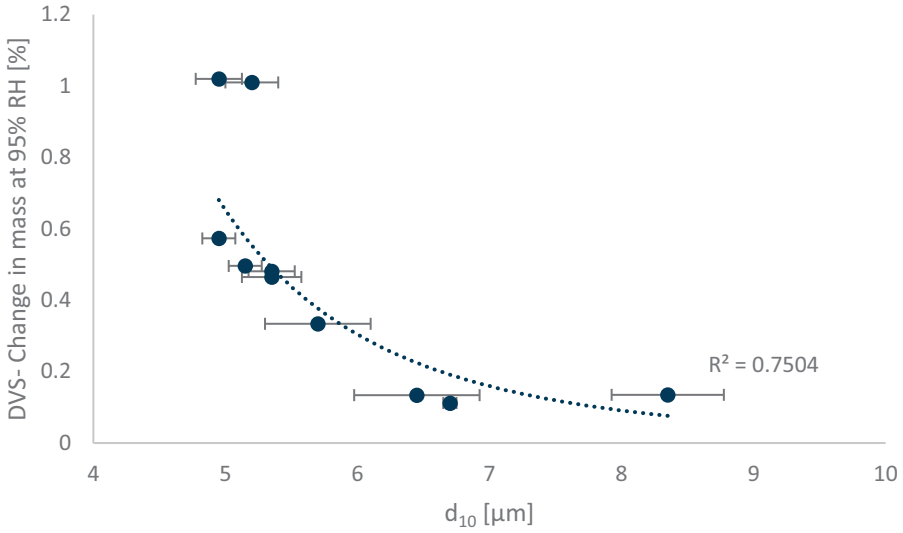

Figure 12. The correlation between the d_{10}-values from the particle size distribution data and the DVS-water uptakes for the ten -20 µm samples of the A-series.

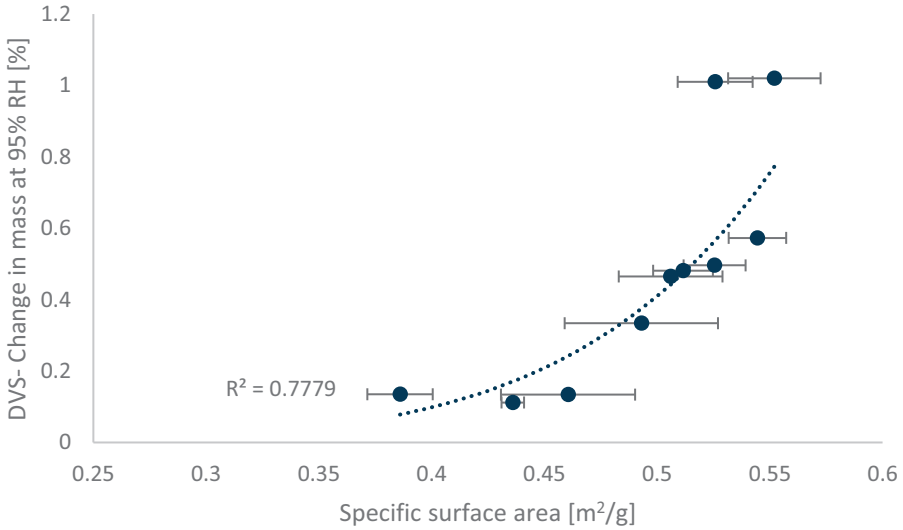

Figure 13. The correlation between the specific surface areas, calculated from the particle size distribution data, and the DVS-water uptakes for the ten -20 µm samples of the A-series.

4 CONCLUSIONS

Samples collected from the first rougher cell in the Aitik copper flotation plant have been analysed for wettability, particle size distribution and mineral content. The samples in the pulp, have a slight variation in mineralogy depending on where they are collected. There is also a particle size variation between the samples in vertical direction. Since it is known that the specific surface area

affects the DVS-results, mineral composition and particle size have to be taken into account when comparing samples.

Even though sampling is complicated near the froth phase there is correlation between wettability characteristics and distribution of valuable and gangue minerals. The fluctuation in fine particle wettability in vertical direction is significant but may be a result of cell hydrodynamics, particle size and/ or mineral distribution. Radial position B where there was a peak in wettability might be an experimental artefact but may also be a result of the complex pulp flow profile in this region (Xia et. al., 2009; Koh and Schwarz, 2011). This might lead to local accumulation of fine hydrophilic particles just below the froth.
The pulp/ froth interface in the B position may be less stable than in A and C thus making sampling in this position less reliable while the A and C sample may have been contaminated by chalcopyrite rich froth.
The concentrate and the samples from the froth phase contain more chalcopyrite, molybdenite and pyrite than the other samples, they also have the lowest DVS-values, indicating higher hydrophobicity. This is as expected since the collector attach mainly to these minerals and render them hydrophobic.
The smallest fraction (- 20 μm) contained a higher amount of chamosite, which is a clay mineral, that can exchange water in its layers. The non-froth samples did adsorb more water when enriched with chamosite. The non-froth samples also take up more water when their specific surface area increases.
The DVS-data for the -20 μm fraction, indicates a difference between the feed and the tailing sample, the feed having a lower DVS value and is thus more hydrophobic than the tailing. This indicates that small, hydrophobic particles in the feed have been floated, leaving more hydrophilic gangue in the tailing.

From this sampling investigation, it has been showed that inside the 160 m^3 flotation cell in Aitik, the hydrophobicity is more or less constant throughout the whole cell but, in the froth phase, there is an increase in hydrophobicity. There is no upgrade of neither the grade nor the hydrophobicity in the large flotation cell (Malm et al., 2016). The smallest particles did contain a lot of chamosite which was shown to correlate to the DVS measurement.

5 ACKNOWLEDGMENT

The authors wish to thank Dr Tommy Karlkvist for his valuable input during the compilation of this manuscript. Boliden Mineral and RISE is acknowledged for permission to publish this paper as well as VINNOVA, the Swedish Governmental Agency for Innovation Systems for financial support.

6 REFERENCES

Buckton, G., Darcy, P., (1995). The use of gravimetric studies to assess the degree of crystallinity of predominantly crystalline powders. *International journal of pharmaceutics*, 123(2), pp. 268-271.

Heng, J., Williams, D., (2011). *Vapour Sorption and Surface Analysis, in Solid State Characterization of Pharmaceuticals (eds R.A. Storey and I. Ymén).* Chichester, UK: John Wiley & Sons, Ltd.

Kawatra, S.K. (2011). Fundamental Principles of Froth Flotation, in SME Mining Engineering Handbook, 3rd Edition, Editor: Darling, P. ISBN 978-0-87335-264-2.

Koh, P. and Schwarz, P., (2011). A novel approach to flotation cell design. SME Annual Meeting, February 27- March 2, Denver, USA, 11-053.

Malm, L., Kindstedt Danielsson, A-S., Sand, A., Rosenkranz, J., Ymén, I., (2018a). Dynamic vapor sorption- A novel method for measuring the hydrophobicity in industrial- scale froth flotation. Proceedings of the 29th International Mineral Processing Congress, September 17-21, Moscow, Russia, paper 431, pp. 1-10.

Malm, L., Kindstedt Danielsson, A-S., Sand, A., Rosenkranz, J., Ymén, I., (2018b). Application of Dynamic Vapor Sorption for evaluation of hydrophobicity in industrial-scale froth flotation. Minerals Engineering, 127, pp. 305-311.

Malm, L., Sand, A., Rosenkranz. J., Bolin, N-J., (2016). Spatial variations of pulp properties in flotation. Implications for optimizing cell design and performance. Proceedings of the 28th International Mineral Processing Congress, September 11-15, Quebec, Canada, paper 354, pp. 1-11.

PANalytical ICDD PDF-2 database, Release 2000, version 2.1.

Susana, L., Campaci, F., Santomaso, A.C., (2012). Wettability of mineral and metallic powders: Applicability and limitations of sessile drop method and Washburn´s technique. Powder Technology, 226, pp. 68- 77.

Tabosa, E., Runge, K., Holtham, P., Duffy, K., (2016). Improving flotation energy efficiency by optimizing cell hydrodynamics, Minerals Engineering, 96-97, pp. 194-202.

Teipel, U., Mikonsaari, I. (2004). Determining Contact Angles of Powders by Liquid Penetration. Particle & Particle Systems Characterization, 21(4), pp. 255- 260.

Wills. B.A., (1997). Mineral Processing Technology. Butterworth-Heinemann, Burlington.

Xia, J., Rinne, A., Grönstrand, S., (2009). Effect of turbulence models on prediction of fluid flow in a Outotec flotation cell. Minerals Engineering 22, pp. 880- 885.

Department of Civil, Environmental and Natural Resources Engineering
Division of Minerals and Metallurgical Engineering

ISSN 1402-1757
ISBN 978-91-7790-314-7 (print)
ISBN 978-91-7790-315-4 (pdf)

LULEÅ
UNIVERSITY
OF TECHNOLOGY